RICE UNIVERSITY

Probabilistic Fragility of Interdependent Urban Systems Subjected to Seismic Hazards

by

Isaac Hernandez-Fajardo

A Thesis Submitted
in Partial Fulfillment of the
Requirements for the Degree

Doctor of Philosophy

Approved, Thesis Committee:

Leonardo Dueñas-Osorio, Chair
Assistant Professor of Civil and
Environmental Engineering

Sátish Nagarajaiah
Professor of Civil and Mechanical
Engineering

Pol D. Spanos
Lewis B. Ryon Professor of Mechanical
Engineering and of Civil Engineering

Houston, Texas

March, 2012

ABSTRACT

Probabilistic Fragility of Interdependent Urban Systems Subjected to Seismic Hazards

by

Isaac Hernandez-Fajardo

Urban service networks have come under increased pressure due to expansion of urban population, decrease of capital investment, growing interdependence, and man-made and natural hazards.

This thesis introduces a simulation-based methodology for the estimation of the fragility of urban networks subjected to earthquake perturbation. The proposed Interdependent Fragility Assessment (IFA) algorithm abstracts the steps required for perturbation-induced damage propagation within and between networks through internal and interdependent links, respectively. Damage propagation uncertainty is accounted by considering conditional probabilities of failure for components and interdependent strengths measuring the likelihood of intersystemic failure propagation.

The IFA algorithm is used in four applications. The first application subjected two simplified models of real interdependent urban power and water networks to selected seismic scenarios. Test results showed that interdependence presence worsens systemic fragility, but that the features of interdependence effects were jointly influenced by local fragility properties and interdependence strengths.

A second application examined the role of cascading failures caused by component overloading in systemic fragility. The results showed that cascading failures worsen

interdependence fragility, and that mitigation actions improving local component capacity have limited effect on controlling interdependent-induced fragility.

Two additional conceptual mitigation measures, component fragility reduction (CFR) and interdependence redundancy enhancement (IRE), were explored. CFR, decreases component seismic fragilities while IRE adds interdependence links to dependent nodes. Test results showed that CFR outperforms IRE; however, their combination achieved comparable fragility reductions. This outcome highlights the potential of synergistic mitigation policies in controlling interdependent systemic fragility.

Finally, the IFA methodology was adapted to use a probabilistic seismic description for the estimation of unconditional systemic fragilities. The hazard description was obtained following an existing approach that uses importance sampling for the generation of intensity maps. The value of the hybrid methodology rests on its capacity to generate unconditional fragility estimates for direct use in risk assessment.

Topics for future work include the development of more sophisticated models of cascading failure, the analysis of optimal mitigation actions using mitigation cost-structures and life-cycle costs, the extension of the IFA methodology for perturbation such as hurricanes and flooding, and interdependent fragility studies of theoretical network models.

Acknowledgements

I would like to express my gratitude to my advisor Dr. Leonardo Dueñas-Osorio, for his continuous support, insight, and patience that contributed greatly to the success of this endeavor.

I am also indebted to the members of the doctoral committee Dr. Satish Nagarajaiah and Dr. Pol D. Spanos whose time, support, and example contributed in many ways to the development of my research.

The work reported here was funded in part by the National Science Foundation under Grant CMMI-0728040.

Contents

Illustrations

Tables

Chapter 1

Introduction and Literature Review

1.1 Motivation

Urban networks, like power, water, gas, transportation, or telecommunication systems, are essential elements of the infrastructure of cities. The productivity and livelihood of corporations and people depend on their continuous operation, while their relevance to society becomes especially evident in the aftermath of strong natural (earthquake, hurricanes) or man-made (accidents, terrorism) perturbations (Davis et al., 2006; EERI, 2010; Eidinger et al., 2010).

In recent years, urban networks have found themselves under increased stress due to urban population growth (United Nations, 2009) (Fig. 1.1), service demand rise (International Energy Agency, 2010), and, in some countries, limited investment on expansion and maintenance (Congress Budget Office, 2008). The resulting infrastructure deterioration and vulnerability has been reported by the media and professional organizations (The Economist, 2011; American Society of Civil Engineers, ASCE, 2009). However, in such reports, the critical role of interdependence as an essential contributor to vulnerability during abnormal operation is not highlighted; furthermore, the fact that network response and interdependence effects are inherently uncertain receives limited attention, despite its impact in infrastructure operation and management and associated decision making.

As networks have become larger and more complex, they have become more in-

(a) 2010

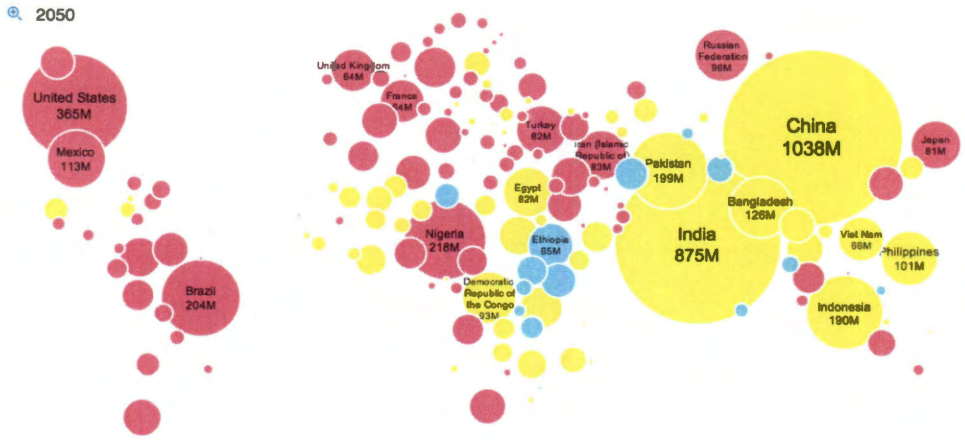

(b) 2050

Figure 1.1 : Urban population growth (1.1(a)) as reported in 2010, and (1.1(b)) forecast for 2050. Larger urban population implies increased pressure on urban infrastructure and greater inoperability risk for cities exposed to strong perturbations like seismic events. Source: 2012.

terconnected (Amin, 2000b). This interconnection is a positive phenomenon during regular operation as it allows easy access to resources needed by other systems to operate as intended. However, the interdependence existence implies that the protec-

tion of an urban network requires the additional protection of components in external systems (O'Rourke, 2007). In fact, the implication is that interdependence between systems is likely to increase the original vulnerability of single networks.

The natural question in relation to the role of interdependence in systemic fragility is how much its impact is (Amin, 2000a). This thesis introduces a methodology to study that quantification problem while considering the randomness of network component responses and interdependence effects triggered by seismic perturbation. The proposed methodology is implemented using a new Interdependent Fragility (IFA) algorithm, based on a proposed description of how earthquake-induced damage propagates within each system and across networks. This propagation mechanism is used to estimate the reduction of the network capacities to fulfill their regular service demands. Results from this IFA strategy can be used to forecast systemic damage in the event of earthquake, which in turn can be used to test mitigation actions, estimate required mitigation expenditures, and design emergency plans to be implemented by public actors (e.g. civil servants, agency managers) or private stakeholders (e.g. utility managers, insurers, businesses).

The proposed IFA methodology targets earthquake events as the perturbation type acting on interdependent systems. Nevertheless, this methodology can be adapted to study other types of natural hazards by changing the input hazard and fragility information, but this thesis chooses to focus on seismic hazards due to the destructive capacity and geographical reach that earthquakes have shown in important cities around the world. The experiences of San Francisco, USA (1905), Tokyo, Japan (1923), or Mexico City, Mexico (1982), Maule, Chile (2010), Tōhoku, Japan (2011) among many others confirm the level of damage that earthquakes can cause in densely populated urban centers.

Additionally, due to their widespread action and intensity, earthquakes are prone to produce scenarios in which interdependence becomes evident: emergency attention slows down when the transportation network is disrupted; the repair of utility systems is delayed, hospitals come under stress when power and water services are not available; businesses are further upset when telecommunications systems are down; water or natural gas pumps may stop working without power; and power itself may stop flowing if thermal power stations are left without natural gas to burn or water to cool down. These examples illustrate how perturbation-induced interdependence enables interaction between urban network fragilities, a condition that may lead to self-reinforcing cycles of damage feedback.

1.2 Basic terminology

Before introducing the details of the IFA algorithm, a basic set of definitions must be provided. This thesis is focused on the concept of *fragility*. Fragility measures the conditional probability, that is the likelihood, of a component or system reaching or exceeding a *performance limit* under the effect of an external perturbation of known intensity. Because of this definition, fragility depends on the magnitude and type of the selected perturbation (e.g., an earthquake inducing a peak ground acceleration of 0.35g at a given location), and on the level of performance targeted as desirable by an analyst, an utility operator or a decision maker. This desired performance target is the *performance limit state* that establishes the threshold dividing the zones of operation at different levels of quality, and failure for a component or a network.

In this thesis, the concept of fragility is applied to individual network components and to complete urban networks. Indeed, the target of the present study is the description of *systemic fragility*, that is the fragility of full networks resulting

from the interaction between component fragilities, internal mechanisms of fragility propagation, and the external fragility spread among networks by the presence of interdependence. When the term *interdependent systemic fragility* is used, the intention is to point out system-level fragility that already includes the effects produced by interdependence.

Another important term used in this thesis is *perturbation.* A perturbation is understood here as any type of phenomenon that may cause the failure of network components. Perturbations can be natural (e.g., earthquakes or hurricanes) or man-made (e.g., accidents or terrorism). Earthquakes are perturbations that are specially strong and widespread but also uncertain, i.e., it is not clear when and how widespread their effect is going to be. Earthquakes as a perturbation are described using two approaches: a basic approach of seismic scenarios and a more complex approach of probabilistic seismic hazard.

Seismic scenarios are expressed in the form of maps indicating the level of seismic intensity at the different locations of the components of an analyzed urban network. These maps are created using a simulation of a single earthquake whose source and magnitude has been specified. The propagation of the earthquake's released energy across the area where the affected network is localized is the source for the intensity values reported in the seismic scenario's intensity map (Jones et al., 2008)

A more complex but also more informative approach for earthquake representation is probabilistic seismic hazard. Seismic hazard, as seismic scenarios, uses seismic intensity maps; however, a seismic hazard characterization generates a set of seismic intensity maps assigning a probability of occurrence to each of them. This characterization is done in such a way that it is possible to estimate the expected annual probabilities of the network fragility by using the simulated seismic intensity maps

(Kiremidjian et al., 2007) allowing the convolution of hazard and vulnerability as required for risk assessment.

1.3 Approaches to interdependence modeling

This thesis uses mathematical graph representations of urban networks to simulate the effects of seismic perturbation of the system components. The proposed methodology tracks how this initial damage triggers additional internal failures due to disconnection of pristine components and flow overloading. These internal failures in turn cause additional failures in external networks due to the dependence of their components in the services provided by external systems. These three effects are combined to estimate the final status of the simulated networks.

The previous process forms the core of a Monte Carlo simulation program in which interdependent networks are subjected to multiple instances of seismic action using a fixed set of seismic scenarios (called here a scenario sweep) or a probabilistic seismic hazard description that uses multiple sampled intensity maps along with their probability of occurrence. Statistical analysis of the performance degradation resulting from this simulation program produces estimates of the likelihood of the single simulated networks exceeding established performance loss targets. These statistics produce the sought systemic fragility values that include the contribution of interdependence.

Previous studies on the effects of interdependence in urban networks use different approaches for the representation of interdependence and the description of systemic vulnerability. Indeed, the interest on the study of interdependence effects on the functionality of urban infrastructure has grown significantly from initial theoretical developments in Mathematics and Physics towards a more direct application in real engineering networks.

The work by Rinaldi et al. (2001) is a defining report on the topic of utility interdependence in terms of a description of its effects and its classification for infrastructure networks. Their classification of interdependencies discussed four basic classes: physical, geographical, cyber, and logical. Physical interdependence occurs when an infrastructure directly depends on the output of another for its regular functionality. Geographical interdependence takes place when infrastructure elements share a spacial location in such a way that disruption to the location itself may induce perturbation to all the elements in the same area. Cyber interdependence is a condition in which the normal functionality of an infrastructure depends on information provided by another system. Finally, logical interdependence describes interdependence conditions that do not match any of the three previous classes. Political and market interactions with infrastructure networks, with human intervention as a defining factor, fall under the scope of this last classification label.

Physical interdependence is considered and modeled by several authors in the field. Lee et al. (2007) model interdependence using physical interconnection links. These authors assign actual flow capacities and demand levels to all network links and solve the resulting supply and demand problem using optimization tools. Their model allows to measure the impact of perturbation in the infrastructure networks (attack or random failures) on the internal flow redistribution. In another approach, researchers like Dueñas-Osorio et al. (2007) and Hernandez-Fajardo and Dueñas-Osorio (2011) model physical interdependence using intersystemic links that describe the likelihood of damage transmission between external components. Their approach includes a probabilistic parameter that makes it appealing for the estimation of physical interdependence effects on systemic fragility, as it involves not only the physical representation of interconnection but also a probability associated to its occurrence.

For the case of geographical interdependence, Johansson and Hassel (2010) explores its impact using a GIS-based description of infrastructure systems, quantifying the magnitude of expected damage caused by attacks or accidents affecting locations used simultaneously by infrastructure elements belonging to different networks.

Cyber interdependence is a recent creation, a byproduct of the information revolution produced by digital telecommunication and the Internet. A critical example of this type of interdependence is the interaction between SCADA (Supervisory Control And Data Acquisition) systems, telecommunication systems, and power networks. Much discussion on the literature has been directed to the likelihood of disruption of the United States power grid by a cyber attack by internal or external antagonists against SCADA systems (Ten et al., 2008). Public attention on the subject of SCADA-Power grid interdependence has increased due to the discovery of computational applications created to disrupt industrial facilities with potential consequences of national scale (Matrosov et al., 2011; Symantec Security Response, 2011).

Finally, Rinaldi et al. (2001) discussed how the California energy crisis occurring from 1996 to 2003 (Healy and Palepu, 2003) showcased the logical interdependence existing between human-decision driven markets, the financial sector, and political decision-makers at the state and national levels.

The discussion of the characteristics and differences of interdependent classes in Rinaldi et al. (2001) provides a basic foundation for the treatment of interdependence effects on urban infrastructure. At the same time, the work does not provide a mechanism or methodology for simulating interdependence effects either in operational conditions or during events or perturbation, although it discusses Complex Adaptive Systems (Holland, 2006) as the proper interpretation of the nature of infrastructure networks. The paper does emphasize the need for further studies and encourages

efforts toward the explicit accounting of interdependence on systemic studies.

Different approaches could be considered as potential answers to the need to model interdependence on urban networks and its consequences. Four alternatives can be highlighted as key approaches due to the nature of their assumptions and the level of detail required for their systemic descriptions: input-output approaches, agent-based methods, empirical methods, and complex networks approaches.

The input-output approach used by authors like Haimes and Jiang (2001) and Barker and Santos (2010) for the description of interdependence interaction between networks and their joint response to perturbation are based on the landmark work by Leontief (1986) for the input-output representation of the interaction of economic sectors. In this input-output approach for utility systems, each infrastructure sector is associated to a column and row in an input-output matrix whose entries describe the level of interaction and potential impact caused in a system by damage in another external to it. This input-output matrix is then incorporated in a linear representation of the future joint status of the networks including the action of external perturbations. With this mathematical description and enough information to populate the input-output interdependence matrix and describe the intensity of perturbations, it is straightforward to evaluate the network *inoperabilities* resulting from direct perturbation and propagated through the input-output matrix (Haimes and Jiang, 2001).

This high-level representation provides a clear description of systemic interdependence and its matrix expression allows the generation of fast estimations of the impact of perturbation of any given network on the total set of infrastructure systems represented. However, the method does not work with direct representations of the interaction between components within individual networks and does not include a description of internal damage propagation phenomena such as disconnection

and cascading failures, likely to occur in the event of strong perturbation. Also, as pointed out by the authors themselves (Haimes and Jiang, 2001), the implicit linearity in the characterization of interdependence may not hold for real-life intersystemic interactions. The research in this thesis builds precisely in that limitation by proposing intuitive urban network representations and goes beyond this basic feature by proposing its own probabilistic interdependence characterization and strategy for the calculation of interdependence effects.

A second approach for network and interdependence description is the use of agent-based simulation. Agent-based strategies use computational simulations for their description of the different elements of infrastructure as agents, i.e., entities whose behavior, interaction, and their emergent response to perturbation are controlled by predefined rules and goals (Zhang et al., 2005). By using this agent-representation, agent-based models describe infrastructure networks as Complex Adaptive Systems, that is systems whose elements called agents behave according to predefined behavioral rules, interact, and eventually are able to produce emergent behaviors (Holland, 2006). This approach to simulating systems combines a bottom-to-top network description with the capacity to specify individual agent behaviors that makes it ideal not only for the description of complex systems like economies and social interactions (Arthur, 1991; Bonabeau, 2002), but also for the interactions of such systems with urban infrastructures (Schoenwald et al., 2004; Ehlen and Scholand, 2005).

The interaction of these components leads to an emerging response of the individual systems to which they belong and also of the system-of-systems described in the simulation. Agent-based methodologies are highly advanced strategies that require considerable computational power and important amounts of information for the description of the behavior of the different components. Their detailed description of

behavior and interaction between actors have contributed to the use of agent-based methodologies for the simulation of emergent response created by the interaction of agent-models representing people (Bonabeau, 2002), a target of particular interest in the field of Economics (Arthur, 1991). For the case of urban infrastructure, Pederson et al. (2006) provide a comprehensive review of agent-based applications developed for modeling infrastructure performance for operational and perturbation-impacted conditions.

Agent-based methodologies for studying urban infrastructure provide a powerful tool to describe the functionality of networks, their interdependence, and their impact of perturbation across scales from system components to societies. However, in relation to the work in this thesis, the problem of studying interdependent systemic fragility, which requires thousands of simulations, does make the use of an agent-type description of components impractical. An urban network component behavior in the context of this thesis is thus limited to the two possible states of failure or survival, while its interactions with other components are conditioned by its location, the network's structure, and a potential role as a supplier to nodes in external networks. A consideration of the response of agents external to the functional performance of urban networks such as businesses, people, and political actors is likely to require the use of agent-based methodologies as part of the high-level problem of the estimation of society-level consequences of systemic perturbation. Such type of analysis holds much value and interest, but it is beyond the scope of the present work.

A third approach to study interdependence between urban networks is the use of empirical data reporting the consequences of catastrophic events. Such data gathered from official sources, private agencies, or press reports is used to estimate the level of failure transmission between different infrastructure networks. Work by Chang

et al. (2007) and McDaniels et al. (2007), for example, have used this methodology to construct and analyze databases of impacts with the objective of identifying interdependent effects. The analysis of such databases allows the researchers to arrive at a characterization of the nature, source, and magnitude of the different impacts across systems. Such information can then be used for the development of recommendations based on the features of the interdependence scenarios identified and their consequences. The results from this methodology provide useful information due to their use of empirical results obtained from real catastrophic events. However, the method itself does not provide a predictive strategy beyond the general lessons learned obtained from previous catastrophic instances. In that regard, this methodology may provide a systematic way of analyzing damage information whose results and conclusions can be used in validation efforts for the predictive methodologies discussed in this thesis.

The final approach for analyzing interdependence effects on urban infrastructure performance is via complex networks analysis. This methodology is based on the representation of urban infrastructure using graph theory concepts, specifically the description of network interconnectivity using mathematical graphs, that is mathematical entities composed of nodes representing real-life facilities (e.g. pumping stations in a water network, electrical substations in power networks, etc) and links representing the connecting elements between facilities (e.g. cables between power transmission towers, pipes in water networks, etc).

Originally used in mathematics and physics, simple directed graphs provide a straightforward, intuitive description of the role, localization, and interaction of components in a network. In particular, the analysis of a network's internal interconnection structure, its *topology*, provides useful insights on the expected systemic response

(Callaway et al., 2000; Albert et al., 2000; Winkler et al., 2011). However, the key feature of this approach is the capacity of direct enhancement of the level of detail of the network description. Based on the basic topological representation, the complexity of the original model can be enriched by adding explicit roles to the network's nodes (e.g., supplier, consumer) or, in a key aspect for this thesis, the systemic fragility of a network can be studied by adding a well-defined description of component-level fragilities for perturbation intensities of interest. Furthermore, given its foundation in graph theory and network analysis, an important amount of mathematical tools and algorithms are available to determine network properties as diverse as the shortest paths between critical network points (Dijkstra, 1959) or the maximum flow the network can carry (Ford and Fulkerson, 1956) under given conditions of supply and link capacities. The next section introduces the key concepts of this approach and describes how previous research and this thesis use it for the study of interdependent systemic fragility.

Under the IFA algorithm described in this research, urban networks are described using the introduced complex networks approach. Using this approach, network interdependence is represented using interdependent links, that is links connecting nodes in different networks. Such links create intersystemic connections between an external provider node and an internal consumer node. Furthermore, each of these interdependent links has an associated *interdependence strength* parameter ($Istr$) that measures the conditional likelihood of failure propagation from the supply node to the consumer component in the event of failure of the external supply component. This interdependence representation is adapted from Dueñas-Osorio et al. (2007), and it is intended to represent the likely failure of a dependent component when its external required providers are disrupted. Consider a pumping station being part of an urban water

distribution system. The pumps in this station depend on the power provided by an adjacent electrical substation which is part of the power distribution grid. If an earthquake occurs in this area and the substation goes offline because of internal physical damage while the pumping station suffers minimal damage, it is possible to end up with a scenario in which undamaged pumps cease to work because of lack of power. Note that in another possible scenario, the pumping station may have diesel generators. In this last eventuality, the water pumps will be able to continue working with no noticeable disruption for as long as the backup system is operational.

The interdependence strength parameter measures precisely that level of dependence between external nodes (also called master nodes) in terms of a probability of failure for the dependent node (also called slave node). For the pumps of the example, if no diesel generators were available in the aftermath of the earthquake (because they were never bought or were poorly maintained) then the $Istr$ for the interdependence link from the power node (the substation) to the water node (the pumping station) will be 1.0, representing certain disruption if the power node fails. In contrast, if the diesel generators were an integral part of the original design of the pumping station, and they were properly maintained, and even tested regularly, $Istr$ may be a small value or simply zero.

This representation of interdependence is a key element in the simulation methodology introduced in this thesis. Previous authors have used this approach for their estimates of systemic fragility (Dueñas-Osorio et al., 2007; Adachi and Ellingwood, 2008; Song and Kang, 2009; Kim et al., 2010; Poljanšek et al., 2012); however, the new IFA algorithm provides a framework for simulating the *evolution* of the interaction of network failures through interdependence links. This evolution of interaction is called here *cycling stabilization* and it is a differentiating feature from previous models that

only considered a single cycle of intersystemic failure propagation. That original rule enforced a policy in which additional interactions, that is potential feedback effects creating additional failures, were not allowed to emerge and hence their effects could not be reflected on the estimations of interdependent systemic fragility. As mentioned above, one of the key contributions of this thesis is the IFA methodology and its capacity to enable such cycling stabilization process.

Other differences of the new IFA methodology with previous work include improved algorithms for the detection of disconnected nodes, for the calculation of systemic fragility, and for the procedure of internal stabilization and interdependent damage propagation. These differences are explained in detail in the inner chapters of this thesis, but their key contribution is their impact on reducing computational expense in the simulation procedure and modeling interdependence phenomena closer to reality. As an example of the gained efficiencies, the new computational implementations reduced the running time of a test case of 10 000 simulations from 15 days to approximately six hours with good approximations to results observed in real cases.

It should be emphasized that the IFA algorithm works as the core of a Monte Carlo simulation program. This choice of using simulation has clear advantages over alternative approaches. One basic alternative approach is the use of analytical solutions to evaluate the expected network response.

The work by Dueñas-Osorio and Rojo (2011) proposes a closed-form solution to the problem of calculating the probability distribution of the reliability of a system with radial topology. Their approach is based in an efficient recursive approach, but because of its definition is limited to the the special case of radial topologies.

Work by White and Newman (2001) and Li and He (2002) propose this type of approach where the internal connecting paths of a network are identified and the

probability of the system is examined through the failure probability of such paths. Such approaches provide valuable tools for the examination of urban network fragility, but they are essentially limited to small systems due to the computational complexity of finding the required disjoint paths (Wang and Silvester, 1993). Furthermore, some important dynamics occurring within a network (internal damage propagation caused by overloading, for example) are not trivial to express in this type of approaches but can be readily integrated in simulation-based approaches like the IFA algorithm.

Another type of alternative approach uses a matrix-based representation of systemic failure events to calculate systemic fragility (Song and Kang, 2009). The key idea of the method is that systemic events leading to failure can be represented in a matrix-form making the calculation of their probability of occurrence straightforward. This approach is extremely efficient if the analyst can successfully identify the mechanisms of component failures leading to the failure of the system. However, that requirement is equivalent to the problem of finding the internal paths used by the previous approach, and so this approach shares the same computational disadvantage of computational complexity with respect to the more general approach of Monte Carlo simulation used in the implementation of the proposed IFA algorithm. Despite the limitations of the close-form solutions, it is clear that if they are computational feasible they must always be preferred to simulation-based approaches due to their advantages in regard to insight and the calculation of importance measures of network components with respect to the estimated systemic fragilities.

1.4 Research contributions and future work

The core objective of the research recorded in this thesis is the creation of a methodology for the realistic estimation of systemic fragility for interdependent networks

subjected to earthquake perturbation. Previous approaches modeling interdependence and network response were either too high-level or too fine-grained in their description of network response to perturbation to be useful to probabilistically capture internal mechanisms of damage propagation. The methodology that provides the closest fit is the complex network approach, specifically in its use of mathematical graphs for the representation of network topologies as used in this research.

The individual network representation is combined here with a model of interdependence to form the basic description of interdependent urban networks. This representation is the basic working model that is enriched by the characterization of the network components behavior using fragility curves and network-level failure propagation principles. This fragility curves allow network components to exhibit a binary response of failure or survival to the action of perturbation. By the virtue of this behavior allocation, it is possible to measure the emergent systemic performance, an implicit function of the response of the different network components and of their dependence on external components.

This enriched model is the target on which the proposed Interdependence Fragility Assessment (IFA) algorithm works. The IFA algorithm is the new strategy proposed in this thesis for the description of failure occurrence, internal propagation within an urban network, and external transmission through interdependent links towards interconnected systems depending on external services. Strategies based on similar models and procedures as the IFA algorithm have been proposed in the literature, but no known approach has included the key novelty of the IFA approach: the explicit representation of interdependence-induced feedback effects on network performance. This feature added to the simultaneous consideration of internal mechanisms of damage propagation like disconnection and cascading failures make the IFA algorithm

a valuable addition to the existing body of literature in the field of interdependent systemic fragility of urban networks.

Using the flexibility of the simulation approach, the proposed IFA algorithm was applied to a series of test cases to measure the effects of earthquake perturbation and internal propagation phenomena in the presence of interdependence. A first test case evaluated the impact of systemic fragility using a sweep of seven seismic scenarios of increasing intensity applied to two simplified versions of real interdependent power and water networks from a location in the US. The intensities of these seismic scenarios were expressed using Peak Ground Acceleration (PGA) for the facilities (nodes) and Peak Ground Velocity (PGV) for the connection elements of the water network. The seismic intensities were in the range from 0.1g (where g stands for standard gravity) to 0.7g, while PGV values were calculated as functions of PGA.

In this first case study, increasing the interdependence strength between the two urban networks led to higher systemic fragility for the water network while it had an almost negligible effect on the power system. Furthermore, the effects on the water network were larger in an earthquake intensity range (0.2g to 0.5g) in which the intensities were large enough to foster disruption but not so excessive as to induce complete direct system collapse. These results illustrate that even though interdependence can cause mayhem in otherwise strong networks (like the test water system), its effects are conditional on the perturbation intensity (difficult to control) and on the fragilities of the interconnected networks (potentially controllable). This insight suggests that the best alternatives to control interdependence consist on achieving full decoupling of the networks or controlling the fragility sources in the individual networks that enable the external fragility propagation.

A second study for the same test networks and seismic scenarios included the

effects of component overloading caused by the direct failure of components. Overloading failures can create a chain reaction of failures when a component overloads and goes offline, the load must be redistributed to other components who in turn may fail themselves. This chain reaction is called *cascading failures* in the literature (Motter and Lai, 2002; Crucitti et al., 2004; Wang and Rong, 2009) and an apparent way of controlling them consists on increasing the local capacity of susceptible components. This mitigation technique called here *local redundancy enhancement* (LRE) was tested for interdependent urban networks using an approach that identifies the number of connecting paths passing through a component with the likely amount of load the element will take in the real network operation. These connecting paths change when elements are removed and such change is interpreted as the likely load change triggered by the perturbation. The capacity of the components is obtained from the number of connecting paths in the pristine network, and this original capacity can be subsequently increased by applying a magnification factor (an α parameter) to represent the mitigation action of local redundancy enhancement. The application of the magnification factor to the original capacities defines the LRE strategy. The results of using local redundancy enhancement against cascading failures and interdependence effects showed that indeed LRE can reduce cascading failures, and by proxy systemic fragility, but its effects are considerably constrained by the fragility of the components of each network and the strength of network interdependence. The test cases showed that the effectiveness of LRE for the weak and less-interdependence-susceptible power network was small under small seismic intensities and nonexistent for large perturbations under which systemic collapse was unavoidable.

For the strong, interdependence-susceptible water network, the LRE effect was large for small seismic intensities bringing down the expected systemic fragility as the

α factor increased; however, increasing the seismic intensity made interdependence effects stronger, inducing a noticeable reduction on the effectiveness of the LRE policy. These trends show that in the case of interdependent urban infrastructure the effectiveness of mitigation measures must be modeled carefully as the different factors involved may compromise the effectiveness of an otherwise sound strategy. In this particular case, the reasonable policy of increasing local capacity proved to be ineffective in a scenario in which the considerable fragility of the power network propagated to the stronger water network through their interdependence.

The mixed results found for the application of the local redundancy enhancement policy emphasized the need for testing alternative mitigation policies. A third case study targeted this issue and used the original interdependent power and water networks and a sweep of seismic scenarios to evaluate the effectiveness of two new mitigation policies at a proof-of-concept level: component fragility reduction (CFR) and interdependence redundancy enhancement (IRE). The CFR policy reduces the fragility of selected components by an amount equal to 25% of their original values, while the IRE policy attaches an additional supply link to each of the dependent components in all interdependent networks. The percentage of reduction for the CFR policy was selected as to reflect the expected maximum reduction of fragility achievable under a reasonable mitigation measure before opting for a policy of complete replacement of the element under analysis. The impact of the mitigation policies was calculated as the average fragility reduction they achieved over all the seismic scenarios. The case study results showed that the CFR policy was more effective than the IRE policy when total reduction in the two networks was considered. This result is to be expected given that the reduction of component fragility leads to less internal failures and hence less interdependence effects. Note, however, that reducing

the fragility of a certain percent of network components (10% and 20% in the test case) by 25% will require higher investments than adding additional supply lines per component as in the case of the IRE policy.

For the same case study, it was found that the combination of the mitigation policies, that is a mixed $CFR+IRE$ policy using less CFR (10% retrofitted components only) and more of the IRE strategy, produced fragility reductions that matched or exceeded the performance of the single policies acting separately. This result highlights the need for a careful review of mitigation policies for interdependent networks; at the same time, this outcome shows that mitigation of the *interdependence interface*, the set of interdependent links between networks, can lead to efficient retrofitting investments to control interdependence effects.

The previous developments on the effectiveness of mitigation measures show a promising avenue for further research on the topic of optimal retrofitting policies. However, the results were conditional on the seismic scenarios used to simulate earthquake perturbation. Therefore, the final contribution in this thesis combines a methodology for the generation of seismic hazard maps proposed by Jayaram and Baker (2010) with the IFA algorithm to obtain unconditional interdependent systemic fragility assessments which account for the uncertainty of site specific seismic scenarios. The new hybrid methodology involves the key operation of generating seismic hazard maps using an *importance sampling* technique originally proposed by Kiremidjian et al. (2007) that reduces the computational expense of sampling seismic hazard maps.

The new hybrid methodology is used to estimate annual probabilities of exceedance (APEX) of systemic fragility that are dependent only on the seismicity of the location of the interdependent networks. Its application to the test interdepen-

dent power and water networks shows that the unconditional interdependence effects have a similar trend as the scenario-based systemic fragility estimates. Indeed, the APEX results for the power network showed small changes under different conditions of interdependence strength as before. Its expected systemic fragility rose only by 14% when interdependence strength was increased from $Istr = 0$ to $Istr = 1$. The same interdependence increase induced a 229% rise in the expected systemic fragility for the interdependence-susceptible water network.

Beyond the illustrative results in the case study, the value of the hybrid methodology rests on its use as a tool that includes a state-of-the-art strategy for probabilistically simulating seismic hazard for the estimation of unconditional interdependence systemic fragility. This tool could therefore be used for analysis directed not only for seismic risk communication purposes, as in the case of seismic scenarios, but ultimately to evaluate the current fragility of interdependent networks exposed to seismic hazard and to measure the impact of mitigation measures, like the CFR and IRE policies, on such fragilities.

Some points for future exploration based on the developments in this research are: 1) inclusion of a model of cascading failures using realistic flow analysis; 2) analysis of optimal mitigation strategies including realistic cost structures of mitigation and life-cycle costs; 3) estimation of interdependent systemic fragility for hazard sources different from earthquake perturbation such as hurricanes and flooding; and 4) execution and comparison of fragility studies for theoretical models of interdependent urban networks.

1.5 Thesis organization

The remaining chapters of this thesis are organized as follows: Chapter 2, *Key Concepts in Complex Networks*, introduces basic definitions for the complex networks approach, disconnection evaluation, cascading failures, interdependence model, paradigms for interdependent damage propagation, and ranking strategies for critical network components. Chapter 3, *Simulation of Damage Propagation and Interdependent Systemic Fragility*, introduces the Interdependent Fragility Assessment (IFA) algorithm and explains its four basic operations of direct hazard action, internal damage propagation, external damage propagation, and systemic performance measure in the framework of a Monte Carlo simulation program for systemic fragility assessment. This chapter also includes two case studies measuring the effect of interdependence strength on systemic performance and the influence of a local redundancy enhancement policy in the reduction of interdependent systemic fragility. Chapter 4, *Mitigation Strategies for Interdependent Seismic Fragility Control on Urban Lifelines Systems* introduces two conceptual mitigation measures, component fragility reduction (CFR) and interdependence redundancy enhancement (IRE) targeting network component fragility and the density of the interdependent interface, respectively as prime enablers of interdependence systemic fragility. A case study of the two conceptual mitigation strategies shows that CFR is more effective than IRE, but that the synergistic combination is likely to produce better results with reduced mitigation intensity and cost. Chapter 5, *Probabilistic Fragility of Interdependent Infrastructure Networks under Network-Consistent Seismic Hazard*, extends the scope of the IFA algorithm by combining it with an existent methodology that generates stochastically-representative network-consistent seismic intensity maps. The seismic intensity maps are used as input to the IFA algorithm and the resulting fragility estimates are used

for the estimation of annual probabilities of exceedance for systemic performance that depend exclusively on the general seismicity of the network location, a type of result generated for the first time in this research. This thesis ends with Chapter 6 discussing *Conclusions and Future Research.*

Chapter 2

Key Concepts in Complex Networks

2.1 Generalities

The complex networks approach to study the systemic fragility of interdependent urban networks rests on the strategy that a graph representation of a network can be used to measure important properties of the represented real systems. Hence, the concept of a mathematical graph is critical. A graph $G(V, E)$ is a discrete mathematical entity formed by a set of nodes V (also called vertices) and the set of links E (also called edges), such that $E \in V^2$, i.e., E is described by ordinated pairs of nodes in V (Diestel, 2005). The size of the set V, the number of nodes in the network, is called the *order* of the graph; the total number of links in the graph is called the *size* of the graph; while the number of links (incoming or outgoing) associated to a node is called the *degree* of the node.

The topological information of a graph can be recorded using different strategies: adjacency matrices, adjacency lists, or incidence matrices, among others (Ahuja et al., 1993). In all the results and computational implementations in this thesis, graph topology is described using adjacency matrices. These data structures are square matrices whose entries can only be zero or one according to the lack or existence, respectively, of a link joining the nodes associated to each entry. For the example network in Fig. 2.1(a), the nodes are labeled from 1 to 5 and each label is associated to the corresponding column and row of the same number in the adjacency matrix in

Fig. 2.1(b). In this figure, note how the existence of links joining node 1 and node 2, and node 1 and node 3 is represented with a one in the entries (1,2) and (1,3) of the matrix, respectively. It is important to note that adjacency matrices are symmetric only when the associated graph is an undirected one (i.e., a graph with undirected links). The graphs used in this thesis for the representation of urban networks are simple directed graphs. Simple directed graphs do not have by default symmetric adjacency matrices because they are directed, and they do not allow loop links, that is links whose source and target nodes are the same. This last property guarantees that the diagonal of the adjacency matrix for the represented networks will be filled with zeros only.

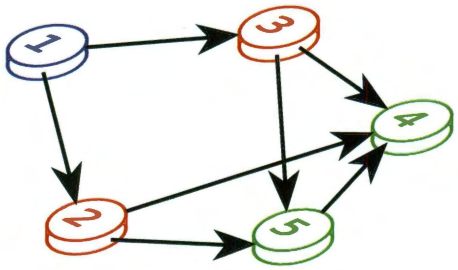

(a) Example network

$$\begin{bmatrix} 0 & 1 & 1 & 0 & 0 \\ 0 & 0 & 0 & 1 & 1 \\ 0 & 0 & 0 & 1 & 1 \\ 0 & 0 & 0 & 0 & 0 \\ 0 & 0 & 0 & 1 & 0 \end{bmatrix}$$

(b) Adjacency matrix

Figure 2.1 : Basic example of a directed simple graph representation of a network. The presence of links between two nodes is represented by a value of one in the associated matrix entry.

Another important definition in dealing with graphs is the concept of paths. A path is a non-empty graph formed by the collection of nodes and links required to connect the path's starting and terminal nodes. A basic operation in graphs is the identification of such connecting paths and different computational tools can be used for such purpose (Dijkstra's algorithm, for example). The identification of such connecting paths has a critical role in the recognition of internal connection routes

and on the functionality of components in the aftermath of a perturbation. This last aspect is explored in more detail later in this section. In the meantime, the next section provides an overview of complex networks research for theoretical network models. Such recent developments have contributed enormously to the use of the complex networks approach for research in more applied fields as it is the case for this thesis.

2.2 Theoretical network models

Early studies on systems' topologies focused on the structure of ideal networks in mathematics and physics, as well as in social and natural sciences (Watts, 2003). The three major developments from such early studies in science and engineering were presented by Erdős and Rényi (1958), Watts and Strogatz (1998) and Barabási and Albert (1999). The first model by Erdős and Rényi (1958) proposed the generation of random graphs, that is graphs in which the probability of existence of a link between any two nodes is the same for every considered pair of nodes.

Watts and Strogatz (1998) proposed a second model for the generation of small-world networks. Small-world networks display short average distances between nodes and important levels of nodal clustering, a behavior known to exist in some social and biological systems (Amaral et al., 2000; Watts, 2004).

Finally, Barabási and Albert (1999) proposed a third model, the Barabási-Albert model, for the generation of scale-free networks. Scale-free networks display the presence of "hubs", which are nodes with a disproportionate amount of network connections relative to the number observed for the average network node. This feature is indeed confirmed by the fact that these networks display node degree distributions $P(k)$ following power laws (i.e. $P(k) \sim k^{-a}, a > 0$). This behavior of the degree of

nodes is displayed by networks such as the Internet and some transportation systems (Cohen et al., 2000, 2001).

The three synthetic models, random graphs, small worlds, and scale-free networks, above are of interest as results based on their topological structures can be used as guidelines for expected systemic behavior in some engineering applications. However, the methodology and examples in this thesis apply only to real networks whose properties are likely to differ greatly from the standard cases described by these theoretical models. Furthermore, studies based on artificial models do not consider the inherent fragility of components or how such fragility propagates to the systemic level, both requirements for the fragility studies addressed in this thesis upon the presence of hazards.

2.3 Error and attack tolerance studies

An important aspect of failure in complex networks is the study of the error and attack tolerance of systems (Albert et al., 2000; Crucitti et al., 2004; Holme et al., 2002). The term *error tolerance* stands for the estimation of the strength of a system to random failures of its components. Typically, error tolerance studies subject a graph model of a system to the random removal of its components. The number of components removed in each trial varies according to the purposes of the study, but the status of the system is usually updated after each removal event (Holme et al., 2002). *Attack tolerance* studies aim to estimate the strength of a system subjected to a removal of its components (usually nodes) based on a specific measure of their importance for systemic functionality. Freeman (1979), Barrat et al. (2008), and Cadini et al. (2009) list the two most used metrics in attack tolerance studies: degree centrality and betweenness centrality. Note that in the context of network science,

the word centrality stands for relevance or importance for the internal connectivity of a networked system. Albert et al. (2000) used the degree centrality metric (i.e. importance based on node degree) to identify the critical nodes to be removed in their error and attack tolerance studies of artificial random and scale-free networks. Later, Albert et al. (2004) performed an attack tolerance study using a betweenness centrality approach on a graph model of the USA power network. The calculation of betweenness centrality assigns an importance value to each node (or link) in a system according to the number of communication paths passing through the node (or link) in question. In their work, the authors found that the power system could be disrupted by targeted attacks on its transmission hubs because of its scale-free-like structure. At the same time, the scale-free configuration of the network was identified as responsible for the robustness of the system to the action of random errors. These two trends are reconciled by considering that error failures remove elements at random and given the hub structure of scale-free networks, it will be more likely that such failures occur at nodes of lesser importance. Similarly, the selection associated to attack tolerance studies will mean that an antagonist will choose to perturb the hubs used by most of the connecting paths within the network in order to maximize the impact of her attack.

Error and attack tolerance studies move closer towards the objective of studying urban network fragility, but they do not include component-level fragility or fragility propagation given their inherently deterministic nature. Nevertheless, the key value of error and attack tolerances studies rests on the introduction of external perturbation and a first approximation to the use of the functionality of nodes as valuable information sources for perturbation design and performance estimation. This thesis builds on this approach for the purposes of systemic fragility. However, the strategy

followed in this work enriches previous models with two key features: the classification of nodes based on their functionality and the assignment of fragilities to each of the components of the system. These enhancements take a simple graph model closer to the actual constitution of urban infrastructure systems.

Before moving into the definitions of component and systemic fragility and system interdependence at the core of this work, an important internal damage mechanism is described in the next section: cascading failures.

2.4 Cascading failures in urban networks

Cascading failures is the term used to describe successive failures within a network associated to a condition of overloading of components rather than to their failure due to direct attack or damage on its physical structure (Motter and Lai, 2002).

The experience of the Northeast Blackout of 2003 (Liscouski and Elliot, 2004) in the US and Canada showed how a series of small perturbations could trigger the collapse of disproportionally large service areas. This specific event was triggered by short circuits caused by tree contact with power lines in Walton Hills, Ohio. These perturbations along with computational and human errors spread until reaching the level of a systemic perturbation of the power network. Furthermore, the failure of the power network in the affected cities led to disruptions on the services provided by other infrastructure systems, i.e, additional interdependence effects like unavailability of telecommunication and water services were generated as a direct consequence of the cascading failures in the power system. Similar experiences have been reported to occur when strong perturbations like earthquakes have affected urban areas (Takewaki, 2011).

Fig. 2.2 presents a basic sketch of the mechanism of generation and propagation

of cascading failures in urban networks. In Fig. 2.2(a), the levels of the blue and red bars, standing for the capacity and demand at each of the networks nodes, guarantee operational stability. However, note that the levels of the bars at some nodes show a condition in which the spare capacity, considered when the current demand is discounted from the current supply, is not high. When node 2 is removed in Fig. 2.2(b), the internal flow patterns of the network reorganize in order to adjust to the new operational situation. An unexpected consequence of such rearrangement is that the new amounts of flow passing through node 4 become larger than the capacity of the node. This imbalance forces the element to go offline and to trigger and additional internal flow redistribution that may lead in the best case to a new stable condition as shown in Fig. 2.2(c) or in the worst case to a new iteration of cascading failures with a potential to become a self-reinforcing catastrophic chain of internal failures.

The previous illustration of cascading failures shows that a flow model is required for the simulation of the phenomenon. However, flow models require additional information sources and higher amounts of computational resources especially when further simulation actions are involved. Instead of using a full flow model, developments in the literature have used centrality metrics as indicators of the expected flow or load to pass through any given network node (Motter and Lai, 2002; Dueñas-Osorio and Vemuru, 2009). One of the most common of such metrics is the already named betweenness centrality, *btwn*, originally proposed by Freeman (1977) for the study of the relative importance of individuals on social networks. Betweenness counts the number of paths connecting different node pairs in a network using a given node as an intermediate connective element. This path count is then normalized by the total number of connecting paths and the resulting quantity is assigned as the betweenness of the node in question. The expression for the calculation of betweenness is shown

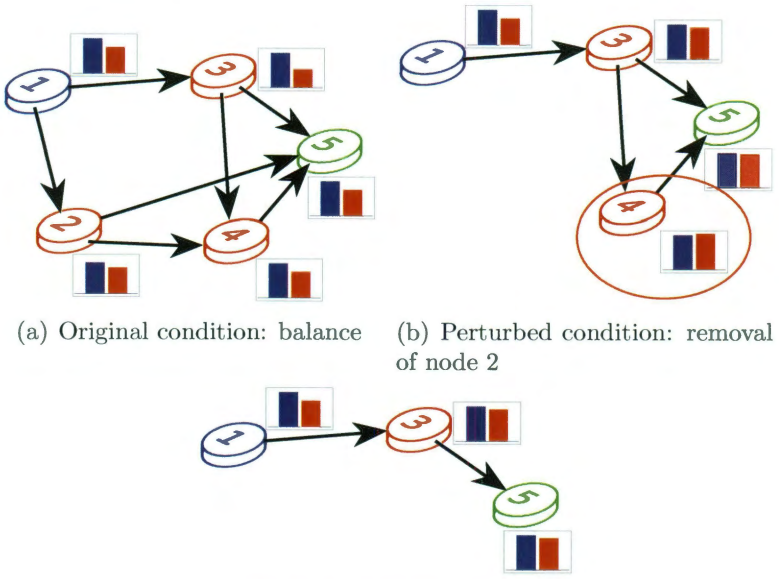

(a) Original condition: balance

(b) Perturbed condition: removal of node 2

(c) Resulting condition after overloading of node 4

Figure 2.2 : Stages in the development of cascading failures with blue and red bar representing the levels of capacity and load in each of the components. Overloading caused by internal flow redistribution after component failures may lead to a situation of self-reinforcing failures in a service network

in Eq. 2.1.

$$btwn(k) = \sum_{s \neq k \neq t} \frac{\sigma_{st}(k)}{\sigma_{st}} \tag{2.1}$$

In this equation $\sigma_{st}(k)$ counts the number of shortest paths between nodes s and t passing through node k, and σ_{st} is equal to the total number of shortest paths between the same nodes. From this definition, it is apparent that the key challenge of calculating node betweenness is the identification of the connecting paths in a network. Such search task is a classical problem in the field of integer programming (Ahuja et al., 1993) and different algorithms have been developed for the purpose (See Bellman (1958) or Dijkstra (1959), for example). Furthermore, a recent algorithm

(Brandes, 2001) has been develop for the reduction of the computational expense of the betweenness calculation itself.

A key feature of the original definition of betweenness is the fact that it does not impose any conditions on the nature of the sources and destinations of the connecting paths used for betweenness calculation. However, in some instances it may be more informative to limit such sources and destinations to selected node sets. For such instances, the standard algorithms must be adapted and the original betweenness denomination becomes an origin-destination betweenness, *O-D btwn*. In this case, the original equation transforms into the expression in Eq. 2.2. with $|SN|$ equal to the size of the network set of supply nodes s, and t limited to elements of the network consumption nodes in set CN.

$$O\text{-}D\,btwn(k) = \frac{1}{|SN|} \sum_{\substack{s \in SN \\ t \in CN}} \frac{\sigma_{st}(k)}{\sigma_{st}} \tag{2.2}$$

With betweenness values assigned to network nodes, a measure of flow (also called demand or more generally, load) has been obtained. However, the capacity of the nodes to transport such loads must be established as well. A common strategy used in the literature to address this requirement is the use of alpha-capacities (Motter and Lai, 2002; Dueñas-Osorio and Vemuru, 2009). These capacities $C_\alpha(k)$ are defined based on the estimations of load obtained from betweenness as shown in Eq. 2.3. This strategy defines alpha-capacities as the product of the original proxy flow measured through betweenness times a magnifying factor $(1 + \alpha)$ used to control the level of spare capacity for each analyzed network element. The value of the magnifying factor is controlled by the α parameter that comes to be associated to the added capacity.

$$C_\alpha(k) = (1+\alpha)O\text{-}D\,btwn(k) \tag{2.3}$$

This amplification strategy is adopted in one of the contributions presented in this thesis with the objective of modeling the impact of increasing local redundancy, or local capacity of components, on the control of the generation of cascading failures leading to increased systemic fragility.

2.5 A model for interdependence between networks

The previous discussion provided a description of cascading failures, a key phenomenon of internal damage propagation, along with a model for the approximation of its effects in urban networks' performance. This section addresses the issue of intersystemic damage propagation caused by the presence of interdependence. The external damage propagation between interdependent networks is called in this thesis *interdependence effects*.

A key result in the discussion of the effects of interdependence in networks was proposed by Buldyrev et al. (2010). These authors developed an study of cascading failures in interdependent theoretical networks subjected to random failures following an error tolerance approach similar to the one described in Section 2.3. Using concepts from network science and percolation theory, the authors measured the robustness of interdependent theoretical networks based on their ability to retain a surviving connected component of interdependent nodes after a series or random node removals. Their study concluded that the presence of interdependence made the interacting networks more fragile specially for the case of scale-free networks in which the original advantage of the presence of hubs for single networks became a liability as even nodes

with small degree could trigger a cascade of failures eventually spreading to the critical hub nodes.

This theoretical result illustrates the importance of considering interdependence as an element of internal perturbation beyond the consequences of the individual fragility of single networks. The change in the paradigm of the robustness of scale-free networks (strong to random failures; weak to targeted attack) was switched by the mere presence of interdependence, an unexpected factor that simply was not considered before as a critical element of infrastructure vulnerability analysis.

In the face of this development, it is important to highlight some crucial limitations in their approach. First, it is clear that the conclusions in their report are based on artificial models that represent only extreme cases of the potential results observed in real networks. A second point is that their representation of interdependence is executed through the use of additional links connecting nodes in different networks without any restriction on the ability of the link to propagate damage. Finally, the work measures systemic performance using the survival of a connected component, i.e., a group of nodes that remains connected, a metric that could be replaced by more informative strategies measuring the effectiveness of service in the aftermath of a perturbation.

These limitations of the theoretical model are addressed in the model used by this thesis for the description of systemic interdependence. Interdependence is described in this thesis based on the approach introduced by Dueñas-Osorio et al. (2007). In this approach, *interdependent links* joining nodes in different networks are used for interdependence description as shown in Fig. 2.3.

These interdependence links [Fig. 2.3(b)] are different from the internal links for each network in the sense that they represent feeding lines from suppliers in an ex-

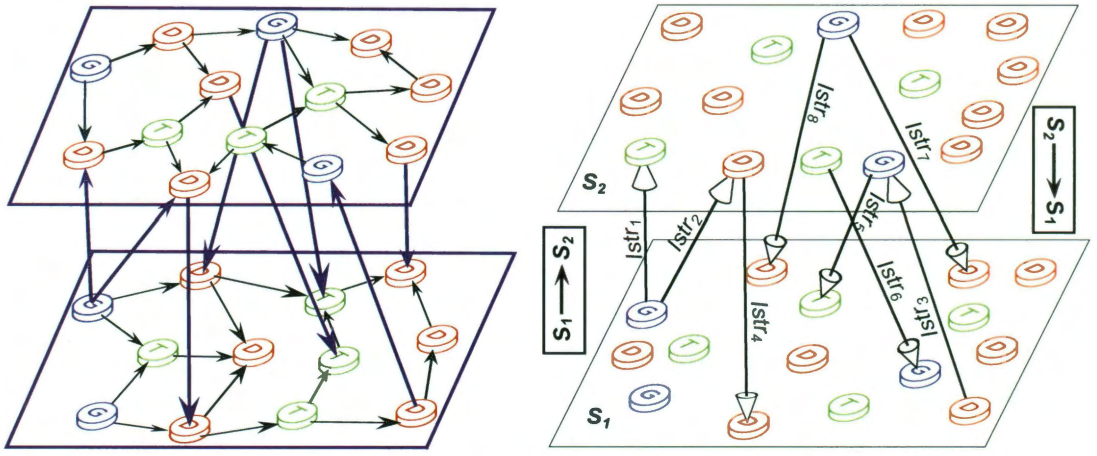

(a) Network and interdependence description (b) Interdependence interface

Figure 2.3 : Sketches representing (2.3(a)) urban networks and (2.3(b)) the interdependence model. A probability, $Istr$, is associated to each of the interdependence links to represent likelihood of damage transmission in the event of perturbation of the supplier node source of each interdependent link. S_1 and S_2 represent two distinct interacting urban networks.

ternal network to consumer nodes in the local network currently under consideration. Note that the supply provided in this way is more likely to be different from the one transported in the local network, but necessary for the normal operation of the recipient node. This dependence relationship is clearly represented in the use of the terminology of *master* node for the external supply link source (tail) of the interdependent link, and *slave* node for the terminal (arrow) consumer node in the local system. An essential feature of this interdependence representation is the association of an interdependence strength parameter $Istr$ to each of the interdependence links representing intersystemic dependence. This parameter is a conditional probability representing the likelihood of perturbation transmission from the external supply node to the local consumer node in the event of failure or disconnection of the master supplier acting as the source of the interdependence link. This relationship is de-

scribed in precise terms by Eq. 2.4, with F standing for the event of failure of a node, and *slv* and *mst* representing generic slave and master nodes in different networks, respectively.

$$Istr = P(F_{slv}|F_{mst}). \tag{2.4}$$

The collection of interdependence links between two networks is called in this thesis the *interdependence interface*. The representation of the connectivity structure of this interface is done by using interdependence matrices Im. Such matrices are similar to adjacency matrices as the existence of links is made explicit by adding a one in the associated entry to a master and supply node ordered pair. However, the matrix itself is rectangular in contrast with the square nature of adjacency matrices. This rectangular property is due to the fact that interdependence matrices associate one given network for the columns and a different network for the rows of the matrix, with both networks potentially having a different number of nodes. A key point regarding interdependence matrices is that two of them are required to represent the interaction between two networks, one for each direction of potential action. Fig. 2.4 illustrates this condition for a case of two small networks S_1 and S_2, one with four and the other with five nodes and a total of three interdependent links in the interdependence interface between the two.

The basic description of interdependence given thus far portrays the phenomenon of interconnection between networks as a rather negative interaction in which the intersystemic connection becomes a pathway for damage transmission. However, interdependence can be interpreted in a more positive light when the possibility of having more than *one* external supplier comes into consideration. For some studies,

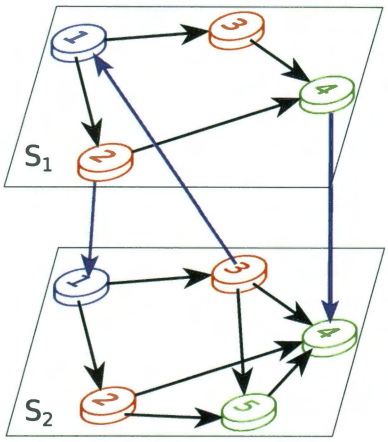

$$Im_{S_1 \to S_2} = \begin{bmatrix} 0 & 0 & 0 & 0 & 0 \\ 1 & 0 & 0 & 0 & 0 \\ 0 & 0 & 0 & 1 & 0 \\ 0 & 0 & 0 & 0 & 0 \end{bmatrix}$$

$$Im_{S_2 \to S_1} = \begin{bmatrix} 0 & 0 & 0 & 0 \\ 0 & 0 & 0 & 0 \\ 1 & 0 & 0 & 0 \\ 0 & 0 & 0 & 0 \\ 0 & 0 & 0 & 0 \end{bmatrix}$$

Figure 2.4 : Illustration of the concept of interdependence matrices for a case of two small interdependent networks. Interdependence matrices are rectangular, unlike adjacency matrices, in order to describe the interaction between networks of different orders.

in particular those related to the modification of the interdependence interface structure, an alternative paradigm for the interpretation of interdependence definition and its strength probability becomes useful. Under this perspective, a new paradigm of *failure avoidance* replaces the original model of *failure transmission* (Fig. 2.5).

The failure avoidance paradigm understands interdependent links as pathways to alternative suppliers of the external resource required by a local component for its normal operation. Note that this definition does not alter the fact that all alternative sources of a single external resource may interact as regular elements of an external network, and it does not constrain the possibility that a local node may require different types of flow from different networks. Note that the definition of the interdependence strength probability does not change, but the new interpretation shifts the association of the $Istr$ parameter from the interdependent links reaching a dependent node to the node itself [Fig. 2.5(b)]. In simpler terms, this shift means

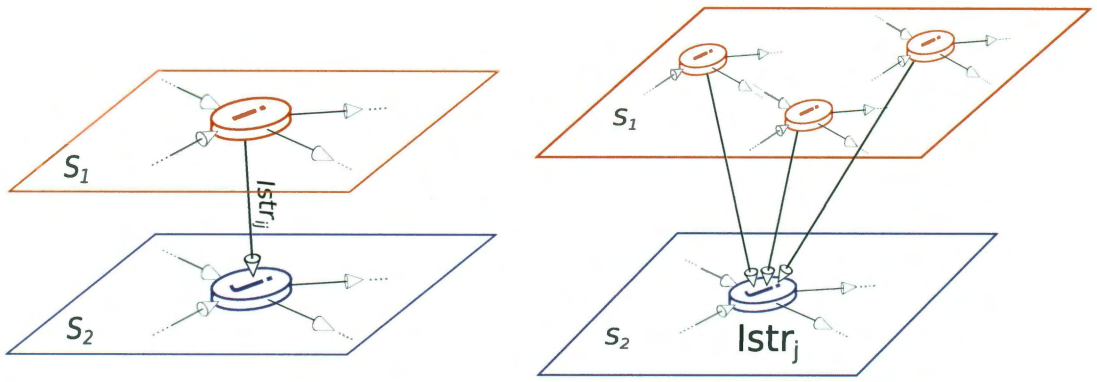

(a) Failure transmission paradigm

(b) Failure avoidance paradigm

Figure 2.5 : Alternative interpretation paradigms for interdependence and interdependent damage propagation in urban networks. The *failure avoidance* paradigm allows a direct identification of the $Istr$ parameter with the probability of failure of redundancy and backup systems at the dependent node

that a node will be exposed to the possibility of interdependence-caused failure only when *all* of its alternatives suppliers of a required resource fail in an external network. This byproduct of the new paradigm implies an implicit reduction on the likelihood of interdependent damage propagation originally described uniquely by the magnitude of the interdependence strength parameter $Istr$. This new interpretation allows a direct identification of the values of the $Istr$ parameter with the probability of failure of redundancy and backup intended to serve a dependent node in the event of failure of the main providers in external networks. A similar interpretation for the original paradigm was proposed by Kim et al. (2009) in their review of the developments proposed by Dueñas-Osorio et al. (2007).

2.6 The concept of fragility and fragility of components

The phenomena of cascading failures and interdependence-induced damage introduced in the previous sections describe scenarios of damage propagation resulting from component interaction within and between networks, respectively. Such phenomena are naturally conditional on the properties of an initial perturbation disrupting the regular operation of stable networks. The concept of fragility attempts to explicitly consider such conditional nature and the expected response of network components subjected to perturbation.

Fragility is defined here as the probability of a component or system under study to exceed a specified performance level under the action of a perturbation of known intensity. In mathematical terms, fragility can be defined using the expression in Eq. 2.5.

$$F(k) = P(S(k) \geq S_o | h = h_o) \tag{2.5}$$

In this equation, $F(k)$ is the fragility of the component k; $S(k)$ is the status or performance of the component k when subjected to a perturbation h of intensity h_o; and S_o is a performance level, target status, or maximum allowable damage state pre-established by the conditions of the analysis or operation of the component.

The fragility of components is commonly specified in the literature using fragility curves (Mosleh and Apostolakis, 1986; Shinozuka et al., 2000; Ellingwood et al., 2004). These curves describe the change in the probabilities of exceedance for the studied component as a function of increasing values of a perturbation. Shinozuka et al. (2000) describe two approaches for the estimation of fragility functions for earthquake events – the perturbation of interest for the developments in this thesis. A first

approach for component fragility estimation is the use of failure reports obtained from earthquake events or from direct experimentation. A second approach is the use of numerical simulations, specifically subjecting computational models of the infrastructure element of interest to the action of artificial or recorded perturbations with the desired intensity characteristics. The use of either approach depends on the nature of the analysis and the availability of information and resources for the execution of the study.

An additional source of generic fragility information for infrastructure networks is Hazus-MH (Federal Emergency Management Agency, 2003). Hazus-MH is a methodology for the estimation of potential losses from selected natural hazards (earthquakes, hurricanes, and floods) developed by the Federal Emergency Management Agency, FEMA. The technical manuals of Hazus-MH provide lognormal models for fragility curves of typical critical components of diverse infrastructure systems ranging from oil transportation systems to power networks. The models of fragility curves in Hazus-MH consider four possible limit states of damage for the performance of components under perturbation: slight, moderate, extensive, and complete (Fig. 2.6). The concept behind these states is that a stakeholder will choose one of such limits as the condition defining the *failure* of a studied component. In simpler terms, the selected state is such that the component is considered failed if its response under perturbation is beyond the specifications of the limit state's definition. This concept is of critical importance because the selection of a state defines the magnitude of the probabilities of exceedance for network components; values that in turn exert a critical influence on the magnitude and characteristics of system-level fragilities. Finally, it is important to understand that even though Hazus-MH concepts for fragility representation have been followed by different authors in the literature (Shinozuka et al., 2000; O'Rourke

and So, 2000; Nielson and DesRoches, 2007; Padgett and DesRoches, 2008), fragility curves from Hazus-MH must be used carefully as they are designed to be used at the national (US) level. Studies for specific cities may choose to generate their own fragility curves to better reflect local conditions of both vulnerability and hazard. In this thesis, the limit state used in the results in this thesis was *extensive*. This limit state represents a condition in which the component results with a level of physical damage that makes it unavailable and unable to restore it back to service or replace it in a short period of time.

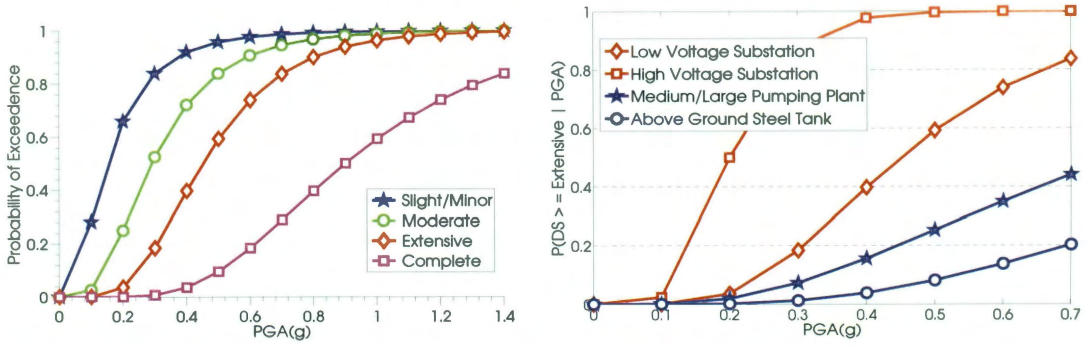

(a) Fragility curves and limit states

(b) Fragility curves for power network elements

Figure 2.6 : Examples of fragility curves from Hazus-MH. Fig. 2.6(a) illustrates the changes in lognormal fragility curves associated to different performance levels of generic components. Fig. 2.6(b) shows fragility curves for different infrastructure components for an *extensive* limit state.

2.7 Emergence of systemic fragility

A basic target for the work presented in this thesis focuses on the characterization of the behavior of a network, its *systemic fragility* as a single entity, as it is influenced by external perturbation, internal weaknesses, and external interdependence effects. To address this point, a clear definition of the term systemic fragility must be given

first. Systemic fragility is the probability of a network as a whole exceeding a given undesirable, pre-established level of performance. This definition does not differ much from the definition for component fragility. However, the new definition has implicit a requirement not present for the case of components. While the response of node due to perturbation is specified as failure (0) or survival (1), network fragility is expressed as a continuous variable expressing the level of performance reduction after perturbation with respect to an initial systemic status.

A node under perturbation fails if its response falls beyond the specification of its assigned limit state. If that is not the case, the component survives. The situation for a networks is different. Of course, it could be the case that a decision-maker is interested only on the total failure or the complete survival of the network. However, given that urban networks cover extensive areas serving considerable amounts of people, the likelihood of an event of zero failures or complete collapse if of little interest for public stakeholders and private shareholders. Instead, the regular approach consists on estimating the expected probabilities of specified levels of partial *systemic degradation* in the event of perturbation. In simpler terms, the target for systemic fragility is the characterization of the probability of increasing levels of systemic performance degradation conditional on a given perturbation intensity.

Thus, this systemic fragility definition requires first the specification of a metric to evaluate systemic performance in the aftermath of a perturbation with the purpose of assessing the systemic degradation used in the definition of systemic fragility. Once the metric has been defined, the additional challenges are limited to the calculation of the metric itself and the design of a strategy for obtaining its probability distribution.

Measuring systemic performance requires the evaluation of the state of the network before and after perturbation. The comparison of these two states, initial and

final, provides a measure of the inherent systemic strength. The status of a network can be measured in multiple ways, but the existing alternatives can be classified into two major groups: *connectivity* approaches and *service-level* approaches. Connectivity approaches for systemic performance focus on exploiting the change in topological properties of a network under perturbation as a proxy to measure systemic performance degradation. Motter and Lai (2002), for example, use the size of the largest connected component left after perturbation as the metric of choice for measuring systemic performance in their study of the strength of critical infrastructure networks such as the Internet and the US power grid. Albert et al. (2000) used the diameter, that is, the average distance of connecting paths between nodes in the system, as the performance metric for their study on scale-free networks. A similar metric, efficiency, is used by Crucitti et al. (2004) in their study of cascading failures in networks. In another approach, Albert et al. (2004) used the connectivity loss metric, counting the reduction on internal connecting paths, for the study of the vulnerability of the US power grid.

The research highlighted above exemplifies the diversity of connectivity-based metrics in the literature. Their key advantage is the exploitation of topological information inherent in the graph representation, which results in efficient systemic performance evaluations. This advantage occurs as part of a trade-off against detailed insight into systemic behavior. Although connectivity approaches do provide important insight on the nature of the response of urban systems, they cannot provide, by their own definition, detailed information on how service levels specific to service types (e.g., pressures, current, etc.) will be affected during a perturbation. This trade-off makes conclusions obtained from connectivity approaches of interest and utility only for initial screening phases of infrastructure fragility studies directed

towards investment decisions.

In contrast to connectivity approaches, service-level approaches require, in addition to the topology of the system, information on service supply and demand levels, capacities, and transportation cost for different network components. All this new information is necessary to obtain a required approximation to a functional model of the system. In simpler terms, to measure perturbation effects on a network's service, it is necessary to be able to understand and predict the resulting flow status of a system after perturbation and that requires additional data sources. These functionality models can range from optimal flow models, such as the one implemented by Lee et al. (2007) in their study of service restoration for urban systems, to models involving the simulation of the physical properties and component behavior of utility systems as done by Nuti et al. (2007) and Mei et al. (2009).

From the descriptions above, it is apparent that service-level approaches lead to deeper insight into systemic performance. However, such insight is obtained at the cost of additional information (not always available), and computational cost. The approach followed in this research seeks informative estimations that can be enriched and updated at a fast pace, a requirement that becomes critical if simulation is used for the description of the probabilistic nature of systemic fragility. In such cases, the demand for computational resources is an important factor for the selection of an appropriate systemic performance metric.

For the test cases in this thesis, it was estimated that a connectivity approach was sufficient to illustrate the introduced methodologies. It is important, however, to highlight at this point that all the results in the test cases present trends that are likely to occur in real networks, but that detailed models of local conditions and more detailed description of systemic performance should be used for decision-making in real

infrastructure networks. Indeed, regarding the trade-off between insight detail and computational requirement of connectivity and service approaches, Hines et al. (2010) established that topological, connectivity metrics are not likely to match the insights obtained from service-based models in the case of real urban networks subjected to error and attack tolerance tests. This caveat limits the usefulness of connectivity based approaches, but not of the methodologies for probabilistic interdependence studies as developed in this thesis which can be equally used with service-based performance metrics if provisions of appropriate computational resources and necessary input data are available and taken into account.

The connectivity metric used in the case studies in this thesis is *Connectivity Loss* (CL), originally introduced by Albert et al. (2004). The definition of CL assumes that network nodes can be classified into three not mutually exclusive categories: supply nodes (SN, also called generation nodes), adding flow to the system; consumption nodes (CN, also called distribution nodes), extracting flow from the system; and transmission nodes (TN, also called transshipment nodes in the literature), acting as connection points between internal supply and consumption nodes. In the terms of the previous classification, Connectivity Loss is defined as the metric measuring the reduction on internal connection paths between supply and consumption nodes in a system after the action of a perturbation. Eq. 2.6 shows the mathematical expression of this definition. In this equation, $|CN|$ is the total number of consumption nodes in a network; CP_o is the original number of paths from the supply nodes to the consumer points; and CP_f is the final number of the same type of connecting paths surviving the action of perturbation.

$$CL = 1 - \frac{1}{|CN|} \sum_{i=1}^{|CN|} \left(\frac{CP_f}{CP_o} \right)_i . \tag{2.6}$$

Fig. 2.7 shows an example of the calculation of Connectivity Loss for a network under a simple perturbation. Fig. 2.7(a) shows the original network highlighting the connection paths from three supply nodes on the left reaching the three consumption nodes on the right. The total of nine paths use the three transmission nodes in the network as intermediate points.

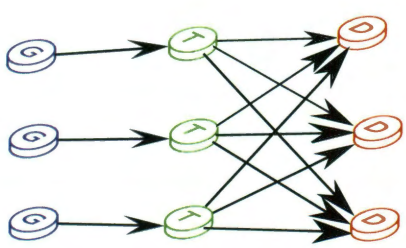

(a) Initial condition: $CL = 0.0$

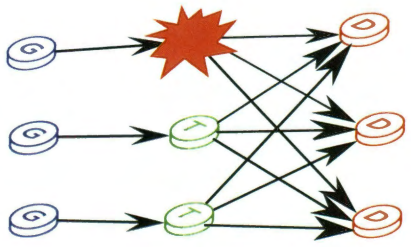

(b) Disabled node: connection reduction

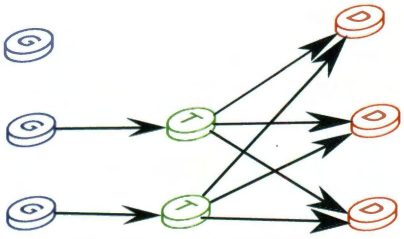

(c) New condition: $CL = 0.33$

Figure 2.7 : Example of Connectivity Loss CL calculation for a network of nine nodes with three elements in each of the supply, transmission, and consumption node sets. 2.7(a) initial condition; 2.7(b) perturbation; 2.7(a) resulting systemic status. CL associates the reduction in internal connecting paths between supply and demand nodes induced by an external action with the fragility of the network itself to the perturbation.

The previous CL expression allows the calculation of systemic performance degradation for a single event of perturbation. The final step towards the estimation of systemic fragility is the estimation of the mean performance degradation. In the case of systemic fragility calculated using Connectivity Loss, the problem rests on the

identification of connection paths and the estimation of their probabilities of failure. Unfortunately, the problem of finding all such labeled paths in a network is known to be an NP-hard (Non-deterministic Polynomial-time hard) problem, that is it is likely (although not yet proved) that no polynomial-time algorithm exists to solve the problem. Regardless of this fact, algorithms like the ones proposed by Abraham (1979), White and Newman (2001), and Li and He (2002) can address the task for networks of reasonable size. An interesting related strategy is proposed by Song and Der Kiureghian (2003) and developed further in Kang et al. (2008), which uses a linear programming technique to calculate bounds of systemic reliability. This procedure is dependent on the inclusion of failure scenarios in the objective function of the linear program and hence it requires the same type of failure path description as in the previous approach.

In this thesis the estimation of systemic fragility is executed using Monte Carlo simulation. The key advantage of using numerical simulation is its flexibility. As it will be shown in the next section, the simulation of interdependent network response to the action of seismic hazards requires the inclusion of different steps whose representation in analytical terms is not straightforward or possible. Simulation allows the integration of the action of initial perturbation with the subsequent phenomena of cascading failures and interdependence damage propagation in a way that its robust and conceptually simple to implement and verify in practice. Authors in the literature like Dueñas-Osorio et al. (2007), Ouyang and Dueñas-Osorio (2011b), and Poljanšek et al. (2012) have used this strategy with positive results. The steps involved on simulating damage evolution and measuring performance degradation required for the statistical estimation of systemic fragility are the topic of the next chapter, *Mitigation Strategies for Interdependent Seismic Fragility Control on Urban Lifelines Systems*,

and the first contribution of this thesis.

2.8 Mitigation actions in urban networks

Very few works have addressed the potential impact of modifying the structure of the interdependence interface between networks as a tool to decrease systemic fragility.

Winkler et al. (2011) studied the properties of generated network interfaces using centrality measures and their propagation role in the event of random failures and hurricane hazards. These authors found that interdependence configurations built based on centrality metrics can offer enhanced response to the action of hazards of importance for specific types of urban networks. In particular, they found that a power-water interface built using an efficiency-based principle showed levels of efficiency reduction, their performance measure, comparable to those observed in real networks under hurricane perturbation.

In another approach, Ouyang and Dueñas-Osorio (2011a) proposed an approach to design interdependence interfaces with the objective of reducing the likelihood of intersystemic cascading failures. These authors produced interface design strategies based on centrality and reliability approaches, testing the effectiveness and efficiency of such methods using a global annual cascade failure effect metric. An application of their techniques to a model of real interdependent power and gas networks subjected to random failures and hurricane hazard shows that reliability-based-designed interfaces perform better than models built based on Euclidean distances. This last result highlights the interaction between the role of interdependence as an enabler of cascading failures and the location of component fragility between individual networks.

These two approaches used general models to test the capacity of artificial interconnection interfaces on reducing the negative propagation effects interdependence

induces. This thesis proposes two conceptual alternative policies to mitigate interdependent systemic fragility. A first alternative, called component fragility reduction (CFR), decreases the component vulnerability to earthquakes by a fixed percentage of their initial value. The aim of this strategy is to address the underlying cause of interdependence, that is the fragility of the components acting as external suppliers to consumer nodes in other networks. A second alternative is called interdependence redundancy enhancement (IRE). This policy is similar to the ones described in the literature as its aim is to modify the interdependence interface as a mechanism to reduce the likelihood of fragility propagation between networks. However, IRE differs from previous approaches in its simplicity. This policy aims to reduce interdependence effects by adding alternative supply sources to dependent nodes in interdependent networks.

A key requirement in the execution of the conceptual policies discussed in this thesis is the need to identify critical nodes in interdependent networks. Indeed, both alternative policies, CFR and IRE, require the identification of the top most fragile or strong components. Under the complex networks approach such identification problem is associated to the importance of a node to the internal stability or efficiency of the network.

The problem of network centrality has been studied by many authors in the literature (Freeman, 1977; Barrat et al., 2008; Newman, 2010) However, this section concentrates on the two selected strategies to rank the importance of nodes in a network used in this thesis: 1. NodeRank and 2. Origin-destination (O-D) betweenness. NodeRank is a ranking strategy based on the PageRank algorithm developed by Page et al. (1999) and used by the websearch company Google. NodeRank builds upon the spectral formulation of PageRank and expands it to measure the importance of

network nodes based on the estimation of their degree of internal connectivity and their fragility against a considered hazard. The key principle to judge internal connectivity is the number of links (or degree) of a node combined with the degree of the nodes to which the same node is connected, thus assessing regional importance. The basic expression for PageRank is described by Newman (2010) as:

$$CR = \beta \left(\mathbf{I} - \alpha D^{-1} A \right)^{-1} \mathbf{1} \tag{2.7}$$

In Eq. 2.7, CR is a vector assigning a ranking to each of the n nodes of the given network. In the inputs, A is the network's adjacency matrix; D is a diagonal matrix of the outdegrees of the network's nodes; α is a scalar required to be smaller than the reciprocal of the maximum eigenvalue of AD^{-1}; $\mathbf{I}$ is the $n \times n$ identity matrix; $\mathbf{1}$ is a $n \times 1$ vector of ones; and β is a column vector of the relative importance of each node. NodeRank adapts the original strategy of PageRank and divides the ranking calculation into two steps. The first step uses a vector of ones for the β factor in Eq. 2.7 to estimate a degree-based ranking. In the second step, the obtained ranking is weighted by a vector of node fragilities according to the hazard under consideration. An additional modification used for the case of interdependent networks is the partial inclusion of interdependence links as part of the outdegree of master nodes. In order to balance the effect of these extra links their number was affected by an arbitrary 0.25 factor before being added to the number of links in the diagonal of D. This factor was included aiming to reflect the presence of interdependence links in the estimates of the importance of a node for the interconnected networks. Note that this value is arbitrary and can be adjusted as desired by the analyst in order to increase the weights of interdependence links in the analysis of importance.

The second ranking strategy, origin-destination betweenness (*O-D btwn*), measures the importance of a node based on the number of shortest paths connecting supply (origin) and consumption (destination) nodes that pass through the node under study. The results of the *O-D* betweenness count are weighted by the fragility of each node in order to arrive to the final ranking values used for the design of mitigation measures. This metric is based on the standard definition of node betweenness (Freeman, 1977), but the inclusion of the *O-D* and node fragility factors force the strategy to focus on the analysis of the critical supply-demand paths that drive systemic fragility.

2.9 Seismic hazard characterization for urban networks

The objective of this work is to address a challenge: the generation of network-consistent probabilistic seismic hazard scenarios to use for the estimation of interdependent systemic performance for risk assessment. The fundamental issue in the here is the generation of simulation scenarios adequate to the study of systemic fragility of networks, that is *network-consistent scenarios.* In this context, a seismic scenario is considered consistent when it includes the natural correlation, due to distances and soil conditions, of hazard intensities at different network sites expected to occur during an earthquake event.

In the topic of earthquake scenarios, Crowley and Bommer (2006) compared the effects of including hazard correlation by comparing loss estimates, total damage ratios in a distributed portfolio of buildings in Turkey, calculated using two competing approaches: an efficient PSHA-based approach (Probabilistic Seismic Hazard Analysis) and a more computationally demanding earthquake catalog simulation plan. The PSHA approach simply combines independent Annual Probabilities of EXceedance

(APEX) loss curves to generate the total loss curve of an spatially distributed portfolio of buildings in Turkey. The earthquake catalog approach generates independent seismic intensity maps that display earthquake effects as they simultaneously occur during an event, satisfying the requirement of inherent hazard correlation at different network sites. Although the annual average loss for both approaches was very close for a test case, Crowley and Bommer (2006) found that the two loss curves were not the same. Indeed, the APEX values for the PSHA curve were larger than those of the earthquake exceedance curve for most of the average damage ratios in the x-axis of the two curves (Fig. 2.8).

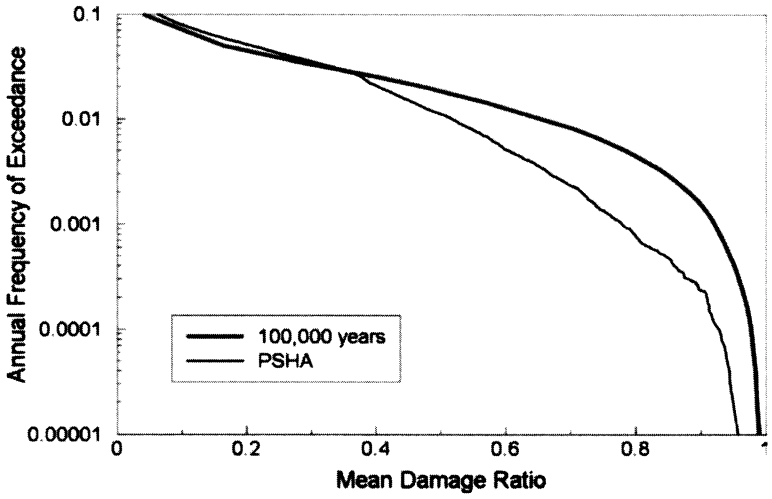

Figure 2.8 : Annual probabilities of exceedance curves for a portfolio of buildings as calculated by Crowley and Bommer (2006) for two competing approaches (regular PSHA and network-consistent hazard maps). The average losses calculated for the each curve are similar, but their behavior at different mean damage ratios (x axis) changes as the damage ratio increases.

The model for generating network-consistent seismic scenarios used in this work is adapted from Jayaram and Baker (2010). The original strategy uses the seismological properties of a fault system and Importance Sampling to generate stochastically

representative network-consistent seismic scenarios. Their fundamental innovation is the inclusion of a correlation structure for ground motion estimates, a factor omitted by previous research. Also important, the Importance Sampling procedure, adapted from (Kiremidjian et al., 2007), noticeably reduces the computational demand of the process of map generation.

The developments in Jayaram and Baker (2010) and Crowley and Bommer (2006) highlight the relevance of network-consistent seismic scenarios for the reliability of probabilistic estimates of network performance. The methodology in this paper adds to their insights by explicitly considering the systemic performance variability present in *each* of the single simulated hazard maps. The estimates developed for the case study in this paper use mean values of systemic performance for the calculation of the probabilities of exceedance instead of using the values of systemic performance obtained from a single damage simulation. This enhancement means that the proposed methodology directly takes into account the variability of network performances on the final probabilistic estimates, a development that allows, for the first time, the calculation of unconditional performance assessment for interdependence urban networks.

Chapter 3

Simulation of Damage Propagation and Interdependent Systemic Fragility

The definitions and developments in the previous section provide the general foundation for the first development in this thesis. In concise terms, the first research objective was to generate a methodology to describe the likely steps a network will withstand from the original inception of perturbation triggering component failures until a final stage of performance stabilization followed by complete collapse or reduced systemic functionality induced by the accumulated damage. The solution provided to this first task becomes instrumental to address a second challenge: the implementation of a practical simulation-based strategy for interdependent systemic fragility estimation.

This section builds upon the basics of the mechanisms of failure of components under perturbation (component fragilities), internal damage propagation induced by triggering damage (cascading failures), and interdependence effects on systemic performance (interdependence model for damage transmission). Such diverse mechanisms are incorporated into an articulated procedure that concludes with the estimation of systemic degradation, which, in the framework of a simulation program, relates to the calculation of systemic fragilities. An approach similar to the developed here but limited to individual networks can be found in Adachi and Ellingwood (2009b). The main developments described in this chapter were published in Hernandez-Fajardo and Dueñas-Osorio (2011).

3.1 Interdependent fragility assessment algorithm

This thesis addresses the first part of the described challenge, the generation of a methodology to describe the likely steps a perturbed urban network undergoes until reaching stabilization, by introducing the Interdependence Fragility Assessment (IFA) algorithm. The IFA algorithm specifies four interacting general operations for the estimation of interdependent systemic fragility (Fig. 3.1). The four operations are named as follows: 1) *Direct Hazard Action* (DHA), 2) *Internal Damage Propagation* (ODP), 3) *Interdependent Damage Propagation*, and 4) *Systemic Fragility Calculation* (SFC). The assumptions and implications used at each of these stages are explained in the following sections.

A differentiating aspect from this methodology is the inclusion of a *cycling stabilization* process for the assessment of performance degradation after seismic perturbation. Previous simulation-based research on damage propagation in networks used an approach that allowed only a single level of interactions between perturbed networks. Instead, the approach introduced here accumulates damage while allowing different cycles of interaction between the perturbed networks. The key abstraction underpinning this approach is that networks reach individually a status of partial stability that may be disrupted by the action of propagated external perturbation. In simpler term, this condition implies that simulated networks do not simply undergo the internal damage propagation (ODP) and external damage propagation (IDP) stages in a single decoupled step, but that they enter a process of joint stabilization in which damage occurring at the ODP stage triggers failures in the next IDP stage, which in turn leads to additional failures that disrupt the partial stabilization achieved by the networks after undergoing the previous ODP phase. This cycling stabilization process concludes when no additional failure is induced during either of

the interacting stages, a condition that can be reached in the same way by complete collapse of all infrastructure systems involved or by a status of reduced functionality in any or all of the interdependent networks.

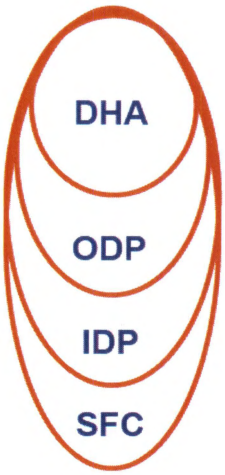

Figure 3.1 : Representation of the interaction between the basic operations of the Interdependent Fragility Assessment (IFA) Algorithm. The organization of the rings denotes the serial nature and complexity increase of the simulation procedure.

3.1.1 Direct Hazard Action (DHA) operation

The Direct Hazard Action (DHA) operation consists of the simulation of direct perturbation action on network components. Two precisions are required for this step, the first with regard to perturbation models and the second to the simulation of component damage. Regarding perturbation, this thesis focuses on the discussion of *seismic* fragility and seismic perturbation. Given the nature of the simulation strategy (Fig. 3.1), the characterization of the perturbation determines the features of the remaining operations and ultimately of the resulting fragility estimates. In this research, two approaches for seismic perturbation description are implemented. In

the first place, *seismic scenarios* are used for the generation of fragility estimates conditional on the properties of such scenarios. A seismic scenario provides a collection of seismic intensities (ground or spectral parameters) that can be used directly in combination with the component fragilities for the simulation of systemic status. The advantage of using scenarios rests on the control of the nature of the perturbation which is exercised in the selection of the representative magnitudes of the perturbation intensities used as input for the IFA procedure. The main limitation of using scenarios is that given their conditional nature, seismic-scenarios-based results can be used mostly for illustration purposes, especially for the communication of potential consequences to non-technical communities or as exploration tools before fully detailed, more complex, and closer-to-reality fragility assessments take place.

The second approach to seismic perturbation is the use of seismic hazard in the form of *probabilistic seismic hazard maps*. This last term stands for seismic intensity maps whose probability of occurrence is known as the result of the analysis of the seismogenic sources that originate them. Fragility analysis executed using this approach are unconditional on perturbation magnitudes and thus can be directly used for seismic risk estimation and decision making purposes. The main constraint associated to the use of seismic hazard maps is its considerable computational demands when used as input for a simulation program.

In spite of this limitation, decision-making dependent on the study of the impact of seismic perturbation on systemic fragility must be carried out using the unconditional type of estimates created by this last approach. Regarding the description of seismic perturbation, the IFA algorithm is independent of the either choice as it will operate without discriminating the sources of perturbation. This statement implies that superior layers of implementation routines must be developed to handle the differences

of the procedures using seismic scenarios or seismic hazard maps. In simpler words, the usage of the IFA algorithm under different approaches requires additional computational routines to guarantee that proper inputs are feed to the procedure, while the IFA procedure itself, and the assumptions used for its development, remains valid for any of the two approaches used for seismic perturbation description.

The second point of order for the Direct Hazard Action (DHA) stage is the nature of the component failures to simulate. First, failure is understood as a binary process. A component either fails or survive, and partial response values are not considered as the selection of a performance limit defines a boundary for the expected behavior of the component. This point means that even though in reality a component may provide some service, if that level of service is inferior to that specified in the performance limit, the component will be marked as failed, following the binary approach followed in this methodology. Note that this criterion is created by the use of fragility curves and must be clearly understood by analyst and decision makers. Second, both nodes and links can fail in a network under perturbation; however, in some cases it is possible to focus the failure simulation in components with the largest share of fragility. Shinozuka et al. (2007), for example, uses such strategy concentrating on the simulation of the fragility of nodes, such as power network facilities, with the objective of simplifying the study of the fragility of power networks. In some other cases, and depending on the nature of the network, such simplifications may impair the accurate characterization of systemic fragility. Note that any type of decision regarding the characterization of damage for the simulation will have an impact on the storage structures and computational demands of the simulation procedure. Such demands must be explicitly accounted by the analyst.

Once a decision has been made on the type of seismic perturbation description to

use and the component failures to simulate, the Direct Hazard Action (DHA) operation can be executed (Fig. 3.2). DHA works simultaneously for all networks and all components involved. For each network element, DHA takes the seismic intensity associated to the provided seismic intensity map as input to establish the probability of failure of components using component fragility functions and their assigned performance levels. For the results presented in the case studies in this thesis, the fragility functions were adapted from Hazus-MH (Federal Emergency Management Agency, 2003) using an *extensive* limit state associated to considerable physical damage of the component that does not imply total collapse but forces the element to be offline for at least more than one week after the perturbation's occurrence.

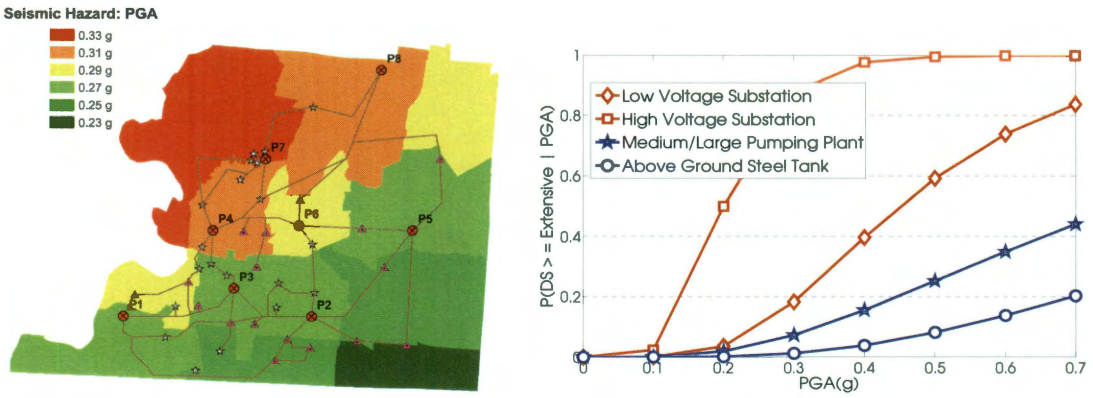

(a) Seismic intensities

(b) Fragility curves

Figure 3.2 : The Direct Hazard Action (DHA) operation of the IFA algorithm uses the intensities of provided seismic maps as input to determine component probabilities of failure from fragility curves. Bernoulli trials determine the status of failure or survival for each of the network components.

Once the probabilities of failure (pof) are obtained from the fragility curves for each component, a Bernoulli random trial (Papoulis, 1991) for each of the networks components takes place. If the random number is larger than the value of the com-

ponent's pof, the component is considered to have survived the effect of the assigned seismic intensity; if the opposite happens, the component's status is updated to failure. The outcome from the DHA operation is thus a binary vector of zeros and ones if only nodes' status are simulated or a binary data structure (a matrix of a cell) when both nodes and links' failures are considered.

3.1.2 Internal Damage Operation (ODP) operation

The vectors or status matrices from the DHA operation are used as an input to evaluate internal damage propagation within each of the independent nodes considered in an interdependence simulation. Two mechanisms are considered in this thesis: *disconnection failures* and *cascading failures*.

Disconnection failures

Disconnection failures occur when surviving network components from the previous stage (i.e. nodes that survived the simulated seismic action) are left isolated from the surviving portions of the system. The main concern regarding nodes in such condition is that they are not available to receive or pass load continuously to other components and hence are failed for all operational purposes. This failure is detected internally by the network if a flow model is executed. However, for graph-based representations, such failures must be detected by searching operations on the surviving network's topology.

Fig. 3.3 shows the basic mechanism of disconnection failures. The key point of these figures is that actual node disconnection is not so much as disconnection from other surviving nodes but rather their disconnection from surviving supply sources. In simpler terms, a surviving node fails if in the resulting surviving network after

perturbation it is left isolated from *all* potential supply sources. If at least one path from the node under study to one of such sources survives, the node will not fail due to disconnection. Note that this disconnection rule is solely topological and does not consider the potential event that flow may not reach the element in question even if the connection path exists. This limitation of the detection strategy is eliminated trivially when flow models are considered.

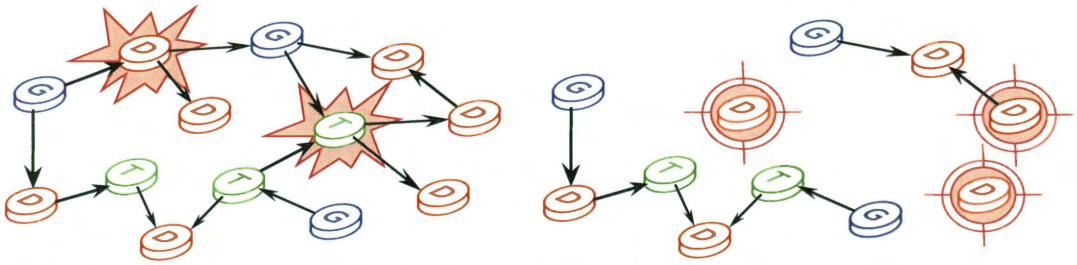

(a) Initial failures (b) Disconnection failures

Figure 3.3 : Occurrence of disconnection failures of surviving components induced by perturbation action. The perturbation in 3.3(a) has the effect of removing the only effective connectors of the three nodes marked in Fig. 3.3(b) leaving them isolated and hence offline.

The detection rule for disconnection nodes in a graph model must resort to a search algorithm on the network topology. Several alternatives may be used for this purpose (e.g., Breadth-first search, Dijkstra's algorithm, Bellman-Ford algorithm). This thesis uses Dijkstra's algorithm (Dijkstra, 1959) for all searches in networks. Dijkstra's algorithm is used here mostly for its versatility, specifically as it is used in this research for identifying node disconnection, calculating Origin-Destination betweenness for nodes, as well as systemic Connectivity Loss. The fundamentals of the search executed by Dijkstra's algorithm can be found in any standard textbook on algorithms [e.g. Ahuja et al. (1993)]. In general terms, the algorithm uses a label-based heuristic to find distances and predecessors in directed graphs with non-

negative link weights, as it is the case for real urban networks whose link weights correspond to the length of the connecting elements between infrastructure facilities. At the beginning of the execution, the algorithm labels all nodes with ∞ as their distance label, with the exception of the user-defined source node which is marked with a zero distance label. The detection of a source for a cycle is done by finding the node with the minimum distance label, i.e., the node with the smallest cumulative distance from the source node. Naturally, at the beginning of the execution this source is the user-defined source node itself.

The search progresses by traveling within the network using the links of the current source node as described in the adjacency matrix of the network under consideration. Note that the adjacency matrix entries (usually zeros and ones) can be easily replaced by the actual lengths of the links connecting each source with its neighboring nodes to make the algorithm use actual distances between facilities. Note that although for this case the link weights are distances, other plausible weights could be transportation costs or any other measure reflecting the difficulty of moving flow within the network under study.

The key step in the search from a source is the update of the distance-labels of the terminal nodes, which originally equal to ∞ are updated to be equal to the sum of the distance label of the predecessor node reaching the target terminal node in the current updating cycle (current source) plus the distance of the connecting link. In this context, the expression *updating cycle* refers to the series of distance-label updating operations occurring before a new temporal source is identified. Of critical importance, this distance label update occurs only if the updated distance is smaller than or equal to the original label for the terminal node. Once all possible terminal nodes are explored and their distance labels are updated, a new source is identified

by finding the node with the minimum distance label. The node so detected becomes the new source and the label updating process starts anew. The described updating rule for distance labels is the local minimization heuristic at the core of the Dijkstra's algorithm and is an instance of the application of the Bellman's optimality principle which states that "an optimal policy has the property that whatever the initial state and initial decision are, the remaining decisions must constitute an optimal policy with regard to the state resulting from the first decision" (Bellman, 1957).

Two issues of importance in the previous description are: 1) how to retrieve the connecting path itself from the original source to a node of interest and 2) the termination criterion for the label-updating process. First, the path retrieval can be executed after the process concludes using a predecessor list that specifies the *last* source node that updated the label of a terminal node. This list is initialized as a zero vector and is constantly updated during the search. Once the algorithm finishes, any given path, and if required the full shortest-path tree rooted at the source node, can be found using a backwards search using the entries of this predecessors vectors and stopping only when the root source node is reached.

The second issue, the termination criterion for Dijkstra's algorithm, can be specified by the user, but in general terms and for the purposes of this thesis the label-updating process concludes when all network nodes have been used as temporal distance-label updating source. In order to use this criterion, an auxiliary list of visited nodes is required. The connection of the criterion with the problem of node disconnection detection is that no source node will be able to update disconnected node labels and hence two events take place: a) the distance label of the disconnected node remains unchanged and equal to ∞ and b) due to its high distance label, the disconnected node will be visited last and its entry in the predecessor vector remains

unchanged and equal to zero. The first event, unchanged distance label equal to ∞, in particular is unique for disconnected nodes (the predecessor entry for the original source is also zero in the second event) and is used in this research to detect nodes disconnected from surviving supply nodes. Naturally, the detection of full disconnection of a node as specified by the definition given above requires the shortest path tree for *each* of the surviving supply nodes. If the list formed by the distance labels of a node obtained using the surviving supply nodes as a source is filled only with ∞, the node is concurrently isolated from all supply sources, what is equivalent to disconnection and an offline status for the component.

Cascading failures

Disconnection failures represent the first level of damage propagation occurring internally in networked systems. It is also a simple mechanism that causes no additional physical damage but loss of functionality for the affected component. As introduced in Chapter 2, cascading failures are a more complex phenomenon involving the interaction between the capacity and the load of components surviving the combined effects of initial seismic damage and disconnection failures.

The main definitions for the simulation of cascading failures were introduced in Section 2.4. The key assumptions in the definition of cascades are the use of a proxy flow on the networks' graph representation and the use of an origin-destination betweenness centrality metric (*O-D btwn*) as reference for both the demanded load and the available capacity of each of the network nodes. Note that the origin nodes referred in the metric are the supply nodes of the network while the destination nodes are the consumption nodes of the same system.

If the classical definition of betweenness is used, tools like the Brandes algorithm

(Brandes, 2001) could be used directly for its calculation. However, the use of *O-D btwn* implies that a different procedure must be used, as the connecting paths to explored are limited to those connecting the supply and consumption nodes in the network under study. The betweenness centrality metric always requires finding connecting paths for its calculation. This thesis uses Dijkstra's algorithm for obtaining such paths. The operations and outputs of this algorithm have been described in the previous section and are used in the same way for the *O-D btwn* calculation. The basic difference in the use of the outputs between the betweenness and disconnection evaluations is the need to retrieve the connecting paths' structure to use them in the post-processing operation counting the number of paths using a particular node as an internal traversing point.

Running Dijkstra's algorithm using each network supply node as the root of the search generates a shortest path tree listing the nodes that need to be traversed from a given source to the destinations of interest (the network consumption nodes). As pointed out before, Dijkstra's algorithm returns a list of predecessors and a list of distance-labels. However, in a key difference, the distance labels were instrumental in disconnection evaluation but it is the list of predecessors which is essential for the calculation of betweenness. Using a backward search from one of the network destination nodes, the structure of the connecting path from destination to source (in that order) is retrieved. Note that the first check for a destination node is to review its distance label entry. If it is equal to ∞ the node is disconnected and the betweenness evaluation must pass to the next destination node. If the node is connected, the backwards search proceeds to retrieve the connecting path structure until the entry with the label of the source node is reached. At each step of this backwards search, an auxiliary vector updates the count of the number of times a

node has been used in a connection path. When all paths for all origin-destination couples have been examined, this auxiliary path-counting vector contains the final path-traversing amounts that are used for the calculation of the *O-D btwn* values.

Two types of *O-D btwn* values are obtained in the IFA algorithm process. The first type is obtained using the pristine condition of each network in such a way that the *O-D btwn* values so calculated are associated to the conditions of flow existent before the onset of perturbation. The second type of values is obtained at every iteration of the IFA process. These values aim to represent the changing flow patterns induced by the removal of components caused by damage simulation from previous IFA operations (DHA, ODP, and IDP). These betweenness values are calculated using a modified adjacency matrix reflecting the cumulative damage of the process, that is a copy of the original adjacency matrix whose entries have been changed to reflect the failure of network links and nodes under the cycling stabilization process. Damage caused by cascading failures is then simulated by comparing the load passing at every stabilization cycle through a node with its alpha-capacity which is calculated as the product of the alpha factor and the original betweenness values obtained from the pristine network condition. Eq. 3.1 brings back the original alpha-capacity calculation expression from Chapter 2 (Eq. 2.3).

$$C_\alpha(k) = (1+\alpha)O\text{-}D\,btwn(k) \tag{3.1}$$

Alpha capacities are used for the purpose of testing the effectiveness of a type of mitigation action called *local redundancy enhancement* (LRE). The strategy inherent in the LRE policy is that enlarging the capacity of network nodes will allow them to cope with surges in demand caused by instability in other network areas. This policy

is implemented by using the α parameter in Eq. 3.1 as a tunable variable with values ranging between 0.25 and 1.5. It must be noted that α can be readily applied to network links; however, for the sake of simplicity, the LRE policy was applied only to nodes in the illustrative examples of this thesis.

3.1.3 Interdependent damage propagation (IDP) operation

The interdependent damage propagation (IDP) operation takes place after the two previous operations (DHA and ODP) have been executed and the simulated networks reach stable conditions. The previous statement requires the interaction of the two operations of internal damage propagation (disconnection and cascading failures) which means that they feed damage into each other until no further damage is created in a process identified here as *cycling stabilization*. This condition of no additional damage is equivalent to local stabilization at the level of independent networks. Naturally, such stabilization can be reached by local absorption of failures under reduced functionality conditions or by total collapse of the simulated interacting networks.

With internal stabilization achieved, the propagation of interdependent damage begins. First, and for each network, failed nodes are detected. According to the interdependence paradigm used (the discussed *failure transmission* or *failure avoidance* paradigms), the next step includes an identification of failed nodes with outgoing interdependent links (i.e. interdependent links using the failed node as a source in the case of the *failure transmission* paradigm) or the confirmation of the survival of at least one of the supply source nodes for a dependent node in an external network (for the *failure avoidance* paradigm). Clearly, the detection procedures require different implementation routines, but once they have been executed and it has been determined that a dependent node is exposed to interdependent damage, the simulation

that concludes the process is the same. Indeed, an exposed node under any of the two approaches is subjected to a Bernoulli random trial to determine its survival or failure due to interdependence effects. For this purpose, the random trial uses the associated $Istr$ parameter as the decision threshold dividing the failure and survival zones in the [0 1] interval. If the drawn pseudorandom number is smaller than the $Istr$ value, the dependent node is considered failed due to interdependence effects. If the drawn value is larger than $Istr$, it is considered that the dependent node managed to survive the failure of its supplier node(s) in the external system under consideration.

Implicit in the previous procedure is the fact that a node that is dependent on different systems must undergo this process of review of the status of its external suppliers and eventual status determination tests for each of its supplier networks. This fact implies that a node can fail due to the absence of at least one of the supply types it requires for its regular functionality as expected to happen in real urban infrastructure networks.

The previous description relates to the simulation of interdependence failures; however, the simulation of the interaction between urban networks as entities brings additional challenges. The key concern on the description of network interdependence simulation is how networks interact and specifically how interdependent failures are communicated between networks. This thesis assumes an instantaneous communication and failure propagation across systems such that for a number of networks, ns, all of them simultaneously affect each other with no explicit hierarchy of interaction. This assumption facilitates the computational implementation discussed in this thesis because it assures that the state of a network will not be updated in the middle of a general cycle of interdependent failure propagation. Such partial update may occur when it is considered that some network pairs (or triads, quartets, or larger groups)

interchange information at a faster rate than others. Indeed, the consideration of different communication speeds opens the door to the need to examine different configurations of failure propagation that are combinatorial in number, a possibility that increases the demand of computational resources.

Note that the instantaneity assumption does not mean, as it may appear, that damage is instantly reflected in the status vectors of an affected network during a stabilization cycle. Quite the opposite, the assumption enforces the use of an auxiliary structure for each network whose entries record interdependence-induced failures independently of which external system caused the event. When all networks have been examined at the end of an interdependent damage propagation cycle, that is when all interdependence effects have been tested and propagated, the contents of these auxiliary structures are combined with the status data structures of the previous cycle to arrive to the resulting damage contents to use in the following stabilization cycle if additional damage is detected. The strategy of recording interdependent damage data without attaching it to a particular master network source guarantees no partial updating in the status of a network and a focus on final network status, i.e., the final network status resulting at the conclusion of the cycling stabilization process, rather than on the causes of such status. This outcome represents a certain loss of information but it provides a trade-off and intuitive mechanism for the simulation of intersystemic interaction in the environment of interdependence-induced damage. In an exploratory work, the author compared interdependent fragility estimates generated using different mechanisms controlling the order of network interaction under interdependence damage for a test using three interdependent urban networks. The results obtained from such test showed only marginal differences between the estimates generated under the different approaches.

Before moving to the last operation of the IFA algorithm, it is important to emphasize that the presence of interdependence acts as an internal perturbation agent triggered as a byproduct of the internal rearrangement that follows after a perturbation. As discussed, interdependence effects are examined only after the collection of simulated systems as a whole has reached an stable condition. This partially stable condition can change because of the external interactions brought into picture by interdependence. It is clear that if interdependence damage is produced, the process in IFA cannot finish. Instead, the new damage condition produced by interdependence will be used to replace the triggering effects originally associated to the simulation of seismic action in the DHA operation. This connection means that the process of stabilization is cyclical and that the cycling persists until all networks have been through the three damage-adding stages of IFA (and in particular the interacting ODP and IDP IFA stages) with no damage being added with respect to the previous stabilization cycle. Once this last event takes place it is considered that the whole macrostructure of interacting networks has arrived to a joint stable condition. It is at that point that the IFA algorithm can move to its final operation of systemic fragility assessment.

3.1.4 Systemic Fragility Calculation (SFC) operation

This stage consists of the computation of the degradation of performance experienced by the simulated networks after the effects of the three previous IFA operations: DHA, ODP, and IDP. The degradation of performance is measured here using the Connectivity Loss (CL) metric, based on the connectivity approach for measuring performance.

As for the cases of disconnection and cascading failures, the key concern in calcu-

lating CL is the identification of connecting paths. However, unlike the betweenness calculation, the interest here rests on the survival of connections rather than in the actual retrieval of the path structure between supply and consumption nodes. In this sense, this task is similar to the disconnection test in the ODP operation, but its scope is limited to the original network consumption nodes as stated in the CL definition in Section 2.7 recreated here in Eq. 3.2.

$$CL = 1 - \frac{1}{|CN|} \sum_{i=1}^{|CN|} \left(\frac{CP_f}{CP_o} \right)_i \tag{3.2}$$

Two factors must be considered when evaluating this expression. First, for each of the simulated networks, the CP_o variable representing the original count of connecting paths for each of the network consumption nodes must be calculated using the pristine information in the unaltered adjacency matrix of the network. The path data so calculated does not change during the execution of the IFA algorithm and hence it can be computed before the algorithm starts. The second factor is that the CP_f variable representing the final count of connecting paths for each of the network consumption nodes must be recalculated after the end of each IFA simulation, that is after the DHA, ODP, and IDP operations have been exhausted by the simulated networks.

For a given consumption node, CP_f can have three possible values: $CP_f = 0$, if the node failed or was left disconnected from the remaining portions of the network; $CP_f = CP_o$ if all its connecting paths survived; or a value $0 < CP_f < CP_o$, describing a condition of partial loss of connection from its original internal suppliers.

The actual value of CP_f is determined in each of the three cases above executing Dijkstra's algorithm with each of the *surviving* supply nodes as a root. Note that

if a supplier fails, no search run is required, but the lost of the connection paths is nevertheless recorded.

In order to illustrate the calculation of CL consider an scenario in which the condition of CP_f is the same for all the network consumption nodes. Under this assumption, the first outcome ($CP_f = 0$) produces a CL equal to one, expressing full loss of the original connectivity between internal consumer points and supply sources. If the second condition occurs, ($CP_f = CP_o$), the CP ratio is one and CL is equal to zero, an outcome stating that the path count and therefore the network functionality was not affected by the seismic perturbation. Finally, if the third outcome ($0 < CP_f < CP_o$) is extended to all consumption nodes, the resulting CL value will be in the range between zero and one, closer to either extreme according to the reduction of connecting paths induced by the seismic perturbation.

3.1.5 Sequential description of the Interdependent Fragility Assessment (IFA) algorithm

The previous sections described the basic operations of the IFA algorithm while emphasizing the internal calculations required at every step. This section presents a sequential algorithm that compiles those in the form of the pseudocode in Algorithm 3.1.

Three aspects are worthy of highlight in this pseudocode. First, the triggering hazard action (the DHA operation) is the shortest and simplest of the four operations, an outcome that reflects the fact that simulating seismic damage in the network components does not demand much resources in comparison with the other operations. Note that although the DHA operation is computationally inexpensive, the routines required to simulate seismic hazard demand much information and require a series of

Algorithm 3.1 Interdependent Fragility Algorithm (IFA)

```
 1: Load descriptions for all urban networks models
 2: for i = 1 → number_of_networks do
 3:     Simulate Direct Damage on components                    ▷ DHA operation
 4: end for                                                     ▷ lines 2-4
 5: if at least a single component failed then
 6:     while At least one new component failure occurred do
 7:         for i = 1 → number_of_networks do
 8:             while Internal Damage Propagation occurs do     ▷ ODP operation
 9:                 Estimate disconnection failures             ▷ lines 7-13
10:             end while
11:             Estimate cascading failures
12:             Update system's damage status
13:         end for
14:         for i = 1 → number_of_networks do
15:             for each slave node in the network do
16:                 if all its master nodes failed then
17:                     Simulate interdependent damage propagation  ▷ IDP operation
18:                     Accumulate external damage effects      ▷ lines 14-22
19:                 end if
20:             end for
21:         end for
22:         Propagate interdependent damage effects
23:     end while
24:     Calculate systemic performance                          ▷ SFC operation
25: else                                                        ▷ line 24
26:     No systemic degradation. Systemic performance = 1.0.
27: end if
```

operations that increase their computational expense specially in the framework of Monte Carlo simulation.

Second, the use of iterations is widespread (lines 2, 6, or 8, for example) in this implementation algorithm. This fact reflects the interactive nature of simulating processes of damage propagation and stabilization after perturbation. In this regard, note that the main body of instructions, including the second and third IFA operations (ODP and IDP), are part of a larger stabilization cycle starting at line 5 and ending

at line 23.

Finally, it must be clear that these instructions (line 5 to line 23, the cycling stabilization process) represent the bulk of actions during *one* simulation with a fixed seismic scenario along with fixed values for the α parameter for cascading failures and $Istr$ probabilities for interdependence effects. This fact means that the IFA algorithm will be applied in successive simulated perturbation scenarios until the statistical analysis of the resulting CL list provides stable estimates of the mean and standard deviation of the resulting systemic fragilities.

3.2 Case study 1: Systemic fragility of interdependent power and water networks under seismic scenarios

This case study discusses numerical results of the application of the IFA algorithm for the estimation of the systemic fragility of simplified yet realistic models of power and water networks subjected to seismic scenarios and interdependence effects. The tasks in this case study cover three majors areas: description of seismic perturbation, network and interdependence properties, and numerical results.

3.2.1 Seismic perturbation

The seismic perturbation used in this test case is based on the seismology of Shelby county in Tennessee as analyzed by Dueñas-Osorio et al. (2007). The Shelby county area has received attention in previous research (Shinozuka et al., 1998; Adachi and Ellingwood, 2009b) due to the hazard created by the New Madrid seismic zone [Fig. 3.4(a)] and the vulnerability of a densely populated city, such as Memphis (Elnashai et al., 2009).

This test case uses seven seismic scenarios labeled according to the maximum

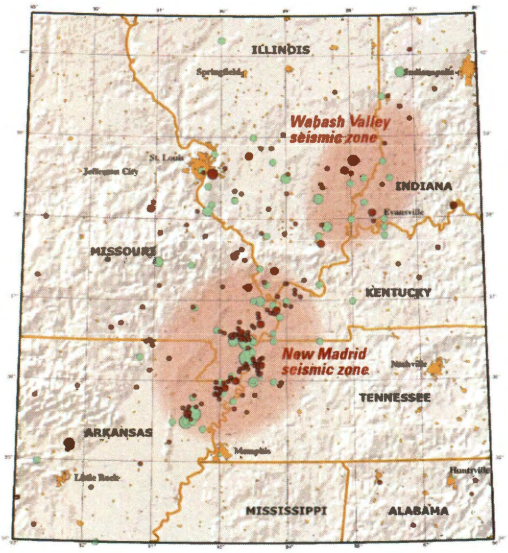

(a) New Madrid seismic zone. Source: Gomberg and Schweig (2006)

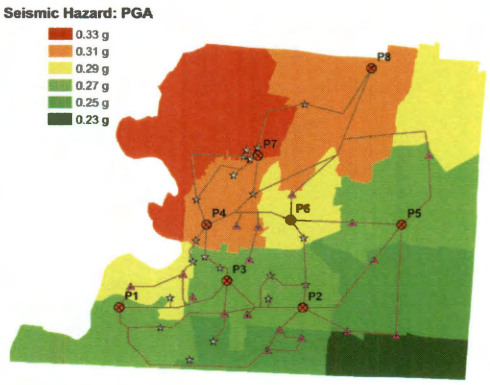

(b) Example of seismic map

Figure 3.4 : 3.4(a) New Madrid seismic zone and 3.4(a) example of seismic intensity scenario used for test case.

observed Peak Ground Acceleration (PGA) among the different network locations for the seismic scenario. These intensities are in the range from 0.1g to 0.7g considering intermediate scenarios every 0.1g. The objective of this seismic sweep is to explore the change in interdependence effects with increasing intensities as it is shown in the fragility results in the next sections.

3.2.2 Test networks and interdependence description

The test power and water urban networks are simplified versions of real networks serving Shelby county (Shinozuka et al., 1998; Hwang et al., 1998). The power network (S_1 label) contains 59 nodes and 73 links. The power nodes are classified into 12 kV substations, 23 kV substations, and gate stations. The eight gate stations (nodes with IDentification Numbers (IDNs) from 1 to 8 play the role of supply nodes, SN;

while the 37 nodes corresponding to the 12 and 23 kV substations are consumption nodes, CN (IDNs from 9 to 45). The remaining 14 nodes (IDNs from 46 to 59) are the network's transmission points, TN. The water network (S_2 label) has 49 nodes classified as large pumps, storage tanks, and delivery nodes. Large pumps and storage tanks are the supply nodes in the water network, while the delivery nodes are its consumption points. The water system has 15 supply nodes (nodes with IDNs from 1 to 15) and 34 consumption nodes (nodes with IDNs from 16 to 49). Figure 3.5(a) provides a wire representation of the structure of the test networks and of the relative location of their components.

The fragility of individual components for the power network is presented in Fig. 3.5(b) (diamonds and squares in red color) as obtained from Hazus-MH. For this network, the fragility of supply nodes is modeled using the curve for high voltage substations, while the fragility of the consumption nodes is modeled using the low voltage substation curve. For the water system, the fragility of supply nodes is described using the fragility functions in Fig. 3.5(b) obtained from Hazus-MH and the type of each supply nodes (either steel tanks or medium/large pumping plant in blue color). In this case study, the fragility of delivery nodes was considered indirectly as a function of the fragility of the supply nodes and the interconnection features of the water system. Note that the fragility of links was not considered for any of the two networks. This assumption has been applied in previous studies (Shinozuka et al., 2007) for the power network as a valid simplification alternative. However, in the case of water networks, the absence of the quantification of factors such as wave propagation, soil deformation, or liquefaction, which are known causes of failures during earthquake events (Idriss and Boulanger, 2008; Orense, 2011), may lead to an underestimation of water fragility and therefore of interdependent effects. This last

effect was found to be of importance in a test application of the IFA methodology proposed in this thesis to a real case of interdependent systemic response to a seismic event (Wu and Dueñas-Osorio, 2012).

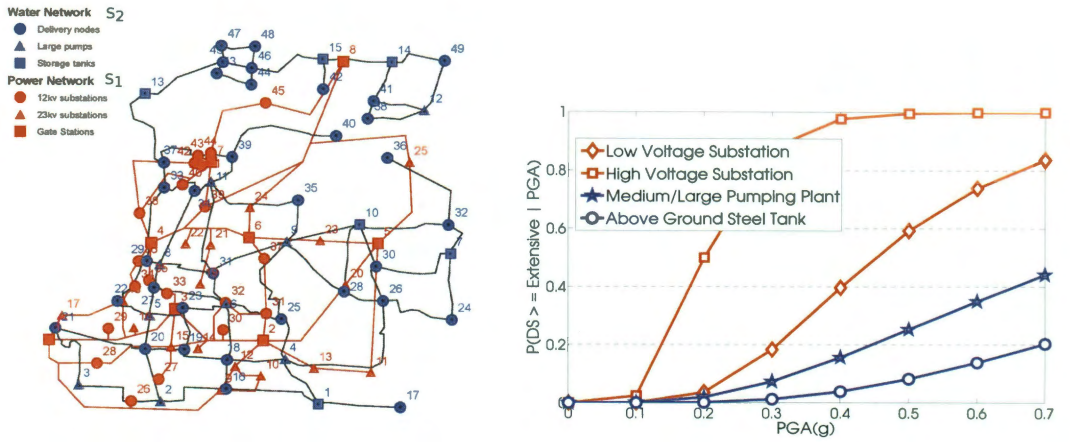

(a) Test urban networks

(b) Fragility curves

Figure 3.5 : Fig. 3.5(a) shows a wire representation of the test power and water networks in Shelby County, TN US. Fig. 3.5(b) displays seismic fragility curves for nodes in both networks. These curves highlight the higher fragility of the critical power supply nodes over the fragility of the water network counterparts.

3.2.3 Interdependence interface

This test case studies the systemic fragilities of the test networks using a failure transmission paradigm of instantaneous interdependence effects propagation and interdependence strengths ($Istr$) ranging from 0.1 to 1.0. While the values of $Istr$ are allowed to change, the structure of the interdependence interface is the same for all case studies. This restriction is important because research on the subject (Ouyang and Dueñas-Osorio, 2011a) has shown that changes in the topology of the interdependence interface can be used as a mechanism to control interdependence propagation, a policy also explored in this thesis in Chapter 4.

The interdependence matrices (Section 2.5) used to represent the interaction of the two test systems were obtained from Dueñas-Osorio et al. (2007) and are displayed in Fig 3.6. The sketches in Fig 3.6 use black dots to represent the existence of links from a master node (labeled in the vertical axis) to a slave node (labeled in the horizontal axis).

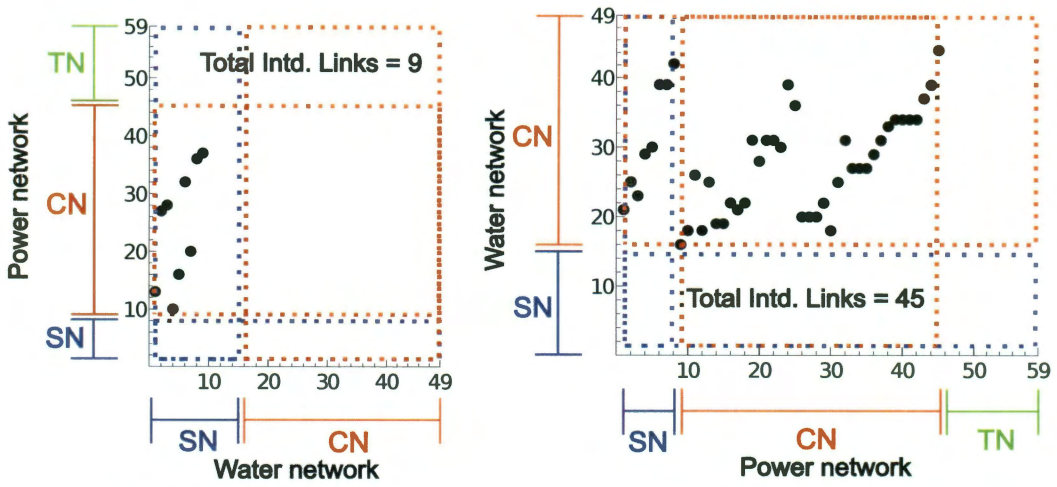

(a) IM_{12} for $S_1 \rightarrow S_2$ (b) IM_{21} for $S_2 \rightarrow S_1$

Figure 3.6 : 3.6(a) shows the interdependence matrices for the action $S_1 \rightarrow S_2$, while Fig. 3.6(b) shows the corresponding $S_2 \rightarrow S_1$ action. Although the number of interdependence links is higher in $S_2 \rightarrow S_1$ than for $S_1 \rightarrow S_2$, their effect is limited by the fragility of the power network elements.

The comparison of Fig. 3.6(a) with Fig. 3.6(b) shows that the number and locations of interdependence links is different for the two directions of interaction. The direction $S_1 \rightarrow S_2$ has nine links acting from consumption nodes in the power network to water supply nodes, while the direction $S_2 \rightarrow S_1$ has 45 links from consumption nodes in the water system acting on power supply and consumption nodes. This imbalance in the number of nodes seems to show that the water network has important influence of the performance of the power networks. However, it must be noted that

the totality of the potential influence of the power system over the water network is concentrated on the *critical* water supply nodes. This influence is considerable, but it is also noticeable that *not all* water supply nodes depend on the power network [Fig. 3.6(a)] and so even complete collapse of the power network cannot trigger the total collapse of the water network. For the case of the water-on-power influence, the distribution of interdependent links covers both supply and consumption power nodes and hence its impact on the power network could be considerable. The results in the following sections will show that the apparent interdependent influence of the water network on the power system is limited by the individual fragility of the power network components, which in turn causes considerable interdependent effects on the water network fragility.

3.2.4 Test specifications and results

The test power and water networks were subjected to seven seismic scenarios, starting at nominal seismic intensity 0.1g increasing at a constant step of 0.1g until reaching the maximum level of 0.7g, and six levels of interdependence strength, 0.1, 0.3, 0.5, 0.7, 0.9, and 1.0. The fragilities of the components and the interdependence interface were left unchanged for all tests. Systemic fragility was measured using Connectivity Loss, CL and all estimates were based in CL lists created after running 10 000 simulations for each of the designed scenarios, a number of simulations that proved enough to generate stable values of expectation and variance of the systemic fragility estimates.

Two types of estimates were sought with these tests: evolution plots and fragility curves. Evolution plots show how the average CL changes during the stabilization cycles leading to the final reported CL values. These plots are useful to visualize the magnitude of the influence of interdependence and the trends of that influence as the

number of cycles increases. The fragility curves generated here are systemic fragility curves. They describe how the probability of networks exceeding a connectivity loss value (an allowable damage level or performance target) changes with increasing values of perturbation. Note that although in practice a decision-maker is likely to choose a preferred performance level (i.e. a single systemic fragility curve), the fragility curves in this test case are generated for several damage levels (0.3, 0.5, 0.7, 0.9, and 1.0) aiming to provide a complete picture of the variations of network response.

Fig. 3.7 displays two sets of plots related to the interdependent effects on systemic fragility. The top set (Figures 3.7a and b) shows how the presence of interdependence affects the mean connectivity loss for a condition of $Istr = 1.0$ and different seismic scenarios. The first observation from these plots is that the inherent power system fragility (stabilization cycle 1) is consistently larger than the water networks' for all conditions of seismic perturbation. This outcome is consistent with the information on the individual fragility of components displayed in Fig. 3.5(b) that shows the fragility of power network components being higher than that of their water network counterparts.

In terms of susceptibility to interdependence (stabilization cycle 2), the trend reverses. The power network results (Fig. 3.7a) show a minimal influence of full interdependence ($Istr = 1.0$) on the expected CL for all seismic scenarios. The result for the water system shows a strong individual performance (cycle 1) that shows important degradation for all the seismic scenarios considered solely under the direct action of the test seismic perturbation. The bottom plots in Fig. 3.7 (Figures (c) and (d)) quantify the interdependence effect on systemic fragility. For the power network, interdependence effects contribute less than 5% of the total systemic fragility, while

for the water network such an effect can be as large as 500% of the initial fragility. These results confirm the interaction between component fragility and interdependence strength as a decisive factor defining the magnitude of interdependence effects. For this test case, the inherent fragility of the power network components proved decisive to curtail the potential influence of the water network on the power system performance. The power network fragility was so high that the system reached a status of complete failure before any interdependence effects could influence the performance. At the same time, that level of fragility impaired the fragility of the water network making the contributions of interdependence many times (as high as five times) larger than the original fragility of the water network.

The bottom plots reveal an additional critical factor for the description of interdependence effects. A close examination of both plots [Figures 3.7 (c) and (d))] shows that interdependence effects are larger in certain PGA ranges. For the power network, the range is limited mostly to the 0.1g seismic scenario. This limited range is explained by the fragility of the power network components. In contrast, the interdependence contribution is more diverse in the case of the inherently stronger water network. Interdependence effects become larger than 100% for high interdependence strengths under seismic scenarios in the range $[0.2g\ 0.5g]$ reaching maximum values for the 0.3g seismic scenario. Thus, the interdependence contributions to water network fragility were limited to a specific band of PGA levels. The lessons from this plots are direct: interdependence can worsen systemic fragility substantially, its effect is manifested early in the stabilization process, and its action is dependent on the intensity of the perturbation and in the inherent fragility properties of the interacting networks.

The second set of results obtained from this case study is displayed in Fig. 3.8.

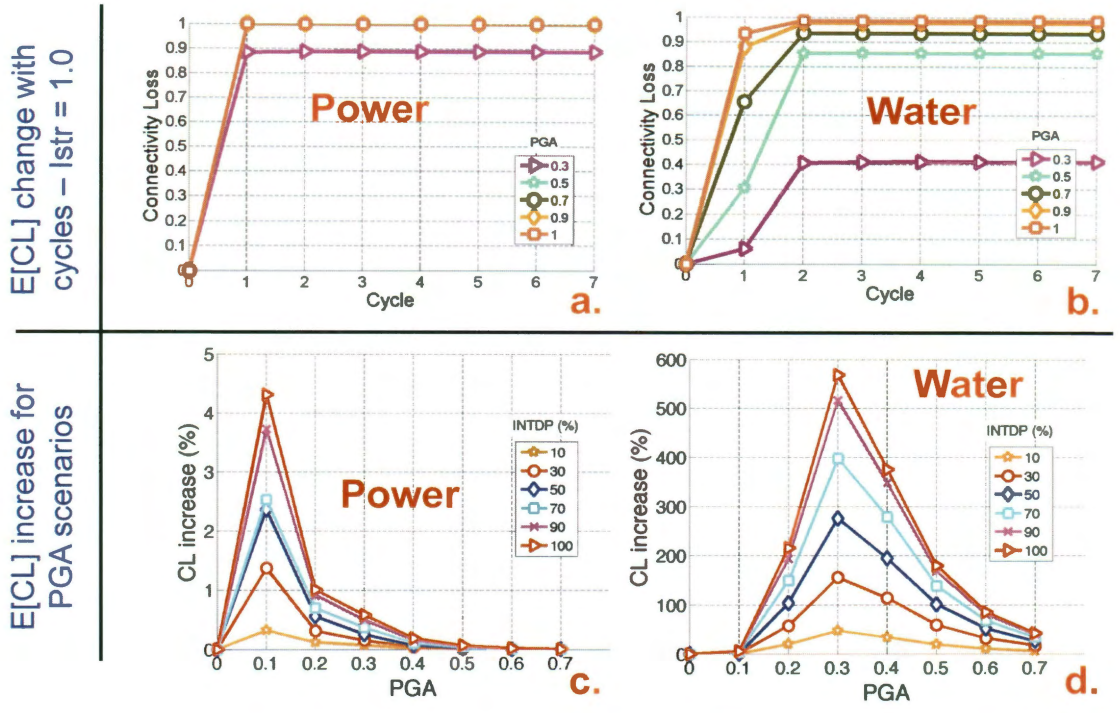

Figure 3.7 : Interdependent effects on systemic fragility for test power and water urban networks. Top figures (a and b) show average change in systemic response as a function of stabilization cycles. Bottom figures (c and d) quantify the increase in systemic performance induced by interdependent effects. Dependence of the water system on the power network triggers considerable fragility increases.

This figure presents fragility curves for the power (Figures 3.8a and b) and water networks (Figures 3.8c and d) for two interdependence strengths $Istr = 0.1$ (Figures 3.8a and c) and $Istr = 1.0$ (Figures 3.8b and d). The comparison of the set of top fragility curves confirms the already described condition of minimal interdependence susceptibility for the power system. The plots show minimal change in their shape and position with respect to the level of PGA intensity in the horizontal axis.

In the same way, the bottom curves showing the change in performance for the water network confirm the condition of dependence of this system on the fragility

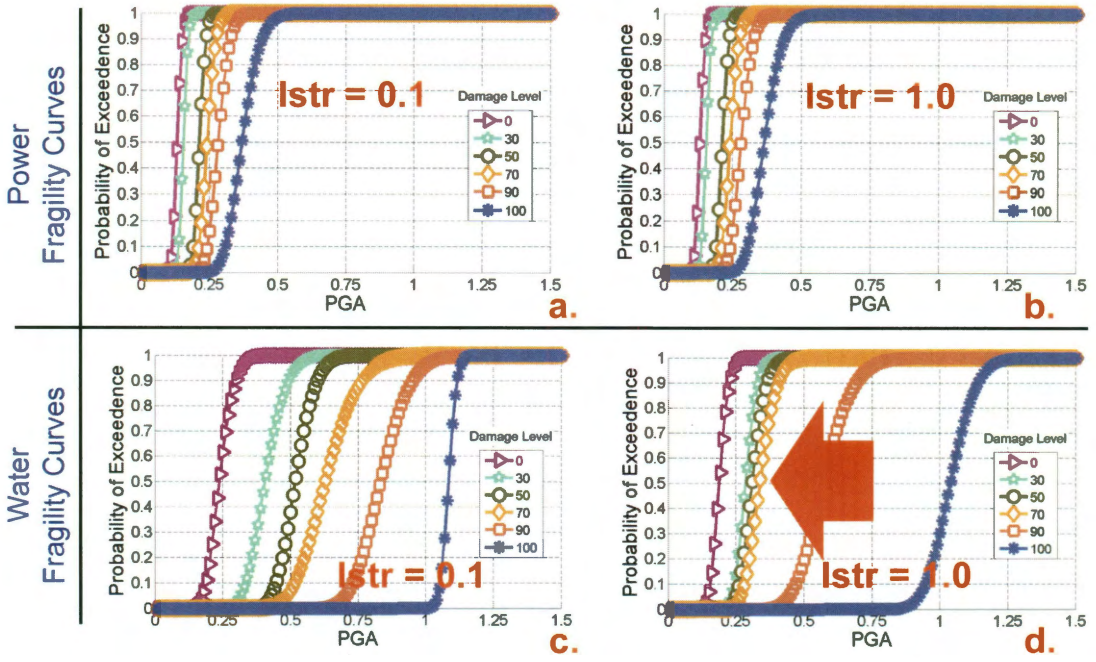

Figure 3.8 : Fragility curves for power (a and b) and water (c and d) test networks under interdependence strengths $Istr = 0.1$ (a and c) and $Istr = 1.0$ (b and d). The fragility curves confirm trends of minimal interdependence influence on the power network fragility and consistent impact of propagated fragility on the water network's expected performance.

propagated from the power network. Curves in Fig. 3.8d display a noticeable shift towards the left, or zones of smaller PGA intensity. This behavior means that smaller levels of PGA intensities are needed to trigger the same connectivity levels observed in the curves in Fig. 3.8c. Also noticeable is the change in the slopes in some of the plots. This change indicates that under the new interdependence condition ($Istr = 1.0$), the water network has become prone to substantial increases of systemic fragility with small increments of the intensity of seismic scenarios.

3.3 Case study 2: Impact of cascading failures and local redundancy enhancement policies in interdependent systemic fragility

This second case study extends the scope of the previous one by including an approximation of the effects of cascading failures in the two interdependent power and water urban networks used as test bed in this research.

As in the previous case, the two test networks are subjected to a sweep of seismic scenarios of increasing intensities under different interdependence strengths, $Istr$. Additionally, this case study includes a model of cascading failures based on the principles discussed in Section 2.4, specifically through the use of the origin-destination betweenness centrality ($O\text{-}D\,btwn$) as a proxy for flow amounts in nodes before and after the occurrence of perturbation.

A key point in this case study is the use of α-capacities, and associated proxy flow capacities using the $(1+\alpha)$ factor, which is at the core of the mitigation policy called local redundancy enhancement, LRE. This policy increases the magnitude of the initial capacity of each of the network nodes in an attempt to limit the overloading likelihood driving the generation and subsequent propagation of cascading failures as explained in the definitions section of this thesis (Chapter 2). The next section discusses in detail the specifications used for the definition of the scenarios in this second case study.

3.3.1 Systemic Fragility Summary Plots, SFSPs

The study scenarios are generated using seismic scenarios of PGA intensities ranging from 0.1g to 0.7g, with a 0.1g increasing step experienced simultaneously by both

networks. The input parameter $Istr$ takes values of 0, 0.3, 0.5, 0.7, and 1.0, while six α-capacities are considered by making α take the values of 0.25, 0.5, 0.75, 1.0, 1.25 and 1.5. This selection of local capacities and interdependence strengths guarantees a considerable exploratory range of local redundancies and interdependence scenarios.

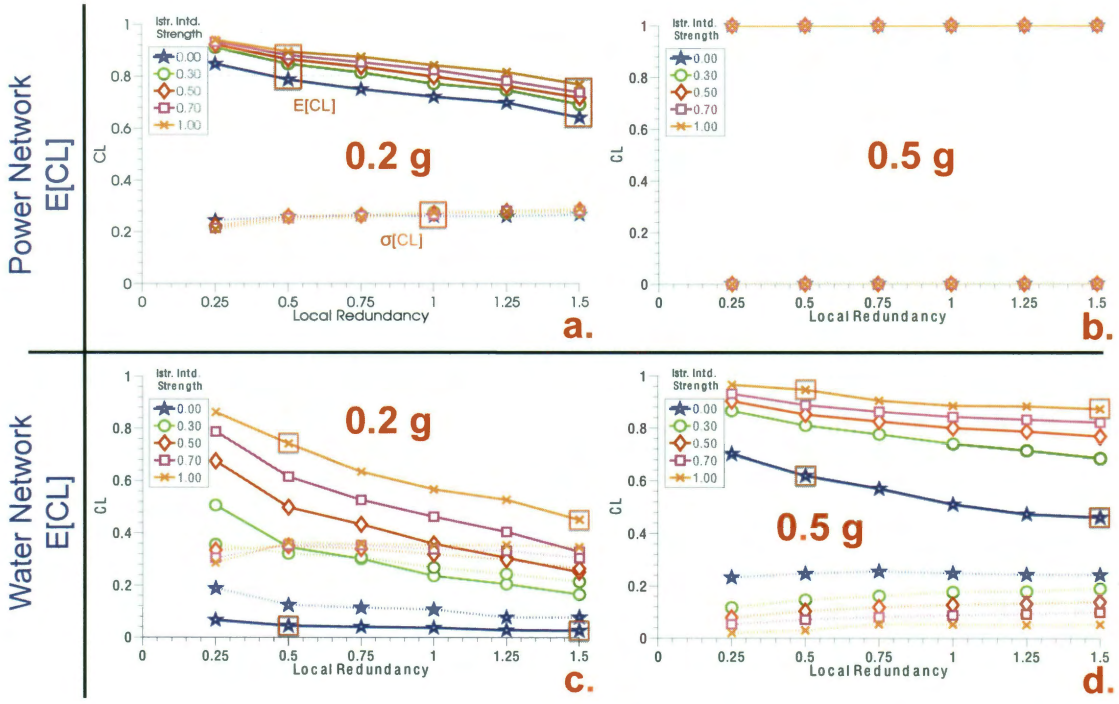

Figure 3.9 : Systemic Fragility Summary plots for PGAs $0.2g$ and $0.5g$. These plots display expected values ($E[CL]$, solid lines) and standard deviations ($\sigma[CL]$, dotted lines) of Connectivity Loss, CL for the test systems (power, S_1, and water, S_2) and different levels of α (Local Redundancy) at I_{str} values.

Figure 3.9 contains Systemic Fragility Summary Plots, SFSPs for PGA values of 0.2g in the first column, and 0.5g in the second. The comparison of the condition of the power network in Figures 3.9a and b produces a first set of insights.

Figure 3.9(a) shows that increasing interdependence strength worsens $E[CL]$, the expected value of the Connectivity Loss metric, for all enhanced local capacity levels

α. At the same time, the figure reveals that adding local redundancy by increasing α reduces $E[CL]$. Nevertheless, the short vertical separation between curves confirms the limited effect of interdependence on the power system. Increasing $Istr$ from 0 to 1 for $\alpha = 0.5$ [leftmost box in Fig. 3.9(a)] increases $E[CL]$ from 0.79 to 0.89, a 12% $E[CL]$ increase. For $\alpha = 1.5$, $E[CL]$ changes from 0.64 at $Istr = 0.0$ to 0.76 at $Istr = 1.0$ (rightmost box), for a 18.7% change. The fact that the changes are measurable, even for higher α values, tells that interdependence is still a factor to reckon with.

In a contrast that highlights the relevance of the perturbation intensity, Fig. 3.9(b) shows that the power system fails surely under $PGA = 0.5g$. This scenario occurs due to the large earthquake fragilities of power components.

For the water system, Fig. 3.9(c) displays trends of increased $E[CL]$ with high $Istr$ values and reduced $E[CL]$ with high α values, as it was the case for the power system; however, it is noticeable that the effects of enhanced local capacity are more pronounced for the water network in the event of interdependence action [change in $E[CL]$ from 0.74 for $\alpha = 0.5$ to 0.45 for $\alpha = 1.5$, under $Istr = 1.0$, top boxes in Fig. 3.9(c)] than in the case of complete independence (0.04 CL for $\alpha = 0.5$ to 0.02 CL for $\alpha = 1.5$, under $Istr = 0.0$, bottom boxes in the same figure). This behavior can be explained by the fact that the water system is in itself strong enough to absorb the damage induced by the small perturbation created by the PGA of 0.2g, leaving the enhanced capacity unused.

Finally, Fig. 3.9(d) describes the water system's response for $PGA = 0.5g$. This figure reveals two key insights. First, the high perturbation level decreases the fragility control effectiveness of adding local capacity. This is illustrated by the small change in CL under $Istr = 1.0$ between $\alpha = 0.5$ and $\alpha = 1.5$ levels (0.94 to 0.87 CL; top

boxes in Fig. 3.9(d)), a 7.4% change, much smaller than the 39.2% observed for the same conditions in Fig. 3.9(c). Second, the larger perturbation intensity shows the local redundancy enhancement potential to control systemic damage in the absence of interdependence effects. The behavior of the $Istr = 0.0$ curve exemplifies this effect; $E[CL]$ drops from 0.62 at $\alpha = 0.5$ to 0.46 at $\alpha = 1.5$, (bottom boxes in Fig. 3.9(d)) a decrease of 0.16, eight times larger than the 0.02 change experienced under $PGA = 0.2g$.

Note that the behavior of the standard deviations of CL changes according to the system's condition and the influence of interdependence and local redundancy. In Fig. 3.9(b), $\sigma[CL]$ is zero for all α levels as the power system surely collapses under the $PGA = 0.5$; while in Figure 3.9(a), the σ curves show similar behavior for different $Istr$ values, as the systemic behavior is not controlled by interdependence but rather by the inherent power system fragility. It is also clear that $\sigma[CL]$ is consistently smaller for the power system relative to the water system, a confirmation of the low variability in the fragility estimates caused by the high fragility of the power components.

Finally, note that although the water system's potential to induce damage back into the power system exists, recent studies on post-event situations suggest that such levels of interdependence action are unlikely to be observed during real earthquake events (Dueñas-Osorio and Kwasinki, 2010). This potential reduction on the power-on-water interdependence impact occurs as a consequence of soil liquefaction and wave propagation factors which increase the fragility of the water network, and reduce the role of interdependence effects.

3.4 Validation

The proposed IFA methodology, the mechanisms of internal damage propagation, and the model of interdependent damage transmission used in this research attempt to represent the expected behavior that real urban networks will exhibit in the event of earthquake perturbation. However, it is clear that uncertainty is present at all levels of failure propagation generation and that the fragility estimates generated using the proposed methodology ultimately represent an underlying random variable whose variability depends on the variability of the seismic hazard, the network components fragilities, and the interdependence strengths of the network interconnections all factors that require important amounts of information for their proper assessment.

Despite these constraints, the utility of these types of IFA models ultimately depends on their capacity to predict at an acceptable level the real outcomes using the methodology in question. From this point of view, the best way of validating the IFA algorithm is to benchmark the quality of fragility forecast estimated from its application to real scenarios. This statement means that the properties of real urban networks subjected to earthquake perturbation of known characteristics must be gathered and analyzed in a post-earthquake effort to verify the level of agreement between theoretical values from a computational model of the affected networks and the real observed levels of systemic disconnection or flow disruption measured by the public authorities and private agencies in a catastrophe zone.

Using such approach, Wu and Dueñas-Osorio (2012) found a matching higher than 90% between the disruption levels observed in the 2010 Chile earthquake and theoretical estimates obtained using the IFA methodology. Noticeably, their study of the interaction between the power and water networks in the Chilean city of Concepción, indicated that the fragility of the water links played an important role in

the global systemic response. The matching between the IFA estimates and the real outcomes observed from the event improved when this factor was included as an additional fragility source in the IFA simulation-based model. This experience supports the validity of the principles used for the generation of the IFA methodology; however, more tests are required to arrive to complete assurance of the reliability of the methodology. In an additional note, Poljanšek et al. (2012) used the approach followed in this thesis for interdependence representation in their study of the fragility of interdependent power and gas networks in Europe.

Chapter 4

Mitigation Strategies for Interdependent Seismic Fragility Control on Urban Lifelines Systems

The previous case study (Case Study 2) introduced a first measure (LRE) to control interdependence systemic fragility as a byproduct of the attempt to control the propagation of internal cascading failures in urban networks. This section introduces two additional mitigation measures acting on two key sources of interdependent fragility: component fragility and interdependence interface. The objective of the this portion of the thesis is to propose two conceptual damage mitigation strategies and evaluate their potential effectiveness in reducing interdependence fragility. The key problem of obtaining *optimal* mitigation policies with implementation details and cost-benefit ratios is beyond the scope of this work and is left as a critical challenge for future developments.

The two conceptual mitigation measures introduced in this section require the selection of critical network components whose properties or external connections are adjusted to enhance the strength of interdependent urban networks against the action of seismic perturbation. Two techniques, origin-destination (O-D) betweenness, introduced before for measuring component centrality, and NodeRank, an importance metric based on the PageRank algorithm used by Google also introduced in the background section, are used for the purpose of identification of critical components in networks. As discussed in Chapter 2, NodeRank ranks network nodes through a combination of fragility values and the results of the PageRank algorithm. The

PageRank ranking estimates are based purely on the topological properties of the network, while NodeRank combines such estimates with the inherent fragility of each component. In the case of origin-destination (O-D) betweenness, the metric measures the number of shortest paths that use a given component when connecting the supply and consumption nodes in a network.

The effectiveness of the implementation plans for the introduced mitigation measures is tested under different conditions of interdependence strength and seismic scenarios by measuring resulting fragility reductions for a selected performance limit state. The following sections explain in detail the mitigation measures and discuss the results obtained from an extensive test case study of two interdependent urban networks based of models of real interconnected systems.

4.1 Mitigation strategies

Two mitigation strategies are used as conceptual measures to reduce the impact of seismic perturbation on systemic fragility: 1) *Component Fragility Reduction*, CFR and 2) *Interdependence Redundancy Enhancement*, IRE.

Component Fragility Reduction, CFR, reduces the fragility of a selected group of nodes by a fixed percentage of their original value. The nodes to intervene are chosen based on their importance for systemic stability and their known fragility to a threat under consideration as determined by a proposed ranking strategy based on centrality measures. The objective of implementing this type of action is to measure the effectiveness of limited (and hence financially feasible) local fragility mitigation on reducing systemic fragility under different conditions of interdependence with other networks.

Interdependence Redundancy Enhancement, IRE, explores the potential of inter-

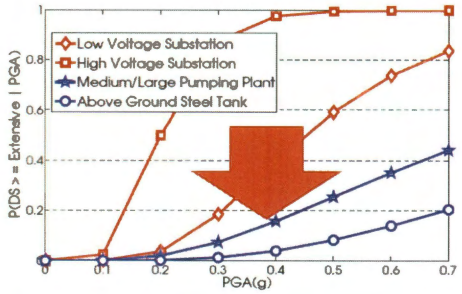

(a) Component Fragility Reduction, CFR

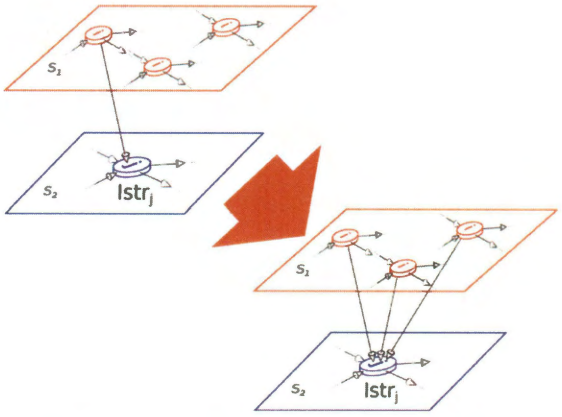

(b) Interdependence Redundancy Enhancement, IRE

Figure 4.1 : Representations of the basic actions used in the conceptual mitigation strategies considered in this chapter. Fig. 4.1(a) represents how the CFR strategy decreases the component fragility of selected critical components. Fig. 4.1(b) shows how the IRE policy increases the number of additional supply lines (interdependence links) for dependent nodes in all networks.

vening the linking interface existing between interdependent networks as a measure to reduce systemic fragility for all interacting networks. The IRE strategy works by adding new interdependence links to the existing interdependence interface with the aim of reducing the likelihood of interdependent damage transmission [Fig. 4.1(b)].

Under the IRE strategy, for a given slave node whose functionality depends on the survival of a single master node, adding an interdependence link is equivalent to providing an additional supply channel for the dependent node. In the updated condition, the failure of the slave node will be conditional not on the failure of a single master node, but on the failure of two of them, an event which, if properly designed, will have a reduced likelihood compared with that of the original interdependence arrangement. Note that this measure reduces the effective fragility by adding connections (link redundancy) between facilities rather than by intervening on the fragility

of facilities, thus representing a direct application of the *failure avoidance* paradigm for interdependence propagation introduced in Section 2.5 (Fig. 2.5). This difference implies that IRE actions may result in a lower total mitigation cost than its CFR counterpart, as it may be the case that adding connecting elements requires less monetary expense than reducing the fragility of a complete facility.

4.2 Case study 3: conceptual mitigation strategies for two test interdependent networks under seismic scenarios

This case study uses the two familiar simplified power and water networks from Shelby county, TN, US as a test bed. The networks are subjected to the seven seismic scenarios used in the previous case studies (Case Studies 1 and 2); however, for the sake of brevity the systemic fragilities of the test networks are calculated now only for the conditions of complete independence ($Istr = 0.0$) and full interdependence ($Istr = 1.0$), that is the two extreme values of the $Istr$ parameter. The interdependence matrices used for the description of the interconnection interface between the test networks are the same as used in previous case studies, but note that they eventually change under the influence of the IRE mitigation policy.

Unlike the two previous case studies, the fragility of the water network has been enriched by the inclusion of the possibility of link failure and by the redefinition of the failure of water consumption nodes as a function of the potential disconnection brought upon them by the failure of their associated links. In the two previous case studies the fragility of such points depended essentially on the failure of its neighbors or in more general terms in their disconnection from surviving internal supply nodes.

The inclusion of link fragility obeys to the fact that several earthquake experiences

(EERI, 2010; Eidinger et al., 2010) have shown that water link failures substantially contribute to the loss of service during an earthquake and to the time required for repairs in the event's aftermath. In this regard, O'Rourke and Lui (1999) state that failure in water pipes is mainly due to either permanent ground movements or wave propagation associated to Peak Ground Velocity, PGV. Of these two causes, this case study models the most common of the two, wave propagation damage, while leaving permanent ground movement fragility as a key aspect to include in future developments. Noticeably, recent research on this topic (Wu and Dueñas-Osorio, 2012) has partially incorporated the issue of ground movement in the study of water network fragility.

To estimate the link fragility associated to wave propagation, this case study uses the expression proposed by Adachi and Ellingwood (2009a) reproduced here in Eq. 4.1,

$$\mathbb{E}[P_f] = 1 - exp\left(-C \times L \times \mu_{PGV}\right) \tag{4.1}$$

In Eq. 4.1, $\mathbb{E}[P_f]$ is the expected probability of failure of the pipe under study; $C = K \times 0.00187$, where K is a parameter obtained as a function of pipe diameter and material; L is the pipe length; and μ_{PGV} is the average value of PGV over the pipe length. Using this equation, the water link fragility is included in the simulation of hazard action of scenarios in the IFA algorithm, specifically at the DHA stage. The resulting link status obtained in a given scenario are used to determine the survival of the network consumption elements. Under this strategy, consumption nodes become failed elements if their associated pipelines fail, that is the consumption point is left isolated from surviving network portions and specifically from the internal supply

nodes and associated paths.

4.2.1 Seismic perturbation and ranking strategies results

The interdependent test power and water networks are subjected to a sweep of seismic hazard scenarios propagated based on the seismology of the Shelby County area. Each of these scenarios is identified by the maximum PGA estimated for the locations of the different components as in the two previous test cases. These scenarios span the same interval from 0.1g to 0.7g with a sampling step of 0.1g. For the water network case, the PGV at each node is calculated as a function of the PGA at the same locations, with the average PGV over a pipe length (required in Eq. 4.1) estimated as the arithmetic average of the PGVs at the link's initial and terminal nodes.

With regard to ranking strategies, Table 4.1 presents the ranking results for both networks using NodeRank and *O-D* betweenness. Both methodologies are applied to the test networks considering their topology and node fragility in the case of NodeRank, and the number of connecting paths using a given network node when connecting supply and consumption nodes in the case of *O-D* betweenness, for their comparison of the importance of a component for the survival of the network it belongs to. This table displays rankings for the top 10% (six power nodes and five water nodes) and 20% (twelve power nodes and ten water nodes) most fragile (for CFR) and top strong (for IRE) nodes in both networks according to the the ranking strategies NodeRank (NR in the table) and *O-D* betweenness (*O-D* btwn in the table). The percentages of intervention represent the author estimation of maximum allowable intervention rates that can take place at the same time for a network under the two modes of intervention (basic and extended) explored in the test case. These values are not meant to be fixed and they can be adjusted without a loss on the

generality of the approaches discussed in this section.

Table 4.1 : Ranking IDNs results for Power (S_1) and Water (S_2) nodes using the NodeRank (NR) and origin-destination (O-D) betweenness ranking strategies. Selection of the top 10% of nodes produces lists of 6 nodes and 5 nodes for S_1 and S_2, respectively.

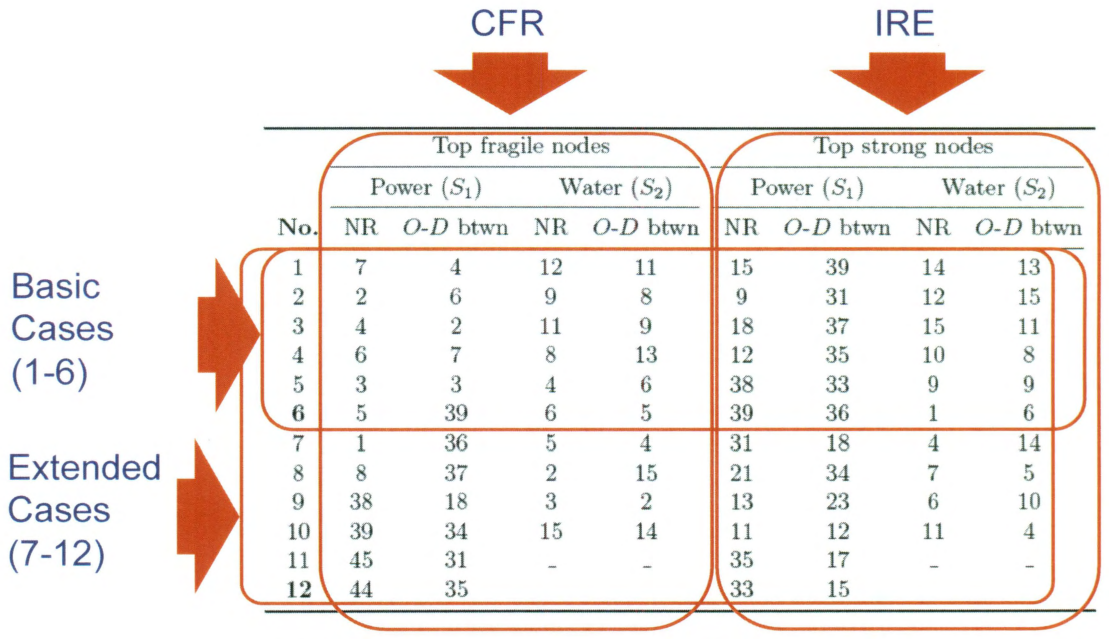

	Top fragile nodes				Top strong nodes			
	Power (S_1)		Water (S_2)		Power (S_1)		Water (S_2)	
No.	NR	O-D btwn	NR	O-D btwn	NR	O-D btwn	NR	O-D btwn
1	7	4	12	11	15	39	14	13
2	2	6	9	8	9	31	12	15
3	4	2	11	9	18	37	15	11
4	6	7	8	13	12	35	10	8
5	3	3	4	6	38	33	9	9
6	5	39	6	5	39	36	1	6
7	1	36	5	4	31	18	4	14
8	8	37	2	15	21	34	7	5
9	38	18	3	2	13	23	6	10
10	39	34	15	14	11	12	11	4
11	45	31	-	-	35	17	-	-
12	44	35			33	15		

4.2.2 Mitigation strategies and comparison cases

The two conceptual mitigation strategies are designed based on the two sets of rankings presented above (Fig. 4.1) and on a fixed fragility mitigation level (25% for CFR) or interdependence interface enhancement (one additional interdependence link under IRE), respectively. These combinations produce six basic cases of mitigation along with six additional cases exploring the effects of more intense actions. Note that as for the case of the number of ranked nodes reported in Fig. 4.1, the intervention

characteristics of the CFR and IRE mitigation policies represent the author estimations of reasonable policies in real cases; in any case, the values can be adapted to reflect a different type of rationality without affecting the generality of the policy implementation.

In the following description of cases, the NodeRank ranking is identified as ranking 1, while the O-D betweenness ranking is referred to as ranking 2. The first two basic mitigation cases (cases 1 and 2) result from applying CFR to the independent networks ($Istr = 0$) using the top 10% fragile nodes (6 nodes for S_1; 5 nodes for S_2) from the rankings 1 and 2, respectively. The next two cases, cases 3 and 4, use rankings 1 and 2 to test the effects of CFR with 25% fragility reduction on a fully interdependent version of the two test networks. Note that both NR and origin-destination betweenness are used simultaneously in every comparison case.

The final two cases, cases 5 and 6, use the top 10% strong nodes in both networks to assess the impact of IRE on the fully interdependent ($Istr = 1.0$) test networks. Note that the strong nodes are used to identify safe sources for the new interdependence links created by IRE. For cases 5 and 6, each slave node is attached to an additional master node as a mean to diversify its external dependence.

The six additional cases, cases 7 to 12, test the effects of mitigation action intensification. For these extended cases involving CFR (cases 7 to 10), the mitigation is intensified by increasing the number of nodes with 25% reduced fragility from 10% to 20% (12 nodes for S_1; 10 nodes for S_2) of the total number of nodes for each network. The final extended cases 11 and 12 increase the IRE mitigation level by adding two interdependence links to each slave node instead of the single one added in the basic cases.

In addition to the 12 cases described, cases 100 and 101 are used to study the

baseline response of both networks before mitigation for the independent and fully interdependent conditions, respectively. Two extra cases, labeled as cases 200 and 201, study the effects of a combination of CFR and IRE. Cases 200 and 201 use the definition of case 3 (CFR, 25%, $Istr = 1.0$) and add to it one and two interdependence links, respectively, to each existing slave node to define mixed $CFR + IRE$ cases.

4.2.3 Results and discussion of mitigation policies

Resulting systemic fragilities for each of the mitigation cases are discussed here as the probability of a network exceeding a 50% Connectivity Loss ($CL \geq 0.5$) obtained after 10 000 simulations for all hazard scenarios. Table 4.2 summarizes the systemic fragilities estimated for each network under each mitigation scenario. Fragility results are obtained by averaging the change in fragility over all seismic hazard scenarios. Note that this procedure implicitly assumes that all earthquake scenarios are of the same likelihood. This assumption is naturally unrealistic and highlights the need for complete probabilistic description of earthquake hazard, a challenge handled in this thesis in Chapter 5. The percentages in parenthesis are calculated with respect to the fragility values of the baseline cases: case 100 for independent networks ($Istr = 0$) and case 101 for complete interdependence ($Istr = 1.0$).

Fig. 4.2 shows typical fragility results used for the calculation of the unweighted averages in Table 4.2. The systemic fragility curves in this figure correspond to the baseline cases 100 ($Istr = 0.0$) and 101 ($Istr = 1.0$). The solid curves show mean probability of the systemic Connectivity Loss metric exceeding 0.5 as a function of PGA. The dashed curves show the relative error of the estimated mean Probabilities of EXceedance (PEX) as a function of the same PGA values. Note that this relative error is of consideration only at $PGA = 0.1$g, a scenario with small impact on final

Table 4.2 : Summary of results for mitigation cases. Amounts in parentheses show the reduction as a percentage of the corresponding base case. All percentages indicate fragility reduction. (* 2 links added)

Baseline Cases

Mixed Cases

				Power (S_1)	Water (S_2)
Case ID	$Istr$	Ranking	Intervention	$\mathbb{E}[P(CL \geq 0.5)]$	$\mathbb{E}[P(CL \geq 0.5)]$
Baseline cases: No intervention					
100	0.0	-	-	0.65 (bl)	0.33 (bl)
101	1.0	-	-	0.66 (bl)	0.56 (bl)
Basic cases: 10% of nodes intervened or intd. link added					
1	0.0	NR	CFR	0.60 (7.7%)	0.28 (15.1%)
2	0.0	O-D btwn	CFR	0.61 (6.2%)	0.26 (21.2%)
3	1.0	NR	CFR	0.61 (7.6%)	0.52 (7.1%)
4	1.0	O-D btwn	CFR	0.61 (7.6%)	0.52 (7.1%)
5	1.0	NR	IRE	0.65 (1.5%)	0.53 (5.4%)
6	1.0	O-D btwn	IRE	0.65 (1.5%)	0.52 (7.1%)
Extended cases: number of nodes/links intervened doubled					
7	0.0	NR	CFR	0.58 (10.8%)	0.24 (27.3%)
8	0.0	O-D btwn	CFR	0.60 (7.7%)	0.23 (30.3%)
9	1.0	NR	CFR	0.58 (12.1%)	0.51 (8.9%)
10	1.0	O-D btwn	CFR	0.61 (7.6%)	0.49 (12.5%)
11	1.0	NR	IRE	0.65 (1.5%)	0.49 (12.5%)
12	1.0	O-D btwn	IRE	0.65 (1.5%)	0.50 (10.7%)
Mixed $CFR + IRE$ cases					
200	1.0	NR	$CFR + IRE$	0.60 (9.1%)	0.47 (16.1%)
201	1.0	NR	$CFR + IRE^*$	0.58 (12.1%)	0.42 (25.0%)

mitigation decisions.

For the $Istr = 0.0$ plot [Fig. 4.2(a)], the power network's PEX curve shows consistently fragility values higher or equal (equality at $PGA = 0.1$g) than the water network's curve (min. difference: 0 at $PGA = 0.1$g; max. difference: 0.91 at $PGA = 0.3$g), a result consistent with the component fragility curves in Fig. 3.5(a) in which the fragility of the critical power supply nodes surpasses the fragility of the water network supply elements. For the $Istr = 1.0$ plot [Fig. 4.2(b)], the fragility differences between the two networks decrease noticeably as observed from comparing cases 100

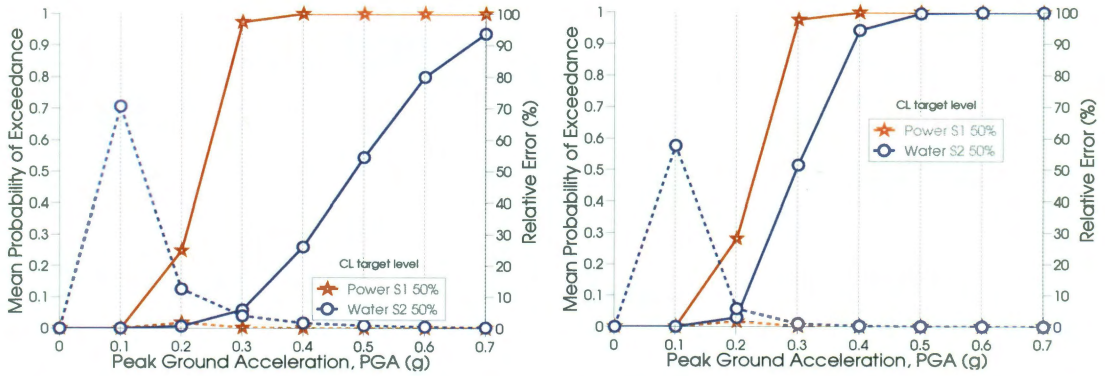

(a) Baseline systemic fragilities for $Istr = 0$ (b) Baseline systemic fragilities for $Istr = 1.0$

Figure 4.2 : $CL > 0.5$ systemic fragility curves for both test networks under independent ($Istr = 0.0$, Fig. 4.2(a)) and fully interdependent ($Istr = 1.0$, Fig. 4.2(b)) conditions. Networks have not undergone mitigation.

and 101. Table 4.2 indicates interdependence effects induced an average fragility increase of 1.5% for the power network and of 69.7% for the water network.

On one hand, the magnitude of these changes emphasizes the fact that negative interdependence effects contribute greatly to the water network fragility increase. On the other hand, the interdependence effects of the water network on the power network are minimal as evidenced in previous case studies. The particular behavior of the power system can be explained by both its own fragility [Fig. 3.5(a)] that allows little capacity to be damaged by external agents (for $PGA \geq 0.4$g), and by the strength of the water network whose connectivity survival reduces the likelihood of interdependence damage transmission from internal cascades.

The basic mitigation cases provide an additional source of insights. In the first place, for $Istr = 0$, CFR basic cases 1 and 2, the 10% node mitigation achieves a maximum (with respect to other comparison cases) 7.7% fragility reduction for the power network and a maximum 21.2% reduction for the water system. These results

can be interpreted as a limited outcome for the power network and a more satisfactory impact in the water network when both networks are independent. Nevertheless, the duplication of efforts in the extended cases (cases 7 and 8) does not lead to a proportional improvement in the fragility conditions. This situation is specially clear in the case of the power network achieving a 10.8% fragility reduction in case 7. Case 7 performs best for the water network in achieving a 27.3% fragility reduction close to the duplication value with respect to case 1 (15.1%).

The performance of the networks under $Istr = 1.0$, CFR basic cases 3 and 4, is noticeable as they achieve the *same reduction values* for both networks (7.6% and 7.1% for the power and water network, respectively). Such parity does not exist in the extended cases (cases 9 and 10) in which case 9 performs better than case 10 for the power network (12.1% against 7.6%), and case 10 surpasses case 9's effects on the water network (12.5% against 8.9% reduction).

A comparison across $Istr$ values of the aggregate fragility-reduction effectiveness of the two ranking strategies (NR and O-D betweenness) shows that O-D betweenness is slightly more effective than NR for the CFR base cases mostly due to its impact on the water network (case 2). However, the NR strategy shows a marginal advantage over O-D betweenness for the CFR extended cases of mitigation. This switching trend and the clearly different network responses to mitigation allows to state that the effectiveness of a local fragility reduction mitigation measure depends on the ranking strategy, the magnitude of the mitigation, and the conditions of interdependence and component fragility of the affected networks. Hence, several ranking alternatives ought to be tested in order to find the best fit for each particular case; that is, no particular preference can be suggested for general applications based on the results of this case study.

Beyond the ranking comparison point, the four CFR basic cases (cases 1 to 4) and their extended cases (cases 7 to 10) in Table 4.2 show that the CFR mitigation policy does decrease interdependent fragility, but the achieved reduction rates are almost never as satisfactory as in the case of independent networks. Indeed, while the maximum reduction ratio under CFR for $Istr = 0$ is 30.3% (case 8, water network), the maximum reduction for $Istr = 1.0$ is 12.5% (case 10, water network). This outcome highlights how the presence of interdependence complicates the task of fragility control. However, at the same time, the same outcome supports the need for adequate interdependence description for a correct evaluation of seismic systemic fragility and mitigation.

The results of the IRE basic cases (cases 5 and 6) show a marginal effect of this mitigation policy on the power network and a considerable impact on the water system. The same trends are observed in the IRE extended cases (cases 11 and 12). In the extended cases, the power network remains at its base case value of fragility reduction (1.5%), that is, the addition of an extra interdependence link does not reduce its fragility any further. However, for the water network, the additional extra link increases the maximum reduction from 7.1% (case 6) to 12.5% (case 11). This response reflects the negative influence of the dependence of the water network on power network elements and shows a potentially very effective way of limiting its effects, without the need for intensive facility-level retrofits.

In terms of ranking comparison, the review of the IRE results shows that maximum fragility reductions are achieved under different rankings and not consistently under one of them. However, the magnitude of the differences between the values is insufficient to create a preference in this case study. Note also that IRE is able to match the fragility reduction levels brought by CFR in basic and extended cases

for the water network but not for the power system. Again, this is a clear indication that IRE targets the negative interdependent effects from the power network increasing the water network fragility, but it is, by its own definition, unable to reduce the mostly inherent fragility of the power network.

Finally, Fig. 4.3 registers the systemic fragility curves for the mixed $CFR + IRE$ cases 200 and 201. The comparison of the curves shows that adding an extra interdependence link in case 201 (for a total of 3 per slave node) leads to a maximum additional fragility reduction of 0.15 (PEX at $PGA = 0.3$g) for the power network and of 0.22 (PEX at $PGA = 0.4$g) for the water system compared to the initial reductions in case 200. The comparison of these new plots with the baseline case 101 [Fig. 4.2(b)] reveals the important gains achieved by mitigation. However, comparing these plots with the fragilities in the case of network independence [Fig. 4.2(a)] demonstrates that additional mitigation for interdependence could generate further fragility reductions per network; that is that the intensity of the mitigation or more mitigation actions could be added to provide additional gains in fragility reduction. As a final note, Table 4.2 shows that case 200 slightly surpasses the fragility reductions brought by the addition of cases 3 and 5. This result indicates that mixed mitigation strategies must be considered as potential optimal mitigation strategies.

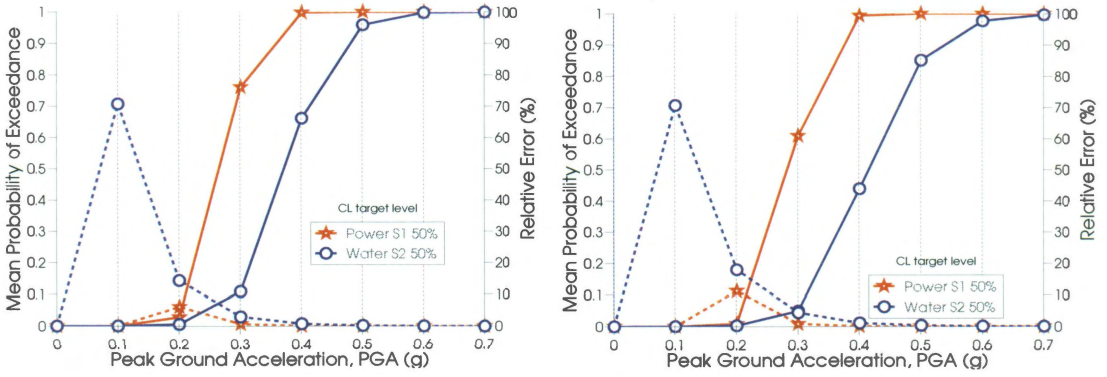

(a) $CFR + IRE$ one intd. link added

(b) $CFR + IRE$ two intd. link added

Figure 4.3 : $CL > 0.5$ systemic fragility curves for both test networks under $Istr = 1.0$ and combined CFR and IRE mitigation policies. With CFR mitigation intensity fixed, Fig. 4.3(a) shows the effects of a IRE policy adding a single link, while Fig. 4.3(b) shows the effects of a IRE policy adding two interdependence links to each dependent node.

Chapter 5

Probabilistic Fragility of Interdependent Infrastructure Networks under Network-Consistent Seismic Hazard

5.1 Generation of Network-Consistent Seismic Fragility Estimates

When an earthquake occurs, seismic intensities impact almost simultaneously all the exposed sites in a network. The collective effect of such perturbation makes the network as a whole reach an undesirable performance level according to the magnitude, the distance, and soil conditions for the event and network locations. This description of systemic seismic damage expects a certain degree of correlation to exist between the intensities at different network locations. A useful mechanism to fulfill this requirement is the use of seismic intensity maps for hazard description and subsequent probabilistic risk assessment.

A catalog of intensity maps preserves in each map the expected correlation of hazard intensities between locations and allows a direct association between the map, its likelihood and the systemic performance calculated using the map as an input the three basic elements required for the assessment of expected systemic performance. In the case of intensity maps, the stochastic nature of seismic hazard requires the use of a sizable collection of them as well as their probabilities of occurrence. The generation of such maps must properly represent the seismological features, the activity, and

the variability of the seismogenic sources while also limiting the number of maps used in fragility calculations for the sake of computational efficiency and practical implementations. The importance of the computational demand factor only increases when additional operations are necessary for the generation of each intensity map (use of a ground motion model, for example), as it is the case for the interdependent systemic fragility assessment procedure introduced in this thesis.

This chapter describes the integration of network-consistent earthquake hazard with interdependent systemic fragility assessment. The seismic hazard assessment methodology discussed here is based on Jayaram and Baker (2010), who provide a strategy for the efficient construction of an earthquake catalog based on Importance Sampling (IS), a variance reduction technique for Monte Carlo simulation. The application of the IS technique reduces the number of required intensity maps compared to regular Monte Carlo simulation. At the same time, the IS formulation delivers formulae for the mean and variance estimates of Annual Probabilities of EXceedance (APEX) for probabilistic interdependent systemic performance assessment executed using the sample seismic maps as input. This calculation of annual probabilities of exceedance for the fragility of interdependent networks is a unique contribution of this thesis.

The calculation of APEX values includes the probability of occurrence of the intensity maps used in the estimation, a feature that makes the resulting APEX-Systemic Performance pairs unconditional probabilistic estimates. This unconditional property represents a positive departure from the previous developments in this thesis which generated fragility estimates based on selected seismic scenarios, that is a few selected seismic intensity maps. The ASPIS (*Assessment of network-consistent Seismic exceedance Probabilities for Interdependent Systemic Performance*) algorithm described

in this chapter compiles the steps required for the generation of seismic intensity maps, the calculation of interdependent systemic performance (IFA algorithm), and the final calculation of APEX estimates for different levels of systemic performance. The fragility estimates obtained using this approach are unconditional properly include the probabilistic features of the seismic hazard and the inherent variability of component fragility and interdependence strength, properties that make these results suitable to be used in decision making regarding maintenance or intervention measures for interdependent urban infrastructure.

5.1.1 Importance Sampling procedure for the generation of hazard scenarios

Kroese et al. (2011) state that a *simple Importance Sampling* procedure transforms the integral in Eq. 5.1 into the expression in Eq. 5.2 through the multiplication and division by an auxiliary importance sampling density $g(x)$.

$$l = \mathbb{E}_f[H(X)] = \int H(x) f(x)\, dx \tag{5.1}$$

In Eq. 5.1, $\mathbb{E}$ stands for the first moment or expectation, H for a function whose expectation is of interest, and f for the nominal probability density function involved in the moment estimation. Its modified version is as shown below:

$$l = \int H(x) \frac{f(x)}{g(x)} g(x)\, dx = \mathbb{E}_g \left[H(X) \frac{f(X)}{g(X)} \right]. \tag{5.2}$$

If $X_1, \ldots, X_N$ are independent, identically distributed samples from $g(x)$, then the integral in Eq. 5.2 can be approximated as

$$\hat{l} = \frac{1}{N}\sum_{k=1}^{N} H(X_k)\frac{f(X_k)}{g(X_k)} \tag{5.3}$$

with $\hat{l}$ standing for an unbiased estimator of the expectation, and the ratio of densities $W_k = f(X_k)/g(X_k)$ identified as the *weight* or likelihood ratio for sample k, with k going from 1 to N, with N being the number of samples used in the approximation.

The formulae for the basic Importance Sample scheme can be extended to a *Weighted Importance Sample* (*WIS*) version after considering that $\mathbb{E}_g[W(X)] = 1$, (given that $f(X_k)$ is a probability density function) which allows for an alternative expression of the expectation in Eq. 5.2 as

$$l = \frac{\mathbb{E}_g[H(X)W(X)]}{\mathbb{E}_g[W(X)]} \tag{5.4}$$

with its estimator $\hat{l}$ expressed as in Eq. 5.5, which is the expression used in Jayaram and Baker (2010) for the definition of an unbiased estimator of a random variable using the importance sampling procedure.

$$\hat{l} = \frac{\sum_{k=1}^{N} H(X_k)w_k}{\sum_{k=1}^{N} w_k}. \tag{5.5}$$

Finally, if the sampling is done sequentially, the weight for a sample $X = (X_1, \ldots, X_n)$, with $f(X) = f_1(x_1)f_2(x_2|x_1)\ldots f_n(x_n|x_{1:n-1})$ and $g(X) = g_1(x_1)g_2(x_2|x_1)\ldots g_n(x_n|x_{1:n-1})$, is calculated as

$$W(x) = \frac{f_1(x_1)f_2(x_2|x_1)\ldots f_n(x_n|x_{1:n-1})}{g_1(x_1)g_2(x_2|x_1)\ldots g_n(x_n|x_{1:n-1})}. \tag{5.6}$$

The next section discusses the application of this Sequential Weighted Importance Sampling (SWIS) strategy for the estimation of the probabilistic performance of *sin-*

gle urban networks. The next section discuss the extension of this methodology to interdependent urban networks.

5.1.2 SWIS for systemic performance assessment

Jayaram and Baker (2010) use the indicator function $I(l_o)$ as the $H(X)$ target function [Eq. 5.1] to estimate the probability of a network exceeding the performance level l_o, $P(L \geq l_o)$, as defined by Eq. 5.7,

$$P(L \geq l_o) = \mathbb{E}\left[I(l \geq l_o)\right] = \int I(l(x) \geq l_o) f(x)\, dx \tag{5.7}$$

with $I(l \geq l_o)$ equal to zero for performance values smaller than the threshold l_o and one for values reaching or exceeding the same limit.

Using the approximation expression in Eq. 5.5 the estimator $\hat{P}$ of the APEX for l_o is (Eq. 5.8)

$$\hat{P}(L \geq l_o) = \frac{\sum_{k=1}^{N} I(l_k \geq l_o) w_k}{\sum_{k=1}^{N} w_k}. \tag{5.8}$$

Finally, Eq. 5.9 presents the expression for the variance of the estimator of the mean.

$$\mathrm{Var}[\hat{P}(L \geq l_o)] = \frac{\sum_{k=1}^{N} [I(l_k \geq l_o) w_k - \hat{P}(L \geq l_o)]^2}{(\sum_{k=1}^{N} w_k)(\sum_{k=1}^{N} w_k - 1)}. \tag{5.9}$$

The key requirements for the calculation of the mean and variance of $P(L \geq l_o)$ in the previous two equations are the values of l_k and w_k, the *specific systemic performance reduction calculated using a sampled map*, and the *weight or likelihood of the sampled map*, respectively. The first of these parameters can be calculated using the IFA algorithm introduced in Section 3, while the second parameter, the weight of

the sample map, depends on the sampling procedure used for the map's generation. The steps of this sampling procedure involved seismological concepts and a set of assumptions which are described in the next subsection.

5.1.3 Simulation of seismic intensity maps

The calculation of intensities for a seismic map is executed using a Ground Motion Model (GMM). A ground motion model is a mathematical model developed with the objective of obtaining seismic intensities based on the magnitude of an earthquake and the distance of its source from target locations.

In the procedure required to simulate a seismic map, the *first step* samples a magnitude from the probability distribution used to describe the capacity of a set of faults to generate earthquakes of different magnitudes [Fig. 5.1(b)]. Once magnitude and fault originating the earthquake are established, the GMM is employed to estimate the sought seismic intensities at the different network location required for running the IFA algorithm. The GMM used in this work follows the expression in Eq. 5.10:

$$\log(Sa_z) = \log(\overline{Sa}_z) + \sigma_z \epsilon_z + \tau_z \eta_z. \tag{5.10}$$

In Eq. 5.10, the seismic intensity of interest is the spectral acceleration Sa_z at a network component site z under a given earthquake magnitude and distance from the event source to the z site. The same formula with different internal parameters, applies for the estimation of other seismic intensity parameters including Peak Ground Velocity, PGV, or Peak Ground Acceleration, PGA.

The first term of Eq. 5.10 is the median value of seismic intensity which is calculated using a deterministic expression within the GMM model; the second term is the *intraevent* residual, and the third term is the *interevent* residual. Of the three

terms, the last two contain a random variable in the normalized parameters, ϵ, the intraevent residual, and, η, the interevent residual.

The *intraevent* residual term ($\sigma\epsilon$) attempts to capture intensity variability between different points (at different geographical locations) during the same earthquake event. The *interevent* residual term ($\tau\eta$) represents the intensity variability at same distances induced by different earthquake realizations (Wesson and Perkins, 2001). The estimation of the deterministic values of the standard deviation terms σ and τ depends on the intensity parameter (Sa, PGA, or PGV) and on the properties of the component at the location of interest (vibration period for Sa, for example). Both parameters σ and τ are provided by the GMM used in this work [See Boore et al. (2003)]. At the same time, ϵ and η are standard normal random variables from which a single realization is required for the evaluation of Eq. 5.10.

Typically, GMMs require the magnitude and the distance from the earthquake location to the network site [Fig. 5.1(b)]. Distances can be found using a GIS tool, while the magnitude sample requires a simulation draw. At the same time, such a draw requires the probability distribution of the *full fault set* inducing a given sampled magnitude m.

For a set of n_f fault sources with individual probability density functions (pdfs) for magnitude generation $f_j(m)$, the *complete* probability density $f(m)$ representing the potential of all seismogenic sources of inducing a given magnitude can be estimated using the total probability rule as shown in Eq. 5.11:

$$f(m) = \frac{\sum_{j=1}^{nf} \nu_j f_j(m)}{\sum_{j=1}^{n_f} \nu_j} \tag{5.11}$$

with ν representing the activity rates of each fault j, which can be estimated using

their seismological properties [See Youngs and Coppersmith (1985), Eq. 11].

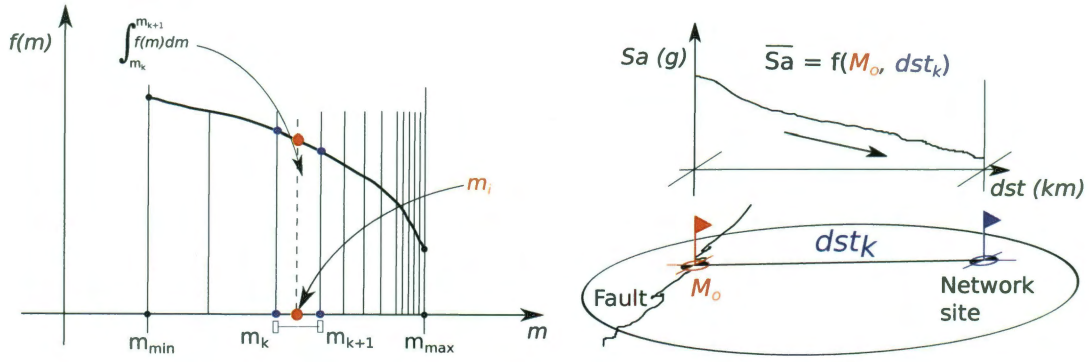

(a) Stratified Sampling (b) GMM illustration

Figure 5.1 : Generation of seismic intensity maps. a) Stratified sampling using $f(m)$ which focuses the sampling on large earthquake magnitudes; b) Interaction between magnitude (M_o), fault, and distance (dst_k) in a GMM for the estimation of seismic intensities (Sa in the image).

Regular sampling using $f(m)$ would produce samples of small magnitude with high probability of occurrence but limited impact on systemic performance equivalent to wasted computational resources. To counter this, the *first step* in the Sequential Weighted Importance Sampling (SWIS) procedure uses a sampling strategy that divides or *stratifies* the sampling domain of seismic magnitudes. Fig. 5.1(a) illustrates the stratification concept. In this division, a single magnitude sample m_i is taken from each sampling interval. The weight or likelihood ratio for each sampled magnitude m_i is calculated as (Eq. 5.12):

$$\frac{f(m_i)}{g(m_i)} = \frac{\int_{m_k}^{m_{k+1}} f(m)dm}{1/n_m} \tag{5.12}$$

with m_k and m_{k+1} defining the lower and upper bounds of the ith sampling interval, respectively. The integral on the numerator, the area under $f(m)$ for the interval $[m_k\ m_{k+1}]$ associated to m_i, corresponds to the likelihood of choosing a sample from

that particular interval, while the denominator specifies the probability of selecting any of the n_m sampled magnitudes. The probability in the numerator is controlled by $f(m)$, while the one in the denominator states that once sampled, the probability of choosing any of the sampled magnitudes is the same: $1/n_m$.

Once a magnitude is sampled, it is necessary to identify which fault from the fault set could cause the event. This second step in the SWIS strategy uses Bayes' theorem to calculate the probability of a fault j being the source of a known magnitude m as shown in Eq. 5.13:

$$f(j|m) = \frac{\nu_j f_j(m)}{\sum_{j=1}^{n_f} \nu_j f_j(m)}. \tag{5.13}$$

The partial weight associated to fault selection is calculated after considering that the value of $f(j|m)$ can be larger than zero for many of the faults, that is, there might be more than one potential source for the sampled magnitude as more than one fault could produce the sampled magnitude. If the total count of such *active* faults is $n_f(m)$, Eq. 5.14 shows the likelihood ratio for an individual fault j causing the sampled magnitude:

$$\frac{f(j|m)}{g(j|m)} = \frac{f(j|m)}{1/n_f(m)}. \tag{5.14}$$

For the two remaining terms of Eq. 5.10, $\sigma\epsilon$ and $\tau\eta$, the required samples for ϵ and η are taken from normal distributions, but their treatment differs for the intraevent and interevent terms. Jayaram and Baker (2008) showed that normalized intraevent residuals (ϵ) at k locations follow a multivariate normal distribution. In practice, this fact implies that obtaining intraevent samples requires a correlation matrix Σ. The same authors in Jayaram and Baker (2009) provide an expression for the estimation

of such correlation structure (Eq. 5.15),

$$\rho_{\epsilon_s \epsilon_t} = \exp(-3h/R) \tag{5.15}$$

with s and t standing for two different network sites, h the distance in km between the same sites, and R the distance parameter in km controlling the decay of spatial correlations. The values of ρ fill the off-diagonal locations of the correlation matrix Σ, while ones fill its diagonal. The value of the R parameter depends on the intensity measure of interest and different estimates are available in the literature (See Esposito and Iervolino (2011), or Goda and Hong (2008), for example). Based on these references, the R value used in the case study at the end of this chapter is fixed at 10 km. More information on the nature and estimation procedures for the R parameter can be found in the references cited above.

With the correlation structure available, the sampling of intraevent values is straightforward. However, conventional sampling from the standard multivariate normal distribution would produce an inefficient number of close-to-the mean samples. To address such situation, Jayaram and Baker (2010) propose a strategy based on shifting the mean by an ms_{intra} value, aiming to obtain samples more likely to induce significant changes on the seismic intensities. This third stage of the SWIS process generates a sample vector $\mathbf{e}$ sampling from the multivariate normal distribution with a vector of means ms_{intra} and the square correlation matrix Σ. The length of $\mathbf{e}$ and the numbers of rows of Σ are equal to the number of nodes in the network under study.

The weight for the third stage is shown in Eq. 5.16. In this case, the weight ratio can be interpreted as a correction factor between the original distribution and

the shifted one used for the sampling. Jayaram and Baker (2010) note that the shift value must be selected with care in order to obtain the desired outcome, and so they provide a diagram (not reproduced here. See Jayaram and Baker (2010), Fig. 1c) for obtaining ms_{intra} values as a function of the number of sites and the average distance between them.

$$\frac{f(\mathbf{e})}{g(\mathbf{e})} = \exp\left(\frac{1}{2}(\mathbf{e} - ms_{intra})^T\Sigma^{-1}(\mathbf{e} - ms_{intra}) - \frac{1}{2}\mathbf{e}^T\Sigma^{-1}\mathbf{e}\right). \tag{5.16}$$

Finally, a similar approach to sampling and weight calculation applies to the fourth SWIS stage: the interevent factor. First, note that because of its definition, the product in the interevent residual $\tau\eta$ must be held constant for all sites for a given seismic map. Given that values for τ are provided by the GMM as a function of the spectral period of the component at a site, the η values must be fixed to comply with the invariability requirement. Jayaram and Baker (2010) enforce the requirement by obtaining a simulated value $\mathbf{t}$ for one of the points (say $\mathbf{t_1}$, for site 1) and calculating the $\mathbf{t}_k$ values for the remaining sites as (Eq. 5.17)

$$\mathbf{t_k} = \frac{\tau_1}{\tau_k}\mathbf{t_1}. \tag{5.17}$$

The sampling itself of the first η ($\mathbf{t_1}$ in the previous illustration) is executed using a standard univariate normal distribution shifted by an amount ms_{inter} specified by Jayaram and Baker (2010) after numerical testing to be in the range between 0.5 and 1.0. The weight associated to the interevent residual including the shifting parameter is calculated using Eq. 5.18. The interpretation of the weight ratio as a correction factor is applied to this calculation as well.

$$\frac{f(\mathbf{t})}{g(\mathbf{t})} = \exp\left(\frac{1}{2}(\mathbf{t} - ms_{inter})^2 - \frac{1}{2}\mathbf{t}^2\right). \tag{5.18}$$

with $\mathbf{t}$ the interevent sample used as referent for the calculation of all other $\mathbf{t}$ values.

The four sequential weights obtained for each of the sampling stages can be compiled to form the weight of a given scenario S. From Eq. 5.5, the weight for scenario $S = (m, j, \mathbf{e}, \mathbf{t})$ can be written as (Eq. 5.19)

$$W(S) = \frac{f(S)}{g(S)} = \frac{f(m)f(j|m)f(\mathbf{e})f(\mathbf{t})}{g(m)g(j|m)g(\mathbf{e})g(\mathbf{t})}. \tag{5.19}$$

The previous discussion applies to the construction of a single intensity map. However, it is evident that the second step of the SWIS procedure, the Bayesian fault procedure, may lead to a family of maps branching out from a common magnitude sample. Moreover, the addition of the interevent and intraevent samples certainly creates additional cases branching out from a single magnitude-fault pair. If the sampling domain for magnitudes is divided in n_m intervals under the stratified sampling strategy, the number of faults is limited to n_f, and a n_{css} number of independent combinations of intraevent and interevent samples are considered, the maximum number of intensity maps to process for the sought APEX mean and variance estimates is equal to the product $(n_m)\,(n_f)\,(n_{css})$. This estimation provides valuable insight into the computational requirements of the SWIS procedure in the light of the additional expense implied by the use of the IFA algorithm for each of the sampled maps, in the quest for unconditional interdependent performance assessments.

5.1.4 Seismic intensity maps and interdependent systemic fragility assessment

The intensity maps and weights generated by the SWIS procedure are used as input to simulate interdependent systemic performance using the IFA algorithm. At this point, the simulation is handling two sources of uncertainty. The first source comes from the hazard simulation itself, and it is assessed by the SWIS process in the variance calculation of Eq. 5.9. A second source of uncertainty is caused by the fragilities of network components which is handled in the sampling procedures of the IFA algorithm.

For any given scenario, the systemic performance value obtained from applying an intensity map to network elements is a random variable itself. Furthermore, the intrinsic variability of such random variable becomes more intricate when interdependence effects on performance are considered. This variability requires an additional simulation plan to determine the mean and variance of the systemic performance, such as CL, under the intensity conditions presented in the map. When such process has been completed for all the intensity maps in the catalog, the triad a) intensity map, b) mean systemic performance, and c) map weight can be used for the APEX estimation in Eq. 5.8. The integration of the two simulation plans, seismic hazard sampling under the SWIS approach and the IFA algorithm the for a single map is presented in the *Assessment of network-consistent Seismic exceedance Probabilities for Interdependent Systemic Performance* ASPIS algorithm below. Note that steps 18 and 19 in ASPIS correspond to the execution of the IFA algorithm for interdependent systemic fragility estimation.

Algorithm 5.1 Assessment of network-consistent Seismic exceedance Probabilities for Interdependent Systemic Performance, ASPIS

1: Load seismological information of faults
2: Stratify magnitude domain
3: **for** each sample interval i **do**
4: Sample magnitude m_i using $f(m)$ (Eq.5.11) ▷ *SWIS step 1*
5: Calculate magnitude sampling weight $f(m_i)/g(m_i)$ (Eq. 5.12) ▷ *lines 4-5*
6: Identify potential fault sources for m_i (Eq. 5.13) ▷ *SWIS step 2*
7: **for** each potential source j **do** ▷ *lines 6-8*
8: Calculate partial weight $f(j|m)/g(j|m)$ (Eq. 5.14)
9: Obtain intraevent sample **e** from multivariate normal distribution with mean ms_{intra} and correlation Σ ▷ *SWIS step 3*
10: Calculate partial intraevent weight ▷ *lines 9-10* (Eq. 5.16)
11: Obtain interevent sample **t** from normal distribution $N(ms_{inter}, 1)$. ▷ *SWIS step 4*
12: Calculate partial interevent weight ▷ *lines 11-12* (Eq. 5.18)
13: Compute total weight for the scenario (Eq. 5.19)
14: Compute seismic intensities for all sites (Eq. 5.10)
15: **end for**
16: **end for**
17: **for** each hazard intensity map **do**
18: Provide seismic intensities at network sites as input for the IFA Algorithm
19: Estimate Mean Systemic Performance (MSP) for the map
20: Match MSP with scenario weight
21: **end for**
22: Estimate APEX using returned lists of MSPs and weights (Eq. 5.8)
23: Estimate APEX estimator's variance (Eq. 5.9)

5.2 Case Study 4: Interdependent Power and Water systems in an Actively Seismic Region

This case study applies the ASPIS algorithm to two interdependent urban networks, highlighting data requirements and procedural details. This section describes the

seismic hazard sources, the interdependent urban networks, and the interdependence characteristics used in the illustrative application example. The section concludes with the interpretation of the resulting plots of annual probabilities of exceedance (APEX) versus systemic performance curves for the two test networks, which are critical for risk-informed decision-making.

5.2.1 Generation of seismic intensity maps

The hazard source is a system of ten realistic, yet from an unspecified location, faults localized with respect to the test utility networks as shown in Fig. 5.2(a). For initial testing, the stratification of the range of magnitudes used 24 sampling intervals. The first six intervals, from magnitudes 5 to 7, are of the same magnitude, (0.33 width) while the remaining 18, from magnitudes 7 to 7.9, were of 0.05 width. The ms_{intra} and ms_{inter} used in the simulation of intraevent and interevent samples, respectively, were made equal to zero as no shifting is used for the sampling (ASPIS alg. steps 9, 11). This decision was made to reduce the complexity of the simulation procedure and seemed to have no impact on the resulting estimates obtained in this case study.

The seismic intensity values for the hazard maps (ASPIS alg. step 14) were obtained using the Ground Motion Model (GMM) proposed by Boore et al. (2003). The estimated PGAs and PGVs served as input to simulate seismic direct damage in nodes and links (IFA alg. steps 2 to 4).

For testing purposes, the total number of scenarios used in the simulation is the product of 24 sampled magnitudes, 10 faults, and 50 combinations of interevent and intraevent samples for a total of 12 000 seismic scenarios to explore. The total number of scenarios proved to be enough to provide stability in the performance estimates in this case study. For each of these scenarios, an independent simulation (IFA al-

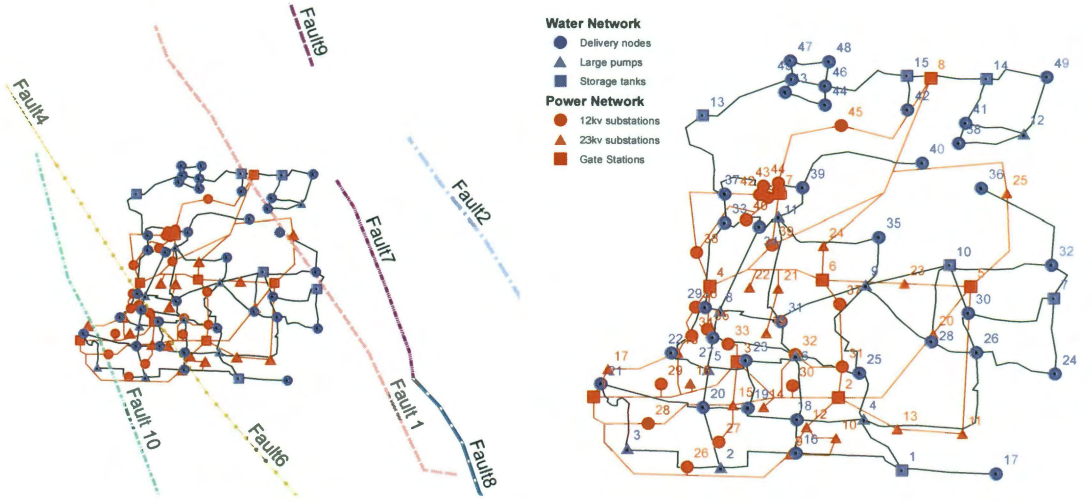

(a) Fault system (b) Test networks

Figure 5.2 : 5.2(a) Realistic faults and their relative unspecified location with respect to the test networks. 5.2(b) Test power and water networks with node IDNs and classification.

gorithm) took place to obtain the mean estimate of the interdependent systemic performance for the networks. This simulation used 500 CL samples to arrive to the final mean estimates used in Eq. 5.8 for APEX calculations.

This fourth test case explores interdependence effects by generating scenarios with complete absence, $Istr = 0$, and full effect of interdependence, $Istr = 1.0$. For simplicity one single $Istr$ value, either zero or one, is extended to all interdependence links in a single scenario. Naturally, the procedure allows the inclusion of independent $Istr$ values for each of the interdependence links in the simulated urban networks.

5.2.2 Results and discussion

Fig. 5.3 presents plots of Annual Probability of EXceedance (APEX) for different systemic performance (CL) levels under three scenarios. The scenario in Fig. 5.3(a) considers $Istr = 1.0$ and includes the effects of water link failures (See section 4.2).

Fig. 5.3(b) shows APEX results for a $Istr = 0$ scenario with water link failures considered, while Fig. 5.3(c) shows estimates for $Istr = 0$ omitting water link failures. The inclusion of the water link failures factors in the scenarios serves two purposes. First, it improves over an important factor not included by Hernandez-Fajardo and Dueñas-Osorio (2011) in their original IFA algorithm; and second, it exhibits the influence of proper *independent* systemic characterization on probabilistic *interdependent* performance.

The plots in Fig. 5.3 can be studied in pairs. A first study set, Set 1, contrasts Figs. 5.3(a) and Fig 5.3(b), with their difference [Fig 5.3(a) - Fig 5.3(b)] presented in Fig. 5.4(a). The two scenarios in Set 1 include the link failure factor but differ in their interdependence level, $Istr = 1.0$ for Fig 5.3(a) and $Istr = 0.0$ for Fig. 5.3(b). This difference in $Istr$ allows Set 1 to display the influence of interdependence effects on unconditional systemic performance. Fig 5.4(a) presents four trends. First, the APEX differences are all positive, meaning that the situation in Fig 5.3(a) is worse than the one in Fig. 5.3(b). Second, the APEX differences are mostly constant along the CL range, but such difference become smaller for larger CL values. It is also clear from the individual figures that the variance of the estimator becomes important for the same, large CL performance values. Third, the APEX differences are larger for the water system for most of the CL range (0 to 0.8) reflecting a larger impact of interdependence in the water network's APEXs than on the power system's performance. Finally, the largest APEX differences are 0.0158 at $CL = 0.35$ for the power network and 0.0566 at $CL = 0.3$ for the water system.

A second study set, Set 2, contrasts the scenarios in Figs. 5.3(a) and 5.3(c). The differences between the two scenarios are presented in Fig. 5.4(b). Set 2 examines the APEX changes brought by full interdependence and water link failures to the net-

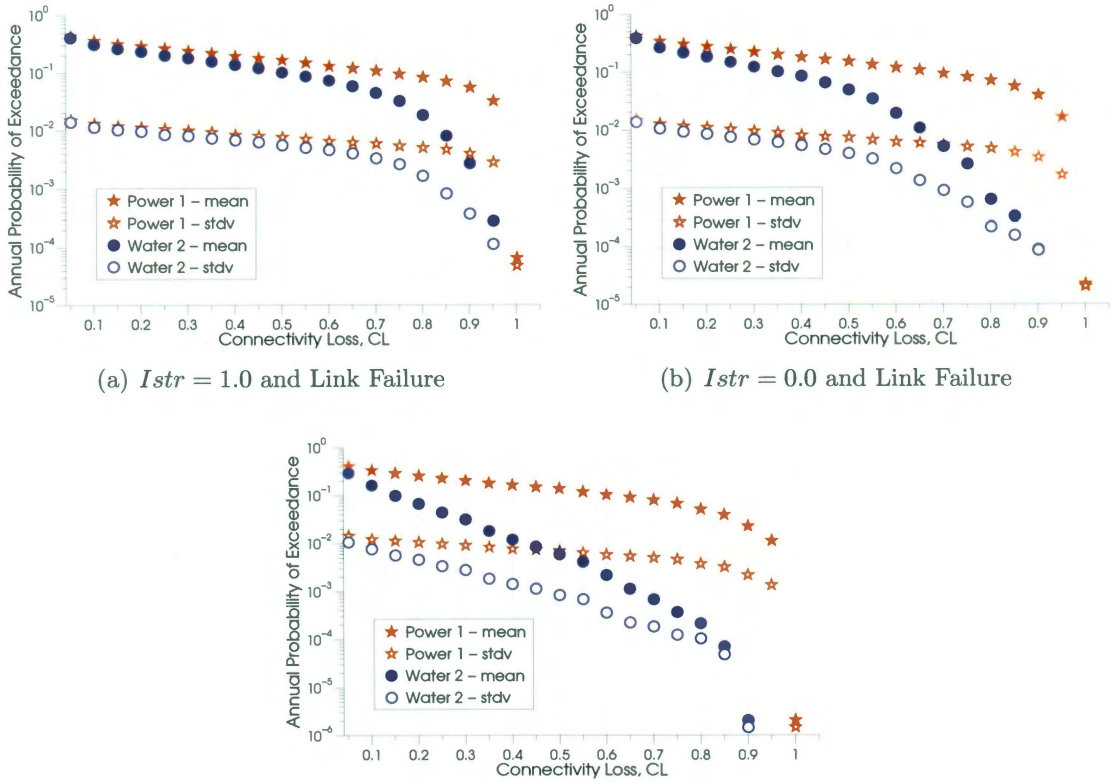

(a) $Istr = 1.0$ and Link Failure

(b) $Istr = 0.0$ and Link Failure

(c) $Istr = 0.0$ and No Link Failure

Figure 5.3 : Summary of Annual Probabilities of test Power (S_1) and Water (S_2) networks exceeding Connectivity Loss (CL) values for a) $Istr = 1.0$ and link failure, b) $Istr = 0.0$ and link failure, and c) $Istr = 0.0$ and no link failure. The inclusion of link failures and interdependence damage propagation increases significantly the water network's APEX values. In contrast, the systemic performance of the power network shows limited sensibility to interdependent effects from the water network.

work' systemic performance. Fig. 5.4(b) shows that these factors have an important influence on the water network, inducing a maximum APEX difference of 0.166 at $CL = 0.3$. It is clear from the same figure that the APEX differences decrease as CL increases, a trend also observed in Set 1. For the power network, the APEX differences behave similarly to Set 1 remaining almost constant with a maximum difference of 0.038 at $CL = 0.35$ and decreasing sharply at the largest CL values.

Finally, Set 3 compares Fig. 5.3(b) with Fig. 5.3(c). This set measures the effect of the water link failures factor in the independent networks. The first trend from Fig. 5.4(c) is that including link failures increases the APEX values for the water network, in this set up to a maximum APEX difference between the link-failures scenario (Fig. 5.3(b)) and no-link-failures scenario (Fig. 5.3(c)) of 0.1194 at $CL = 0.15$. The results for the power network are interesting as no differences should occur for this set ($Istr = 0$). The differences observed can be attributed to the internal variability of the systemic performance estimation, specifically the variability of the mean CL estimates used in the ASPIS algorithm (Step 19).

The trends observed from the three comparison sets provide support for three statements for this case study. First, from Sets 2 and 3, it is clear that considering water link failures increases the APEX for the water network. This fact emphasizes the need for proper modeling of independent networks as a first basic step for more complex analysis. Second, from Sets 1 and 2, interdependent effects have a clear effect on the water network in which the maximum APEX difference increased from 0.056 to 0.166. Moreover, these sets support the hypothesis that interdependence effects induce more damage in dependent networks with a considerable level of fragility of their own even when accounting for the considerable joint uncertainty of hazard and vulnerability. Finally, the power network also shows higher APEX values in both Sets 1 and 2, but the magnitude of the change is never as large as for the water network. Indeed, the power network profile in the plots of Fig. 5.3 changes very little for all scenarios and the APEX differences remain in the 10^{-2} range in all study sets. This behavior supports the notion of an effectively decoupled power network as a result of its larger component-level fragility. Hernandez-Fajardo and Dueñas-Osorio (2011), using the same test networks, propose a similar explanation based on results

from scenario-based earthquakes. In the light of this similarity, it is important to note that the results just described are unconditional systemic performance estimates independent from fixed scenario events and hence ready to use in risk-based decision-making, and mitigation analysis, while accounting for life-cycle costs.

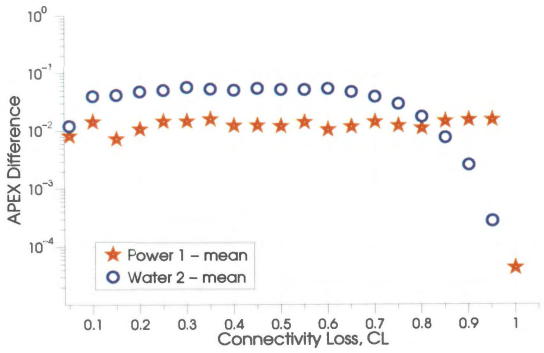

(a) Set 1: Fig. 5.3(a) - Fig. 5.3(b)

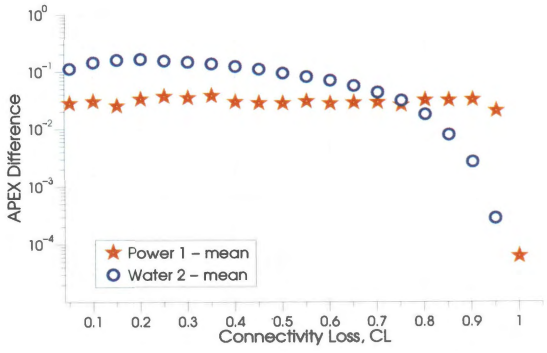

(b) Set 2: Fig. 5.3(a) - Fig. 5.3(c)

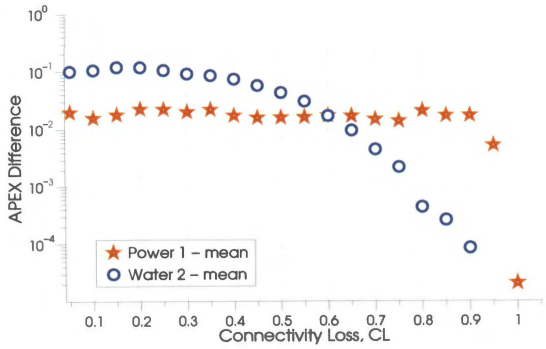

(c) Set 3: Fig. 5.3(b) - Fig. 5.3(c)

Figure 5.4 : APEX differences for comparative sets 1 through 3. Set a) comparison of Figures 5.3(a) and 5.3(b); b) comparison of figures 5.3(a) and 5.3(c); and c) comparison of figures 5.3(b) and 5.3(c).

Chapter 6

Conclusions and Future Research

The study of the fragility of critical infrastructure is a basic task for private managers and public stakeholders alike. The productivity of cities and the well-being of urban populations depend on the protection and continuous operation of infrastructure urban networks like the power grid, the gas infrastructure, or the water delivery systems. Their expansion, induced by growing urban population all over the world, has lead to an explosion in their interdependence, a phenomenon that although essential for their normal functionality becomes a path for fragility interchange between systems in the event of external perturbation. This thesis focused on the study of the effects of interdependence on the fragility of urban systems subjected to the action of earthquake perturbation. Such study was performed from the perspective of modeling interdependent infrastructure networks using a complex systems approach, that is using mathematical graphs, nodes and links representing network facilities and their communicating elements, for the representation of the structure, properties, and response of real systems. The contributions in this thesis included 1) the development of the Interdependence Fragility Assessment (IFA) methodology to describe perturbation action, internal damage propagation, and interdependence effects on interacting networks; 2) the use of the proposed IFA methodology to test the effects of cascading failures and local redundancy enhancement (LRE) on the fragility of interdependent networks; 3) test of conceptual fragility mitigation policies such as component fragility reduction (CFR), and interdependence redundancy enhancement (IRE) for interde-

pendent fragility reduction; and 4) the development of a methodology that combines a mechanism to sample probabilistic earthquake hazards with the IFA methodology for the generation of unconditional interdependent systemic fragility estimates useful for risk assessment and decision making. In additional work independent from the results in this thesis, Wu and Dueñas-Osorio (2012) applied the IFA algorithm to a model of interdependent networks affected by earthquake hazard in the aftermath of the 2010 Chile earthquake. The cited work produced supportive outcomes in terms of the predictive accuracy of the IFA estimates with respect to the actual levels of disruption observed in the real networks.

The previous developments are explained in more detail in the following paragraphs. The first development advanced previous research by proposing a numerical simulation strategy called Interdependent Fragility Assessment (IFA) algorithm. The IFA algorithm simulates internal damage propagation, interdependent damage transmission, and failure feedback between interconnected networks subjected to earthquake action. The element of failure feedback was not explored by previous research and was shown to have only a marginal influence on test interdependent fragility estimates.

The second development combined the IFA algorithm tool with a strategy to model the occurrence of operational cascading failures on infrastructure networks. This effort tested the influence of two combined negative effects, interdependence and cascading failures, on systemic fragility, and also evaluated the effectiveness of local redundancy enhancement (LRE) as a measure of systemic fragility control. Cascading failures and interdependence effects were found to work together to worsen fragility estimates when urban networks were exposed to seismic hazards. Also, the local redundancy mitigation policy proved to be of limited effect against cascading

failures, especially in the event of seismic scenarios of high intensity (Peak Ground Acceleration, PGA in the second case study in this thesis). The effect of local redundancy was also limited on its control of global interdependence effects and hence alternative mitigation measures were proposed and examined.

The third work explored mitigation alternatives for interdependent fragility reduction. Two mitigation strategies were tested: Component Fragility Reduction (CFR) program and Interdependence Redundancy Enhancement (IRE) policies. The application of the IRE policy used an alternative interdependent failure propagation paradigm for the IFA algorithm. In a critical development, a new paradigm of interdependence propagation, *failure avoidance*, replaced the original failure transmission model and was successful on guiding the reduction of interdependent effects on systemic fragility. Both mitigation strategies produced considerable fragility reductions, but the CFR mitigation policy consistently outperformed the IRE policy. Nevertheless, $CFR + IRE$ combinations showed comparable outcomes highlighting their potential in terms of investment impact by addressing single system fragility reductions as well as interdependence-induced fragility reductions, without being as intensive as CFR-only mitigation actions.

The four and final development combined an existing methodology for sampling seismic hazard induced by seismic faults with the IFA algorithm to use probabilistic seismic hazard descriptions on the assessment of systemic fragility to facilitate risk-based decision making. The application of the new hybrid methodology allowed the estimation of annual probabilities of exceedance for systemic fragility values. The trends and variations observed in the fragility estimations provide unconditional information beyond the scope of scenario-based analysis used in previous efforts in the field, and make the results informative for life-cycle and other long-term decision

making planning, retrofit, and growth evaluations.

This summary shows new contributions and consolidation of the understanding of the factors and interactions likely to have an impact on the fragility of complex urban networks. In all these developments the estimation of fragility is the key objective and the IFA algorithm is the main synthesizing tool. A detailed review of the IFA algorithm's structure as a central contribution of this thesis reveals its key building blocks and how such critical portions influenced the developments in this thesis; such review is presented below.

The IFA algorithm first models direct damage created by hazard action; internal damage propagation in all networks is the next step; while the main procedure corresponds to the simulation of interdependence damage propagation. These steps are followed by the estimation of systemic performance, the final product of the simulation procedure which is used for the generation of systemic fragility estimates. Each of these stages contains an operational principle and a set of key assumptions explored in detail throughout the thesis. The first stage is associated to the model of hazard impacts on network components. Three of the four efforts in this thesis used a selection of seismic scenarios which are useful to quantify the impacts of interdependence and the effects of local seismic fragility. However, the fourth contribution proposed a hybrid procedure to include fully probabilistic seismic hazard descriptions on the study of interdependent systemic fragility. Such studies provide the right type of information that decision-makers should use for investment allocations instead of the conditional estimates provided by single scenario results.

The second IFA stage controls internal damage propagation. The original IFA algorithm included disconnection failures as an internal mechanism, but the second contribution incorporated an important discussion on the issue of cascading failures,

a factor assessed before for independent networks but new to the study of the fragility of interdependent urban infrastructure.

The third IFA stage considers interdependence effects. Interdependence is represented in this thesis using interdependence links connecting nodes in interacting systems and establishing a dependence relationship between a master provider node in one system and a slave recipient node in an external network. The event of failure of the master node in the relationship triggers the potential of observing an external node failing due to the elimination of a vital external provider. Such type of failure is said to occur due to interdependence effects. Of key importance, an inherently negative paradigm, *failure transmission*, for interdependence simulation used in the first two contributions and based on previous research in the field was replaced in the third contribution by an alternative paradigm, *failure avoidance*, that highlights the advantages brought by interdependence in terms of alternative supply sources to dependent infrastructure nodes.

The final step of the process of the IFA algorithm is the calculation of systemic performance. The objective of such step is the measure of the reduction of systemic performance induced by the cumulative action of the previous stages of the IFA algorithm. The way of calculating such reduction in the case studies in this thesis was through measuring the reduction of internal connecting paths between the supply and consumption nodes of the studied urban networks using a metric called Connectivity Loss, CL. Connectivity Loss averages the connectivity reductions experienced by consumption nodes in a network after the action of perturbation. The probability of reaching or exceeding a CL level determines the fragility of a system to the cumulative action of initial perturbation, internal damage propagation and interdependent effects. It should be noted that although all result reported in this thesis used CL,

the proposed IFA algorithm is inherently independent of the mechanism selected for measuring systemic performance degradation and systemic fragility.

The previous descriptions show the guiding role of the IFA algorithm in the developments presented in this work. However, of equal relevance is the discussion of its assumptions and limitations. A key feature of the IFA algorithm is its *simultaneity* assumption. This assumption states that the operation of internal systemic update occurs in parallel in all analyzed networks, i.e., all processes of systemic update and systemic disruption occur at the same time for all networks without any single network leading any of such processes. In a similar manner, failures in external networks due to interdependence are stored temporarily during an updating cycle (Section 3.1) and are only propagated after all sources of interdependent failures have been examined. These assumptions ease the comprehension of the updating process as well as its computational demand for practical implementation. However, it is possible to consider interdependence interactions in which such assumptions do not hold. Whether differences in the relative times of systemic update interdependence failure propagation have an impact in the assessment of systemic fragility is a matter that demands physics-based models including not only an explicit time factor of flow dynamics, but also an analysis of the variations of supply and demand for the networks affected by seismic hazard. An exploratory work on this subject using seismic scenarios and three interacting networks with equal propagation times tested alternative orderings in the propagation of interdependent damage finding only marginal differences in the resulting fragility estimates; hence, the instantaneous approach could be used as an initial interaction description paradigm fragility assessment studies.

The previous point leads naturally to the issue of the details of systemic characterizations. This thesis represented networks using enriched graph representations

capturing the structure of connections between components as well as the individual fragilities that are the basic sources of systemic fragility. This representation is both efficient and sufficient for first-level analysis of connectivity-based fragility. However, public decision-makers and private stakeholders interests may be closer to alternative ways of measuring systemic fragility and their forecasts. Probabilistic estimations of number of customers affected and their spacial distributions may be a key target for public decision-makers as such quantities and allocations may influence their estimates of expected perceived damage and of the investment amounts required for retrofitting and emergency planning. The same type of forecast holds critical value for private stakeholders in terms of investment decisions, degree of interaction required between utility managers, demands for alternatives supply sources, and the expected amount of resources required to revert networks to their original condition after a perturbation event. Such outcome types could be modeled to a proper accuracy level only by using physics-based models of the typical operational conditions of the networks involved in a clearly circumscribed realistic urban scenario. Note that the IFA methodology still applies for such models and that the level of detail required at each of its steps increases with the demand level requested by the purposes of the analysis.

The two key challenges of such realistic scenarios are the data requirements and the amount of computational resources required. For the first point, it is reasonable to expect that such an ambitious analysis could only be executed with the willing participation of the different utility administrations involved and hence the issue of data requirement would only be a partial obstacle. For the second point, the study of systemic response using physics-based models will surely require a considerable investment of computational resources used mainly for the purpose of simulation. This constraint is clear but given the inherent parallel nature of simulation, the time

required to obtain the sought results depends mostly on the development resources allocated by the interested parties.

Finally, and beyond the IFA algorithm and the analysis of interdependent systemic fragility, the issue of fragility mitigation links modeling to practice. The fragility mitigation measures tested in this study were of two kinds: component intervention and interdependent interface intervention. These mitigation types represent indeed the basic structures that can be altered in networked systems, but more complex techniques may be tested according to the different profiles and interests of a of a decision-maker. Targeted survival, for example, is an interesting policy in which during a perturbation scenario resources are mobilized from certain zones to support others in more critical condition. Hospitals, government offices, and other key facilities may be ring-fenced during a scenario through adequate design and retrofitting of key points within a network. For each of these mitigation policies a key constraint exists: investment efficiency. The assessment of different ways of implementing a policy to find out which specific mechanism provides the best cost-benefit ratio is a key goal that in order to be achieved requires a clear understanding of the cost-structures of the different intervention steps. Furthermore, cost-benefit ratios should be extended to include the life-cycle costs of such mitigation mechanisms so that the important costs of maintenance and operation are signaled and included in the pre-decision assessments.

Additional topics for future work are: 1) inclusion of an alternative model of cascading failures effects based on more realistic flow analysis; 2) analysis of optimal intervention strategies including realistic cost structures and life-cycle requirements; 3) extension of the interdependence model to include the effects of alternative types of hazards, like hurricanes or flooding; 4) use of the probabilistic hazard model developed

in the fourth contribution for the study of the effectiveness of mitigation policies; and 5) execution of interdependent systemic fragility studies for theoretical models of urban networks.

Finally, it is worthy to state that currently researchers working in projects in the US (Tang et al., 2009) developing standards for the design of interdependent lifelines, the EU (Poljanšek et al., 2012), studying the interdependent fragility of interconnected energy grids, and the UK (Hall et al., 2012), aiming to adequate the local infrastructure to future challenges, are likely to adapt the basic ideas proposed in this research to gain insights in and benchmark the systemic behavior and response of diverse sets of interdependent infrastructure networks.

References

Abraham, J. (1979). An improved algorithm for network reliability. *Reliability, IEEE Transactions on R-28*(1), 58–61.

Adachi, T. and B. R. Ellingwood (2008). Serviceability of earthquake-damaged water systems: Effects of electrical power availability and power backup systems on system vulnerability. *Reliability Engineering & System Safety 93*(1), 78 – 88.

Adachi, T. and B. R. Ellingwood (2009a). Serviceability assessment of a municipal water system under spatially correlated seismic intensities. *Computer-Aided Civil and Infrastructure Engineering 24*(4), 237–248.

Adachi, T. and B. R. Ellingwood (2009b). Serviceability assessment of electrical power transmission systems under probabilistically stated seismic hazards: case study for Shelby County, Tennessee. *Structure and Infrastructure Engineering 5*(5), 343–353.

Ahuja, R. K., T. L. Magnanti, and J. B. Orlin (1993). *Network flows: theory, algorithms, and applications.* Prentice Hall, Englewood Cliffs, N.J.

Albert, R., I. Albert, and G. L. Nakarado (2004). Structural vulnerability of the North American power grid. *Phys. Rev. E 69*(2), 025103.

Albert, R., H. Jeong, and A.-L. Barabasi (2000). Error and attack tolerance of complex networks. *Nature 406*(6794), 378–382.

Amaral, L. A., A. Scala, M. Barthélémy, and H. E. Stanley (2000). Classes of small-world networks. *Proceedings of the National Academy of Sciences 97*(21), 11149–11152.

American Society of Civil Engineers, ASCE (2009). *Report Card for America's Infrastructure.* American Society of Civil Engineers.

Amin, M. (2000a). National infrastructures as complex interactive networks. In T. Samad and J. Weyrauch (Eds.), *Automation, Control, and Complexity: An Integrated Approach*, pp. 263–286. John Wiley and Sons.

Amin, M. (2000b). Toward self-healing infrastructure systems. *Computer 33*(8), 44–53.

Arthur, W. B. (1991). Designing economic agents that act like human agents: A behavioral approach to bounded rationality. *The American Economic Review 81*(2), pp. 353–359.

Barabási, A.-L. and R. Albert (1999). Emergence of scaling in random networks. *Science 286*(5439), 509–512.

Barker, K. and J. R. Santos (2010). A risk-based approach for identifying key economic and infrastructure systems. *Risk Analysis 30*(6), 962–974.

Barrat, A., M. Barthlemy, and A. Vespignani (2008). *Dynamical Processes on Complex Networks.* New York, NY, USA: Cambridge University Press.

Bellman, R. (1957). *Dynamic Programming.* Princeton University Press.

Bellman, R. (1958). On a routing problem. *Quart. Appl. Math. 16*, 87–90.

Bonabeau, E. (2002). Agent-based modeling: Methods and techniques for simulating human systems. *Proceedings of the National Academy of Sciences of the United States of America 99*(Suppl 3), 7280–7287.

Boore, D. M., J. F. Gibbs, W. B. Joyner, J. C. Tinsley, and D. J. Ponti (2003). Estimated Ground Motion From the 1994 Northridge, California, Earthquake at the Site of the Interstate 10 and La Cienega Boulevard Bridge Collapse, West Los Angeles, California. *Bulletin of the Seismological Society of America 93*(6), 2737–2751.

Brandes, U. (2001). A faster algorithm for betweenness centrality. *Journal of Mathematical Sociology 25*, 163–177.

Buldyrev, S. V., R. Parshani, G. Paul, H. E. Stanley, and S. Havlin (2010). Catastrophic cascade of failures in interdependent networks. *Nature 464*, 1025–1028.

Cadini, F., E. Zio, and C.-A. Petrescu (2009). *Using Centrality Measures to Rank the Importance of the Components of a Complex Network Infrastructure*, pp. 155–167. Berlin, Heidelberg: Springer-Verlag.

Callaway, D. S., M. E. J. Newman, S. H. Strogatz, and D. J. Watts (2000). Network robustness and fragility: Percolation on random graphs. *Phys. Rev. Lett. 85*(25), 5468–5471.

Chang, S., T. McDaniels, J. Mikawoz, and K. Peterson (2007). Infrastructure failure interdependencies in extreme events: power outage consequences in the 1998 Ice Storm. *Natural Hazards 41*, 337–358.

Cohen, R., K. Erez, D. ben Avraham, and S. Havlin (2000). Resilience of the Internet to Random Breakdowns. *Phys. Rev. Lett. 85*, 4626–4628.

Cohen, R., K. Erez, D. ben Avraham, and S. Havlin (2001). Breakdown of the Internet under Intentional Attack. *Phys. Rev. Lett. 86*(16), 3682–3685.

Congress Budget Office (2008). Testimony before the Committee on the Budget and the Committee on Transportation and Infrastructure, U.S. House of Representatives. Technical report, CBO.

Crowley, H. and J. Bommer (2006). Modelling seismic hazard in earthquake loss models with spatially distributed exposure. *Bulletin of Earthquake Engineering 4*, 249–273.

Crucitti, P., V. Latora, and M. Marchiori (2004). Model for cascading failures in complex networks. *Phys. Rev. E 69*(4), 045104.

Crucitti, P., V. Latora, M. Marchiori, and A. Rapisarda (2004). Error and attack tolerance of complex networks. *Physica A 340*, 388–394.

Davis, T., H. Rogers, C. Shays, H. Bonilla, S. Buyer, S. Myrick, M. Thornberry, K. Granger, C. Pickering, B. Shuster, and J. Miller (2006). A Failure of Initiative: Final Report of the Select Bipartisan Committee to Investigate the Preparation for and Response to Hurricane Katrina. Technical report, US House of Representatives.

Diestel, R. (2005). *Graph Theory* (Third ed.), Volume 173 of *Graduate Texts in Mathematics*. Springer-Verlag, Heidelberg.

Dijkstra, E. W. (1959). A note on two problems in connexion with graphs. *Numerische Mathematik 1*, 269–271.

Dueñas-Osorio, L., J. Craig, and B. Goodno (2007). Seismic response of critical

interdependent networks. *Earthquake Engineering & Structural Dynamics 36*(2), 285–306.

Dueñas-Osorio, L. and A. Kwasinki (2010). Quantification of lifeline system interdependencies after the 27 February 2010 M_w 8.8 offshore Maule, Chile earthquake. Earthquake Spectra. In press.

Dueñas-Osorio, L. and J. Rojo (2011). Reliability assessment of lifeline systems with radial topology. *Computer-Aided Civil and Infrastructure Engineering 26*(2), 111–128.

Dueñas-Osorio, L. and S. M. Vemuru (2009). Cascading failures in complex infrastructure systems. *Structural Safety 31*(2), 157 – 167.

EERI (2010). The Mw 8.8 Chile Earthquake of February 27, 2010. Technical report, Earthquake Engineering Research Institute. Available online at http://bit.ly/dV6hTP. Retrieved on 01/20/2012.

Ehlen, M. and A. Scholand (2005). Modeling interdependencies between power and economic sectors using the n-able agent-based model. In *Power Engineering Society General Meeting, 2005. IEEE*, pp. 2842 – 2846.

Eidinger, J., A. Tand, and T. O'Rourke (2010). Report of the 4 September 2010 Mw 7.1 Canterbury (Darfield), New Zealand Earthquake. Technical report, Technical Council on Lifeline Earthquake Engineering. Available online at http://bit.ly/xOjRui. Retrieved on 01/20/2012.

Ellingwood, B. R., D. V. Rosowsky, Y. Li, and J. H. Kim (2004). Fragility assessment of light-frame wood construction subjected to wind and earthquake hazards. *Journal of Structural Engineering 130*(12), 1921–1930.

Elnashai, A., L. Cleveland, T. Jefferson, and J. Harrald (2009). Impact of new madrid seismic zone earthquakes on the central usa, vol. 1 and 2. Technical report, Mid-America Earthquake Center.

Erdős, P. and A. Rényi (1958). On random graphs. *Publicationes Mathematicae Debrecen 6*, 290–297.

Esposito, S. and I. Iervolino (2011). PGA and PGV Spatial Correlation Models Based on European Multievent Datasets. *Bulletin of the Seismological Society of America 101*(5), 2532–2541.

Federal Emergency Management Agency (2003). *HAZUS-MH MR4 Technical Manual.* Washington D.C.: Federal Emergency Management Agency.

Ford, L. R. and D. R. Fulkerson (1956). Maximal flow through a network. *Canadian Journal of Mathematics 8*, 399–404.

Freeman, L. (1977). A set of measures of centrality based on betweenness. *Sociometry 40*(1), 35–41.

Freeman, L. C. (1979). Centrality in social networks: Conceptual clarification. *Social Networks 1*, 215– 239.

Goda, K. and H. P. Hong (2008). Spatial correlation of peak ground motions and response spectra. *Bulletin of the Seismological Society of America 98*(1), 354–365.

Gombèrg, J. and E. Schweig (2006). Earthquake hazard in the heart of the homeland. Technical report, U.S. Geological Survey.

Haimes, Y. and P. Jiang (2001). Leontief-based model of risk in complex interconnected infrastructures. *Journal of Infrastructure Systems 7*(1), 1–12.

Hall, J., J. Henriques, A. Hickford, and R. Nicholls (2012). A fast track analysis of strategies for infrastructure provision in great britain: Technical report. Technical report, Environmental Change Institute, University of Oxford.

Healy, P. M. and K. G. Palepu (2003). The Fall of Enron. *The Journal of Economic Perspectives 17*(2), pp. 3–26.

Hernandez-Fajardo, I. and L. Dueñas-Osorio (2011). Sequential Propagation of Seismic Fragility across Interdependent Lifeline Systems. *Earthquake Spectra 27*(1), 23–43.

Hines, P., E. Cotilla-Sanchez, and S. Blumsack (2010). Do topological models provide good information about electricity infrastructure vulnerability? *Chaos 20*(3), 033122.

Holland, J. H. (2006). Studying complex adaptive systems. *Journal of Systems Science and Complexity 19*(1), 1–8.

Holme, P., B. J. Kim, C. N. Yoon, and S. K. Han (2002). Attack vulnerability of complex networks. *Phys. Rev. E 65*, 056109.

Hwang, H. H. M., H. Lin, and M. Shinozuka (1998). Seismic performance assessment of water delivery systems. *Journal of Infrastructure Systems 4*(3), 118–125.

Idriss, I. and R. Boulanger (2008). *Soil liquefaction during earthquakes.* Oakland, CA: Earthquake Engineering Research Institute. Monograph MNO-12.

International Energy Agency (2010). Key world energy statistics. Technical report, International Energy Agency, IEA.

Jayaram, N. and J. Baker (2010). Efficient sampling and data reduction techniques for probabilistic seismic lifeline risk assessment. *Earthquake Engineering & Structural Dynamics 39*(10), 1109–1131.

Jayaram, N. and J. W. Baker (2008). Statistical tests of the joint distribution of spectral acceleration values. *Bulletin of the Seismological Society of America 98*(5), 2231–2243.

Jayaram, N. and J. W. Baker (2009). Correlation model for spatially distributed ground-motion intensities. *Earthquake Engineering & Structural Dynamics 38*(15), 1687–1708.

Johansson, J. and H. Hassel (2010). An approach for modelling interdependent infrastructures in the context of vulnerability analysis. *Reliability Engineering & System Safety 95*(12), 1335 – 1344.

Jones, L., R. Bernknopf, D. Cox, J. Goltz, K. Hudnut, D. Mileti, S. Perry, D. Ponti, K. Porter, M. Reichle, H. Seligson, K. Shoaf, J. Treiman, and A. Wein (2008). The shakeout scenario. Usgs open file report 2008-1150. cgs preliminary report 25. version 1.0, U.S. Geological Survey and California Geological Survey.

Kang, W., J. Song, and P. Gardoni (2008). Matrix-based system reliability method and applications to bridge networks. *Reliability Engineering System Safety 93*(11), 1584–1593.

Kim, Y., J. Song, B. Spencer, and A. Elnashai (2010). Seismic risk assessment of complex interacting infrastructures using matrix-based system reliability method. In *Safety, Reliability and Risk of Structures, Infrastructures and Engineering Systems*, pp. 2889–2893. Taylor and Francis Group, London.

Kim, Y., B. Spencer, A. Elnashai, and J. Song (2009). Seismic performance assessment of interdependent lifeline systems. *International Journal of Engineering Under Uncertainty: Hazards, Assessment, and Mitigation 1*(3-4), 173–181.

Kiremidjian, A., E. Stergiou, and R. Lee (2007). *Issues in seismic risk assessment of transportation networks*, Volume 6, pp. 461 – 480. Springer Netherlands.

Kroese, D. P., T. Taimre, and Z. I. Botev (2011). *Handbook of Monte Carlo methods.* Wiley, New Jersey.

Lee, E. E., J. E. Mitchell, and W. A. Wallace (2007). Restoration of services in interdependent infrastructure systems: A network flows approach. *IEEE Transactions on Systems, Man, and Cybernetics, Part C 37*(6), 1303–1317.

Leontief, W. (1986). *Input-output economics.* New York: Oxford University Press.

Li, J. and J. He (2002). A recursive decomposition algorithm for network seismic reliability evaluation. *Earthquake Engineering & Structural Dynamics 31*(8), 1525–1539.

Liscouski, B. and W. Elliot (2004). Final Report on the August 14, 2003 Blackout in the United States and Canada: Causes and Recommendations. Technical report, U.S.-Canada Power System Outage Task Force.

Matrosov, A., E. Rodionov, D. Harley, and J. Malcho (2011). Stuxnet Under The Microscope. Technical report, ESET.

McDaniels, T., S. Chang, K. Peterson, J. Mikawoz, and D. Reed (2007). Empirical framework for characterizing infrastructure failure interdependencies. *Journal of Infrastructure Systems 13*(3), 175–184.

Mei, S., F. He, X. Zhang, S. Wu, and G. Wang (2009). An improved OPA model and blackout risk assessment. *Power Systems, IEEE Transactions on 24*(2), 814 –823.

Mosleh, A. and G. Apostolakis (1986). The assessment of probability distributions from expert opinions with an application to seismic fragility curves. *Risk Analysis 6*(4), 447–461.

Motter, A. E. and Y.-C. Lai (2002). Cascade-based attacks on complex networks. *Phys. Rev. E 66*(6), 065102.

Newman, M. (2010). *Networks: An Introduction.* New York, NY, USA: Oxford University Press, Inc.

Nielson, B. and R. DesRoches (2007). Analytical seismic fragility curves for typical bridges in the central and southeastern united states. *Earthquake Spectra 23*(3), 615–633.

Nuti, C., A. Rasulo, and I. Vanzi (2007). Seismic safety evaluation of electric power supply at urban level. *Earthquake Engineering & Structural Dynamics 36*(2), 245–263.

Orense, R. (2011). Soil liquefaction during the 2010 Darfield and 1990 Luzon Earthquakes: A comparative study. In *Proceedings of the Ninth Pacific Conference on Earthquake Engineering Building an Earthquake-Resilient Society.*

O'Rourke, M. and X. Lui (1999). Response of buried pipelines subject to earthquake effects. Technical report, MCEER. SUNY Buffalo.

O'Rourke, M. J. and P. So (2000). Seismic fragility curves for on-grade steel tanks. *Earthquake Spectra 16*(4), 801–815.

O'Rourke, T. D. (2007). Critical infrastructure, interdependencies, and resilience. *The Bridge 37*(1), 22–29.

Ouyang, M. and L. Dueñas-Osorio (2011a). An approach to design interface topologies across interdependent urban infrastructure systems. *Reliability Engineering & System Safety 96*(11), 1462 – 1473.

Ouyang, M. and L. Dueñas-Osorio (2011b). An efficient approach to compute generalized interdependent effects between infrastructure systems. In *Journal of Computing in Civil Engineering. Available online.*

Padgett, J. E. and R. DesRoches (2008). Methodology for the development of analytical fragility curves for retrofitted bridges. *Earthquake Engineering & Structural Dynamics 37*(8), 1157–1174.

Page, L., S. Brin, R. Motwani, and T. Winograd (1999). The pagerank citation ranking: Bringing order to the web. Technical Report 1999-66, Stanford InfoLab.

Papoulis, A. (1991). *Probability, Random Variables and Stochastic Processes* (3rd ed.). McGraw-Hill Companies.

Pederson, P., D. Dudenhoeffer, S. Hartley, and M. Permann (2006). Critical Infrastructure and Interdependency Modeling: A Survey of US and International Research. Technical report, Idaho National Laboratory.

Poljanšek, K., F. Bono, and E. Gutiérrez (2012). Seismic risk assessment of interdependent critical infrastructure systems: The case of european gas and electricity networks. *Earthquake Engineering & Structural Dynamics 41*(1), 61–79.

Rinaldi, S., J. Peerenboom, and T. Kelly (2001). Identifying, understanding, and analyzing critical infrastructure interdependencies. *Control Systems Magazine, IEEE 21*(6), 11–25.

Schoenwald, D., D. Barton, and M. Ehlen (2004). An agent-based simulation laboratory for economics and infrastructure interdependency. In *American Control Conference, 2004. Proceedings of the 2004*, Volume 2, pp. 1295 –1300 vol.2.

Shinozuka, M., X. Dong, T. C. Chen, and X. Jin (2007). Seismic performance of electric transmission network under component failures. *Earthquake Engineering & Structural Dynamics 36*(2), 227–244.

Shinozuka, M., M. Q. Feng, J. Lee, and T. Naganuma (2000). Statistical analysis of fragility curves. *Journal of Engineering Mechanics 126*(12), 1224–1231.

Shinozuka, M., A. Rose, and R. Eguchi (1998). *Engineering and Socioeconomic Impacts of Earthquakes - An Analysis of Electricity Lifeline Disruptions in the New Madrid area.* Buffalo, N.Y.: Multidisciplinary Center for Earthquake Engineering Research, MCEER, Monograph 2.

Song, J. and A. Der Kiureghian (2003). Bounds on system reliability by linear programming. *Journal of Engineering Mechanics 129*(6), 627–636.

Song, J. and W.-H. Kang (2009). System reliability and sensitivity under statistical dependence by matrix-based system reliability method. *Structural Safety 31*(2), 148 – 156.

Symantec Security Response (2011). W32.Duqu. The precursor to the next Stuxnet. Technical report, Symantec.

Takewaki, I. (2011). Preliminary report of the 2011 off the Pacific coast of Tōhoku Earthquake. *Journal of Zhejiang University SCIENCE A 12*(5), 327–334.

Tang, A., S. Werner, and A. S. of Civil Engineers. Technical Council on Lifeline Earthquake Engineering (2009). *TCLEE 2009: Lifeline Earthquake Engineering in a Multihazard Environment : June 28-July 1, 2009, Oakland, California.* American Society of Civil Engineers.

Ten, C.-W., C.-C. Liu, and G. Manimaran (2008). Vulnerability assessment of cybersecurity for scada systems. *Power Systems, IEEE Transactions on 23*(4), 1836 –1846.

The Economist (April 28 2011). America's transport infrastructure. Life in the slow lane. http://www.economist.com/node/18620944.

United Nations (2009). DESA Population Division. World Population Prospects: The 2008 Revision and World Urbanization Prospects: The 2009 Revision. http://esa.un.org/wup2009/unup/. Retrieved on January 05 2012.

Wang, J. and J. Silvester (1993). Maximum number of independent paths and radio connectivity. *Communications, IEEE Transactions on 41*(10), 1482 –1494.

Wang, J.-W. and L.-L. Rong (2009). Cascade-based attack vulnerability on the US power grid. *Safety Science 47*(10), 1332 – 1336.

Watts, D. (2004). *Small worlds : the dynamics of networks between order and randomness.* Princeton, N.J. Woodstock: Princeton University Press.

Watts, D. J. (2003). *Six Degrees: The Science of a Connected Age* (1st ed.). W. W. Norton & Company.

Watts, D. J. and S. H. Strogatz (1998). Collective dynamics of "small-world" networks. *Nature 393*(6684), 440–442.

Wesson, R. L. and D. M. Perkins (2001). Spatial correlation of probabilistic earthquake ground motion and loss. *Bulletin of the Seismological Society of America 91*(6), 1498–1515.

White, D. R. and M. Newman (2001). Fast Approximation Algorithms for Finding Node-Independent Paths in Networks. Technical report, Santa Fe Institure Working Paper.

Winkler, J., L. Dueñas-Osorio, R. Stein, and D. Subramanian (2011). Interface network models for complex urban infrastructure systems. *Journal of Infrastructure Systems 17*(4), 138–150.

Wu, J. and L. Dueñas-Osorio (2012). Calibration and validation of a seismic damage propagation model for interdependent infrastructure systems. In Preparation.

Youngs, R. and K. Coppersmith (1985). Implications of fault slip rates and earthquake recurrence models to probabilistic seismic hazard estimates. *Bulletin of the Seismological Society of America 75*(4), 939–964.

Zhang, P., S. Peeta, and T. Friesz (2005). Dynamic game theoretic model of multilayer infrastructure networks. *Networks and Spatial Economics 5*(2), 147–178.